

IAEA-TECDOC-464

**CURRENT TRENDS
IN NUCLEAR BOREHOLE LOGGING TECHNIQUES
FOR ELEMENTAL ANALYSIS**

PROCEEDINGS OF A CONSULTANTS MEETING
ORGANIZED BY THE
INTERNATIONAL ATOMIC ENERGY AGENCY
AND HELD IN OTTAWA, CANADA
2-6 NOVEMBER 1987



**A TECHNICAL DOCUMENT ISSUED BY THE
INTERNATIONAL ATOMIC ENERGY AGENCY, VIENNA, 1988**

CURRENT TRENDS IN NUCLEAR BOREHOLE LOGGING TECHNIQUES
FOR ELEMENTAL ANALYSIS
IAEA, VIENNA, 1988
IAEA-TECDOC-464

Printed by the IAEA in Austria
June 1988

PLEASE BE AWARE THAT
ALL OF THE MISSING PAGES IN THIS DOCUMENT
WERE ORIGINALLY BLANK

The IAEA does not normally maintain stocks of reports in this series.
However, microfiche copies of these reports can be obtained from

INIS Clearinghouse
International Atomic Energy Agency
Wagramerstrasse 5
P.O. Box 100
A-1400 Vienna, Austria

Orders should be accompanied by prepayment of Austrian Schillings 100,—
in the form of a cheque or in the form of IAEA microfiche service coupons
which may be ordered separately from the INIS Clearinghouse.

FOREWORD

Nuclear borehole logging techniques have a potential to provide immediate and representative information about elemental concentrations in geological media. Several techniques are well established and widely used while other techniques have been emerging during recent years because of improvements in instrumentation.

The Agency convened the consultants' meeting in order to assess the present technical status of nuclear borehole logging techniques, to find out the well established applications and the development trends.

This report contains a summary report giving a comprehensive overview of the techniques and applications, and a collection of research papers describing work done in individual institutes.

The consultants' meeting was held in conjunction with a research coordinated meeting (RCM) on "Nuclear borehole logging techniques for the determination of rock characteristics". The progress reports on the RCM presented at the meeting are not included in this report but all participants of the RCM participated in writing the summary report.

The Agency is grateful to the Geological Survey of Canada which hosted the meeting, the main organizer of the meeting, Mr. Quentin Bristow, who also chaired the meeting and all participants who contributed to the meeting by presenting papers and contributing to the fruitful discussions.

EDITORIAL NOTE

In preparing this material for the press, staff of the International Atomic Energy Agency have mounted and paginated the original manuscripts as submitted by the authors and given some attention to the presentation.

The views expressed in the papers, the statements made and the general style adopted are the responsibility of the named authors. The views do not necessarily reflect those of the governments of the Member States or organizations under whose auspices the manuscripts were produced.

The use in this book of particular designations of countries or territories does not imply any judgement by the publisher, the IAEA, as to the legal status of such countries or territories, of their authorities and institutions or of the delimitation of their boundaries.

The mention of specific companies or of their products or brand names does not imply any endorsement or recommendation on the part of the IAEA.

Authors are themselves responsible for obtaining the necessary permission to reproduce copyright material from other sources.

CONTENTS

1. INTRODUCTION	7
2. NUCLEAR TECHNIQUES FOR ELEMENTAL ANALYSIS	8
2.1. Natural γ -ray spectrometry	8
2.2. Prompt gamma neutron activation analysis	9
2.3. Prompt inelastic neutron activation analysis	10
2.4. Delayed gamma neutron activation analysis	10
2.4.1. DGNAA with thermal neutrons	11
2.4.2. DGNAA with high energy neutrons	11
2.5. Spectral γ - γ , γ -density	12
2.6. Neutron porosity measurement	12
2.7. Energy dispersive X-ray fluorescence	13
3. APPLICATIONS	14
3.1. Applications of natural gamma ray spectrometry	14
3.2. Applications of γ - γ and spectral γ - γ logging	15
3.3. Applications of activation analysis techniques	16
3.4. Applications of neutron porosity measurement	17
4. FUTURE TRENDS	19
5. TECHNICAL AND ECONOMICAL BENEFITS	20
6. CONCLUSIONS	21
Downhole assaying in Canadian mineral deposits with the spectral gamma-gamma method ...	23
<i>P.G. Killeen, C.J. Mwenifumbo</i>	
Quantitative nuclear borehole logging based on neutron excited gamma reactions	31
<i>M. Borsaru, P.L. Eisler, J. Charbucinski</i>	
Elemental concentrations from gamma ray spectroscopy logs	55
<i>J.S. Schweitzer, D.V. Ellis, J.A. Grau, R.C. Hertzog</i>	
Borehole capture gamma ray spectrometry in very dry rock	67
<i>F.E. Senftle, J.L. Mikesell</i>	
Nuclear quantitative analysis of P, Si, Ca, Mg, Fe, Al in boreholes on a phosphate mine	93
<i>J.-L. Pinault</i>	
Analysis of boron, samarium and gadolinium in rock samples by neutron capture gamma ray spectrometry	105
<i>C.W. Tittle, M.D. Glascock</i>	
The Monte Carlo Library Least-Squares Analysis principle for borehole nuclear well logging elemental analyzers	111
<i>K. Verghese, R.P. Gardner, M. Mickael, C.M. Shyu, T. He</i>	

Advances in bulk elemental analysis using neutron interactions	123
<i>T. Gozani</i>	
The assay of gold and platinum in rocks and ore — an option	135
<i>C.G. Clayton</i>	
List of Participants	153

1. INTRODUCTION

The analysis of elemental concentrations in boreholes require techniques which are element specific, sufficiently sensitive to detect anomalies as well as economically recoverable deposits, and penetrating enough to overcome mineral heterogeneity and enable determination in water filled boreholes.

These specifications can in principle be found only in nuclear methods. In spite of the obvious advantages on in-situ analysis in mineral exploration, the techniques have not found the widely spread use, which could be expected. The main reason is that the logging systems developed until now have not filled all the requirements mentioned above. The analyzers are either specific and sensitive but not penetrating enough, or penetrating but not sensitive enough. Calibration presents a significant problem rendering accurate quantitative analysis difficult.

Recent years have brought new promising development mainly because of improved measuring electronics and computers. Therefore it is time to review the current status and development trends in borehole logging techniques for elemental analysis.

The meeting was convened by the Agency in Ottawa, with the Geological Survey of Canada acting as host, to provide a forum for scientists to present the results of their work and to discuss the present status and future development trends of the techniques.

The technical proceedings include a summary report together with the written versions of all the papers presented. This summary describes the individual nuclear techniques, and their main applications. The summary was produced by working groups of two or three of the participants whose areas of expertise were most relevant to the technique in question.

The research papers describe development work and applications made in the different institutes represented by the participants.

2. NUCLEAR TECHNIQUES FOR ELEMENTAL ANALYSIS

2.1. Natural γ -Ray Spectrometry

The method involves the detection of natural gamma radiation which is used to determine the concentrations of the three naturally occurring radioelements, potassium, uranium and thorium. Detection can be made with either scintillation detectors (usually NaI(Tl), CsI(Na), or BGO) or solid state detectors (usually high purity Germanium) operating at liquid nitrogen temperature.

At present the use of scintillation detectors dominates the applications primarily because of difficulties associated with cooling problems and low detector efficiency of solid state detectors. Maximum count rate is limited by the concentrations of Th, U and K. However, solid state detectors have the advantage of very high energy resolution which make it possible to do uranium and thorium determinations without assumptions regarding radioactive equilibrium in the U and Th decay series.

In addition to K, U, and Th determinations, natural gamma-ray spectrometry is used as an aid to lithological correlation and mineral identification, determination of organic material of higher U content, and detection of alteration associated with mineral deposits.

Recent technological developments indicate that room temperature solid state detectors will soon become available and their usage will therefore become greatly increased. In addition, increased knowledge about effects of variations in measurement parameters, both of the boreholes and of the equipment, now make it possible to improve interpretations using computer models, which at the same time take advantage of recent developments in the field of computer technology. Hence higher accuracy of quantitative measurements can be expected in the near future.

Natural gamma-ray spectrometry encounters a problem when radioelement concentrations are low and the natural gamma-ray flux is statistically difficult to work with in computing results. The solution to the problem lies in the area of increasing the detector efficiency or detector size if hole diameter permits.

Another important problem exists in the area of calibration standards. At present, calibration models for uranium logging (with gross count gamma-ray equipment) exist in many countries. Model boreholes for calibration of thorium and potassium are relatively rare and some attention should be directed to their establishment in the future.

2.2. Prompt gamma neutron activation analysis

The prompt production of gamma-rays resulting from the capture of slow ("thermal and epithermal") neutrons is the basis for prompt gamma neutron activation analysis (PGNAA).

The resulting gamma-rays are specific for the nuclei that capture the thermal neutrons. Hence the presence of specified gamma-rays and their intensity allows for the quantitative determination of the elemental concentration in the neutron interrogated object (e.g. stream of coal, ores, formation around borehole probe, etc.).

Because of the prompt production of thermal neutrons at depth in the sample and the resulting gamma-rays are of high energy (0.5 to 11 MeV), PGNAA is ideal for non-intrusive on-line measurement of bulk samples and streams and borehole measurements.

A PGNAA system is composed of a neutron source and its shielding, sample presentation, detection system and data processing system. As all practical sources of neutrons (isotopic or electronically generated) are of high energy (1 to 14 MeV), the neutrons from the source must be externally (e.g. by use of polyethylene) or internally moderated by the hydrogen present in the sample (as in the case of coal). The most common and readily available neutron sources are the isotopic sources ^{252}Cf , Am-Be other alpha-Be and the 14 MeV neutron generator. The sources are listed according to ease of moderation. Thus, in most cases cost and complexity will be in favour of the ^{252}Cf source.

The PGNAA technique has been researched, developed and applied over a period of more than three decades. The last decade shows major improvements and the maturity of the technique.

The main stumbling block to seeing a wide beneficial industrial use of PGNAA is bridging the general acceptance gap between the developer and/or manufacturer of such systems and the potential user, and demonstrating the material properties, e.g. mineralogy, that may be determined from elemental concentrations.

2.3. Prompt inelastic neutron activation analysis

The prompt production of gamma-rays resulting from the inelastic scattering reaction $(n, n'\gamma)$ is the basis for prompt inelastic neutron activation analysis. Prompt gamma-rays can also be produced by other fast neutron reactions (n, X) where X can be a proton, deuteron, tritium alpha or 2 neutrons.

The technique is complementary to PGNAA. The resulting gamma-rays are different but are also generally specific to the nuclei that interact with the fast neutrons.

The PINAA is better suited for analysis of low and medium atomic weight elements such as carbon, nitrogen and oxygen, where the PGNAA response is low.

The most practical source for the PINAA is the electronic neutron generator based on the fusion reaction (D, T) which prolifically generates 14 MeV neutrons. For some applications, when the wealth of gamma-ray lines generated by the 14 MeV neutrons is not beneficial, an (α, Be) (e.g. $^{241}\text{AmBe}$) source with a lower average neutron energy $\sim 5\text{MeV}$ is more appropriate.

Most of the 14 MeV neutron generators for borehole exploration are pulsed so that one can combine PINAA during the pulse and PGNAA during the ensuing die-away time of the thermalized neutrons.

2.4. Delayed Gamma Neutron Activation Analysis

Delayed gamma neutron activation analysis (DGNAA) is the detection of specific gamma-rays produced by the decay of radioactive nuclei formed through neutron absorption by a stable nucleus. From a practical point of view, radioactive nuclei with half lives ranging from about 1 sec to

about a few months are of the greatest interest. In general, DGNAAs techniques, as compared with other analytical techniques, are favoured for minor and trace element analysis because of the reduced background which is one of the major factors contributing to improved sensitivity. Maximum data rates require the use of the largest intensity neutron sources consistent with radiation safety. Inorganic scintillators can frequently be used when only a few elements are of interest. A more complete multi-element analysis usually requires a semi-conductor detector which has much better resolution than can be achieved with scintillators. In the DGNAAs technique the delay between neutron irradiation and gamma-ray detection can be adjusted to enhance the selectivity for specific elements. DGNAAs can be performed either with thermal or high-energy neutrons.

2.4.1. DGNAAs with Thermal Neutrons

Isotopic neutron sources, e.g. ^{252}Cf , are currently used for thermal DGNAAs (future developments on d,d or γ,n accelerators may also be suitable), and the lowest energy neutron sources are preferable to minimize interference from high-energy neutron-induced reactions. A unique advantage of this technique is the unambiguous association between the detected gamma-rays and the specific elements in the rock. This advantage occurs because thermal neutron capture will create only radioactive isotopes of the original element.

2.4.2. DGNAAs with High Energy Neutrons

Neutron generators based on the d,t reaction are used to produce high-energy neutrons ($E = 14\text{MeV}$) that can be used for DGNAAs. In extended media, such as a borehole, the neutron flux will contain both high-energy and thermal neutrons. High-energy neutrons can create radioactive nuclei of elements other than the original element. This can result in improved sensitivity for particular elements (e.g., Si, Fe, O ...). Particular gamma-rays may now be produced from more than one element, and unlike thermal DGNAAs, require improved resolution and precision to allow unambiguous quantitative analysis of elemental concentrations. The higher energy and intensity of the source neutrons increase the importance of careful shielding to protect the detector and eliminate background from the spectrometer.

2.5. Spectral γ - γ , γ -Density

The method involves emission of γ -rays by a source in the probe and the detection of the gamma-rays backscattered from the rocks surrounding the borehole. Variations of the method involve counting with one or more detectors at different distances from the source and applying simple (single window) or sophisticated (multichannel) energy discrimination techniques.

Most commercial logging companies use multiple-detectors but very simple energy discrimination, and no energy stabilization. The information is primarily limited to density determinations. Often information is qualitative showing only density variations, although some systems have been properly calibrated in density models and quantitative density data are possible.

There is a trend towards more widespread use of calibration models and hence quantitative measurements. In addition the incorporation of the spectral gamma capability arising from developments in natural gamma-ray spectral logging are making it possible to obtain much more information in the form of spectral gamma-gamma data that allows a simultaneous determination of density and average photoelectric absorption cross section. At the same time spectral stabilization methods have improved and are being incorporated in these probes for more accurate measurements. In favourable environments (e.g. iron deposits) elemental determinations can be made from spectral γ - γ data. It is also possible to combine both natural spectral γ and spectral γ - γ measurements in a single detector in a single run in a borehole.

Multi-element deposits are difficult to analyze, for example, when barite is present in association with the element of primary interest.

2.6. Neutron Porosity Measurement

Though intended to be specific to hydrogen, which is then regarded as a measure of porosity, neutron porosity devices tend to be influenced by the solid rock matrix. Nevertheless, these devices, especially when coupled to a complementary method such as the gamma-gamma density log,

are capable of precise porosity determination, because hydrogen is so often directly related to porosity. All existing neutron porosity devices determine hydrogen through strong influence on either the neutron slowing length or the slowing down time.

These methods, as presently implemented, are just as sensitive to hydrogen found in the solid component as to that associated with fluids, which is the basis for porosity estimation. Thus, bound hydrogen, as in hydrates or clays, adversely affects the porosity measurement. Means of reducing these effects are worthy of investigation.

The three practical neutron sources for neutron porosity logging are: (1) californium-252; (2) alpha-beryllium sources such as Am-Be; and (3) d-t sources (neutron tubes). On the average, these sources have increasing fast neutron energy in the order listed. In that same order, porosity sensitivity decreases, while depth of investigation and matrix effects increase.

If thermal neutrons are detected as the primary measurement, the indicated porosity is also influenced by the thermal absorption cross section (σ) of the formation. This, in part, explains the interest in laboratory methods for rapid determination of σ in rock samples. The epithermal slowing down time porosity logging method promises to alleviate some of the difficulties.

The useful character of the neutron porosity log has found very wide application on the oil industry and is being used increasingly in other fields such as coal and hydrology.

2.7. Energy Dispersive X-ray Fluorescence

Because of the relatively low energies involved, this technique has limited application, except in shallow, dry boreholes for mine control.

An increased use of high resolution detectors, as a result of the increased lifetime of cryogenics, and more rapid, if not instantaneous, data analysis are the only significant developments forecast for the future.

The most important area of application is believed to be in assessing the ore grade of tin deposits in regions where hard rock mining prevails.

3. APPLICATIONS

The following is not intended as a comprehensive description of all possible applications of the known techniques, or all the techniques which are needed for a complete evaluation of a specific geological formation or ore. The discussion is limited to the most important established applications and the most important development trends.

3.1. Applications of Natural Gamma-Ray Spectrometry

Passive gamma-ray spectrometry is primarily used in uranium mining exploration for determination of uranium concentrations in the presence of thorium and potassium. It is also used for lithological correlations in non-uranium mining related problems, especially in situations where gross gamma-ray counting fails. In some geological environments characteristic radioelement ratio can be established to delineate certain zones of interest, and in many cases characteristic radioelement concentrations and/or ratios are associated with economic mineralization.

In general determination of K, U and Th by natural gamma-ray spectrometry is extremely useful for solving geological problems, such as the North Sea oil exploration problems.

The future should see increased usage of natural gamma-ray spectrometry to solve geological problems through the associations of minerals of interest with characteristic variations in K, U and Th. Examples are gold associated with potassium alterations, uranium associated with phosphorus deposits, and radioelements associated with tin/tungsten deposits. Characteristic radioelement distributions are also associated with differentiation at the time of cooling of magma.

Natural gamma-ray spectral logs also have a potential for geothermal reservoir identification.

In an active geothermal field, potassium rich hydrothermal fluid-flows which are connected with some magmatic activity, rise up through permeable zones such as fractures, and this potassium tends to precipitate in formations which are located in the path of hydrothermal fluid-flows.

It was found that the concentration of potassium in altered rocks can be easily detected by the use of a natural gamma-ray spectral log. This detection method can be applied not only for recognition of hydrothermal potassium minerals such as K-feldspar and Sericite in drill wells, but also for interpretation of distribution of potassium caused by hydrothermal activity. The natural gamma-ray spectral log is a useful tool for the evaluation of geothermal hydrology in an active geothermal field.

Future applications include the detection of man-made radioisotopes associated with nuclear waste disposal and related environmental problems.

3.2. Applications of γ - γ and spectral γ - γ logging

The method is primarily used for density determinations, usually for coal logging. Zone thickness and ash determinations can often be computed from the density log.

In general density logging is widely used in coal, oil, and gas exploration as a lithological tool for correlation purposes and for determining the pore volume of rocks.

Spectral gamma gamma logs provide lithological information resulting from the different effective atomic numbers of different rocks. Quantitative determinations of the concentrations of certain heavy elements can be made with a properly calibrated system. More accurate quantitative density computations can also be made based on the spectral γ - γ data.

Spectral γ - γ logs may also be used in geotechnical applications for density of soils and stability of benches in open pit mining, dams and other foundation problems.

In general there is a very high potential for widespread application of spectral γ - γ techniques in both developed and developing countries. This is primarily because there is a natural progression from familiarization with spectral logging to spectral gamma-gamma logging. In addition the radioactive sources involved are relatively weak. Interpretation of γ - γ spectra is also easier than interpretation of neutron-gamma spectra. Methods to realize this potential as soon as possible should be developed.

3.3. Applications of Activation Analysis Techniques

All elements of interest manifest, to various degrees, clear signatures in PGNAA and/or PINAA. The actual application depends on technical feasibility (e.g. levels of concentration required for a given element, background, interferences, etc.) and ultimately on economic issues. Only the technical considerations are discussed in this summary.

PINAA has been used for the last 15 years (but unfortunately not extensively) for the quantitative determination of: -Al, P, S, Fe, Ni, Zn, Pb and a few other intermediate elements in ore and ore processing. Carbon is being measured in ash from power stations prior to its use in cement manufacture. Carbon and oxygen are now measured using (α , Be) or 14 MeV neutron sources, in addition to non nuclear techniques, to determine relative amounts of water in light and heavy oil near the extraction point and to determine oil content of subsurface geological formations.

PGNAA has an increasing importance in borehole logging for oil and gas evaluation and the geosciences by providing absolute elemental concentrations.

For coal exploration the new trend is to develop nuclear borehole logging techniques for elemental analysis, particularly the PGNAA and DGNAA based on HPGe and Am-Be as well as ^{252}Cf sources. It has been found in the laboratory that more than 20 elements could be detected by using this method. They are as follows: C, H, S, N, O, Si, Fe, Al, K, Na, Ca, Mg, Mn, Cl, Zn, B, Cd, Gd, Ge, V, Ti, Sm, As, Pb, Au.

These techniques can be used to determine not only the location and thickness of the coal measures, but also the ash content and the calorific value of the coal, and the concentrations of toxic elements (As, ...) and useful by-products (Ge, Gd, Ti, Sm, Au, etc.). Moreover, an evaluation of the formation can be made from the concentration ratio of Si, Fe, Al, etc.

The main problem is the leading edge technology involved in fabricating a probe containing the HPGe detector which is needed, and in dissipating the heat which is generated during logging. An additional problem is separating the radiation flux induced in the borehole fluid from that of the formation from which the elemental analysis must be made.

The advantages of PGNAA are also demonstrated by its emerging applications in on-line analysis. PGNAA has gained in popularity over the last decade, finding use in on-line elemental analysis of coal moving on belts or chutes. The main use is in the determination of sulphur content to ensure compliance with environmental regulations. Most of the existing on-line instruments (there are about ten of them currently in use) can determine a few elements (such as Fe and Ca) in addition to sulphur. One system can determine most of the eleven elements in coal directly, and can infer the concentration of the rest (e.g. Na, Mg).

Two PGNAA instruments are now installed in cement plants, one for full elemental analysis and the other for Ca and Fe. There are numerous laboratory applications of PGNAA that have been reported, that include the determination of phosphorus in phosphate ore using a Ge detector; the elemental composition of rocket propellant; and the boron content of large samples and nitrogen content in explosives.

3.4. Applications of Neutron Porosity Measurement

Neutron porosity measurements are mainly used for hydrocarbon exploration and production. For quantitative interpretation of neutron logs additional information concerning the rock matrix such as sigma values are needed. Several kinds of neutron logs have found wide application in the petroleum industry. These include:

1. Single detector probes
 - (a) Neutron-thermal neutron
 - (b) Neutron-epithermal neutron
 - (c) Neutron-gamma

2. Dual detector probes
 - a, b, c as above

3. Multiple detector probes
 - (a) Combination of 2(a) and 2(b) in one probe
 - (b) Proposed multi-detector probes whose purpose is to correct for borehole effects

Neutron porosity logs provide information on total hydrogen content in rocks (including hydrogen content in rocks, in organic matter, in water and hydrogen bound in mineral matter) when coupled to a complementary method such as gamma-gamma density or the PGNAA technique. Neutron porosity measurements can be applied for determining the most important coal characteristics like calorific value or the moisture and mineral matter (ash) content of coal.

A type of neutron log called a moisture gauge has been used for studying soil and rock properties related to building foundations, bridges, highways and other structures. Another application has been the location of the best producing horizon in a water well for general use and for irrigation.

4. FUTURE TRENDS

Significant progress has been made in recent years in the performance and reliability of logging probes. In oil exploration and production boreholes the greater reliability and extended lifetime of neutron tubes is already having a significant effect on the quality and value of extracted information and this trend is expected to continue.

In minerals exploration the development of efficient cryogenics now allows high resolution gamma-ray detectors (HPGe) to be used downhole so that a vastly increased amount of data has now become available. In particular, this is giving rise to accurate determination of elemental concentrations which in turn is leading to important advances in formation analysis.

Significant progress has also been made in high level data transfer from the probe to the logging equipment located at ground level.

The application of micro- and mini-computers in the logging equipment now permits rapid assessment of the characteristics of underlying studies, but perhaps the most important development in computer application is in the modelling of real situations through the development of sophisticated Monte-Carlo and associated codes. This latter development, in particular is expected to have a profound effect on all aspects of operational strategies and on data interpretation in the future.

5. TECHNICAL AND ECONOMICAL BENEFITS

Activities involved in the identification, evaluation, recovery, and processing of geologic material require the acquisition of remote samples and subsequent analysis at a distant location. In-situ nuclear techniques generally provide technical and economical benefits. Technical and economical benefits are not mutually exclusive. The following two paragraphs will emphasize the technical and economical aspects, respectively.

Samples acquired by remote acquisition must necessarily be small and discrete. The techniques of acquiring the samples are frequently costly and time consuming. Once acquired, they undergo subsequent analysis which can be both costly and time consuming. Because of the size of the samples, they are generally not statistically representative of the material from which they were taken. Nuclear analysis techniques can ameliorate these limitations. They typically are sensitive to volumes that are 100-1000 times larger than the remotely-acquired samples. In-situ nuclear analyses are continuous, faster, frequently cheaper, and produce results which are more statistically significant.

The most important economic consequence of in-situ nuclear analysis is the more accurate and complete description of the region under investigation. Improvement of the data quality allows better economic evaluation. The costs associated with discrete sampling can be minimized. Immediate analysis permits better control and improved efficiency of all operations. An additional benefit is the better understanding of any resources and the geological environment. The stringent requirements of modern geologically-related operations necessitate quality control that can only be achieved with the maximum amount of rapidly available data.

6. CONCLUSIONS

Nuclear techniques have assumed a major role in obtaining data on geological strata for geoscience purposes, for in-situ evaluation of oil, gas, and mineral resources, and for on-line control of process streams, especially for mineral production. The techniques employed include the measurement of gamma-ray scattering, neutron scattering, and elemental-specific spectroscopic measurements of either natural activity or gamma-rays induced by neutron interactions. The technical complexity of the techniques range from very simple to highly advanced, providing a range of applications that can be applicable at all levels of technological sophistication. These techniques have demonstrated the ability for more precise evaluation of extended media leading to more efficient evaluation and processing of geological material. Recent advances have also demonstrated the utility of nuclear-measured parameters for determining other material properties. Optimum use of these nuclear techniques can be enhanced by hardware improvements, analysis enhancements through a better understanding of the measurement physics and the relationship of the measurements to geological properties, and greater education and training to permit wider use of established analysis techniques.

The present status and future of the different techniques can be summarized as follows:

1. Although problems of low counting rates and tool calibration exist, the use of natural gamma-ray spectroscopy has proved eminently useful for the determination of Th, U, and K, lithological correlation, detection of regions of alteration of ore bodies, etc.
2. Borehole elemental analysis using gamma-rays produced both by radiative capture or inelastic scattering have been well tested over the past 15 years, and these methods are gaining recognition as useful analytical techniques. The technology is in place, and therefore, once it has gained more widespread acceptance by geologists, it should become a standard method of borehole analysis.

3. Borehole elemental analysis by delayed gamma-ray spectroscopy is attractive for specific elements with appropriate half-lives and neutron absorption cross-sections. The method has the advantage of a better signal-to-noise ratio than prompt gamma-ray techniques, but the disadvantage of requiring a strong neutron source.
4. Spectral γ - γ and γ -density logs are improving in quality and use primarily because of better calibration techniques and more useful data. The γ -density measurements can be helpful in correcting a porosity determination, so that quite accurate porosity measurements can be obtained.
5. Neutron porosity logs are well established and commonly used means for determination of total hydrogen content of rocks when coupled to a complementary method such as gamma-gamma density log. Most important applications are in exploration for oil, gas, coal and water.
6. New technology, especially computer data reduction techniques and new electronic counting systems, is expected to improve all the borehole activation methods.

DOWNHOLE ASSAYING IN CANADIAN MINERAL DEPOSITS WITH THE SPECTRAL GAMMA-GAMMA METHOD

P.G. KILLEEN, C.J. MWENIFUMBO
Mineral Resources Division,
Geological Survey of Canada,
Ottawa, Ontario, Canada

Abstract

The Borehole Geophysics Section at the Geological Survey of Canada is conducting research into the Spectral Gamma Gamma (SGG) logging method with the objective of developing a borehole assay technique suitable for use in Canadian mineral exploration and mine development. The SGG method is based on the different interactions of gamma rays with matter. After gamma rays from a radioactive source have interacted with rock the gamma ray energy spectrum contains information about the atomic number (Z) of the elements in the rock. A special radioactive source holder has been designed to attach to the nose of a spectral gamma ray logging probe in order to make SGG measurements. A series of different collimators designed to focus the gamma rays radially out into the rock at angles of 90°, 60°, 45° and 30° to the probe, and a series of different spacers to permit variations in source-detector spacing have been fabricated from tungsten. In addition, sources with different gamma ray energies (Cobalt 60, Cesium 137, Iridium 192) have been tested. A number of experiments have been conducted, varying all of the above parameters and the energy windows. The SGG probe has been field tested using some of the experimental configurations in boreholes intersecting different types of mineralization. The high Z values of lead in lead deposits is easily detectable and semi quantitative assay logs have been produced. Barite and pyrite associated with gold mineralization has also been detected and sphalerite-rich zones have been delineated in a zinc mining area.

1. INTRODUCTION

Direct assaying techniques for use in boreholes have numerous advantages over assaying of drill core taken from the hole. These include rapid return of results compared to laboratory analysis of core, the possibility of assaying the borehole wall in sections where core recovery may have been poor, and perhaps most importantly, the large sample volume analyzed in the borehole compared to the core size.

Borehole assaying techniques that have been tried, with varying degrees of success, are generally based on nuclear techniques such as X-Ray Fluorescence (XRF) and Neutron Activation Analysis (NAA). The low penetration of X-rays in rock severely restricts the sample volume, and the neutron based techniques have met with resistance related to the elaborate safety precautions required in handling the relatively strong radioactive sources involved.

One nuclear technique, Spectral Gamma Gamma (SGG) logging, appears to offer the significant depth penetration of gamma rays as well as the possibility of minimizing radiation safety problems by appropriately designing a logging tool with a relatively weak gamma ray source. In addition the technology for natural spectral gamma ray logging is already well developed, and can be adapted for SGG logging [1].

The possibilities for elemental analysis based on the different interactions of gamma rays with matter, (in this case rocks and minerals) was first described by Czubek in 1966 [2]. The dominant interaction is Compton scattering in which gamma rays are reduced in energy by scattering as they collide with electrons in the outer shells of atoms. The second type of interaction is photoelectric absorption in which a gamma ray loses all its energy in a collision with an electron and ceases to exist. The probability of photoelectric absorption is roughly proportional to the fifth power of the atomic number, Z , of the element with which the gamma ray interacts, and inversely proportional to about the third power of the gamma ray energy E . The probability of Compton scattering is roughly proportional to Z/E . Thus, if a spectral gamma ray logging tool is used to measure the distribution of energies of gamma rays from a radioactive source after they have interacted with rock as shown in Figure 1, the shape of the spectrum will contain information about the atomic number of the elements in the rock. In particular, as shown in Figure 2 the observed count rate at low energies will be greatly reduced if heavy elements (i.e., high Z) are present in the rock. An example of practical work in this area is that of the CSIRO in Melbourne in which an iron ore assay method was developed for use in mines of Western Australia [3].

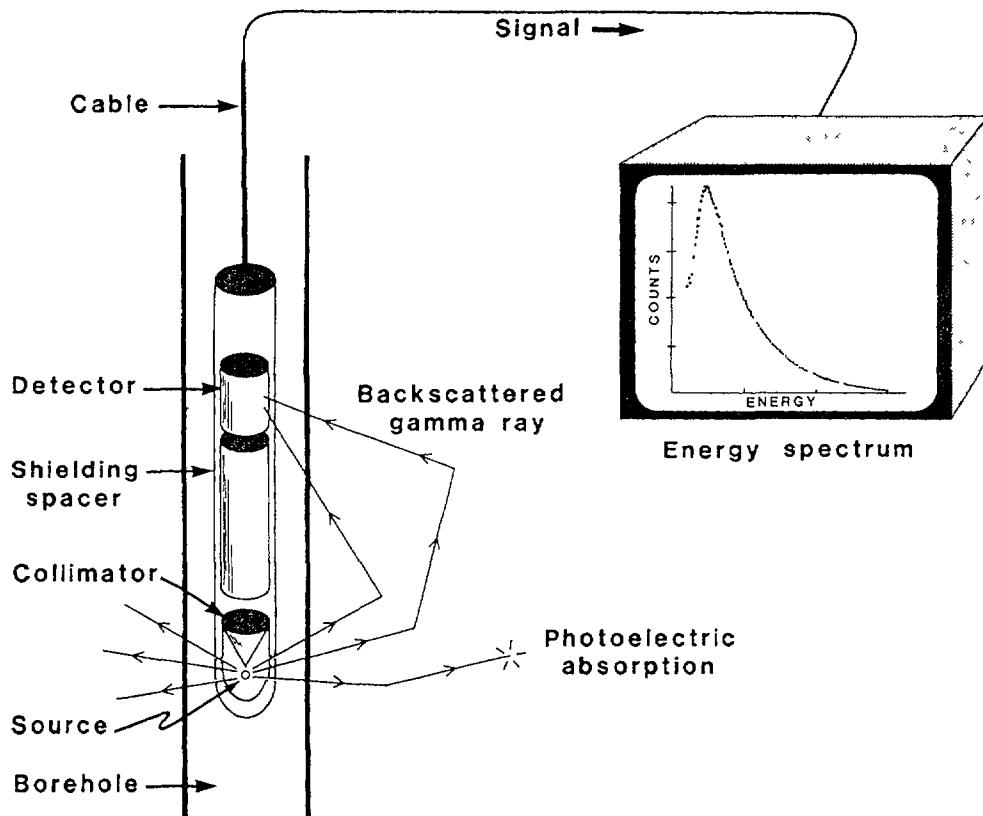


Figure 1: The spectral gamma gamma method consists of recording the energy spectrum of backscattered gamma rays from a source in the borehole probe as shown. The main components of the probe; source, collimator, spacer, and detector are indicated.

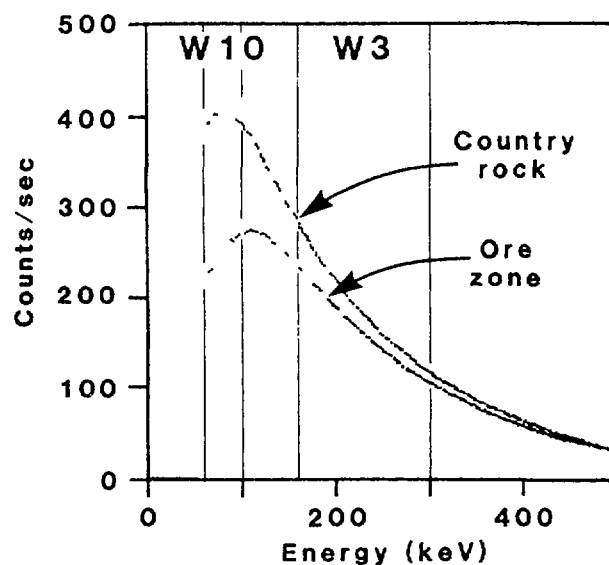


Figure 2 Typical gamma ray spectra recorded in country rock and an ore zone containing heavy elements. The increase in effective atomic number of the ore causes an increase in photoelectric absorption of low energy gamma rays. The resultant decrease in count rate at low energies is evident. The ratio of count rate in appropriate energy windows (e.g. W3/W10) can be used to indicate the presence of heavy elements in the form of a spectral ratio log of a borehole.

2 THE SPECTRAL GAMMA GAMMA PROBE

At the GSC, a special gamma-ray source holder has been designed to attach to the nose of a spectral gamma ray logging probe in order to make SGG measurements. In making the measurements it is important to optimize the source-detector spacing and the collimation angle at the source. A series of different collimators designed to focus the gamma rays radially out into the rock at angles of 90°, 60°, 45° and 30° to the probe, and a series of different spacers to permit variations in source-detector spacing have been fabricated from tungsten (see Figure 3). Tungsten provides high gamma ray attenuation, and permits the use of short source-detector distances if desired. The source holder is omni-azimuthal and is designed for use in the slim holes (e.g., AQ, 46 mm) commonly drilled in Canadian mineral exploration. The source can be of relatively low strength compared to those commonly used in gamma gamma density probes because the collimators are radially symmetrical focussing gamma rays at the appropriate angle, outward into the borehole wall in all directions. In the gamma-gamma density type of probe commonly used for coal and petroleum well logging, the gamma rays are usually strongly collimated in a narrow beam and therefore most of the gamma radiation emitted by the source is not utilized. This is because the probe must be "side walled" in the large diameter holes for consistent measurements. In addition to the different collimators and source detector spacings, sources with different gamma ray energies (Cobalt 60, Cesium 137, Iridium 192) have been tested.

The principle of the SGG log can best be understood by referring to the two spectra shown in figure 2. The positions of a low energy window (W10) and a high energy window (W3) are indicated in the figure. When there is a change in the density of the rock being measured, the count rates recorded in both windows will increase or decrease due to the associated change in Compton scattered gamma rays reaching the detector. However, if there is an increase in the content of high Z elements in the rock, the associated increase in photoelectric absorption will cause a

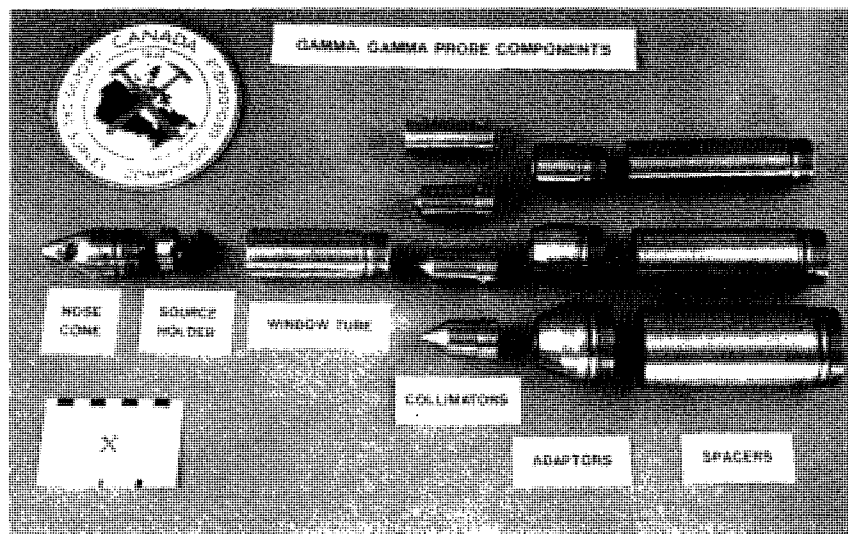


Figure 3: Experimental spectral gamma gamma probe components showing the source holder, four collimators (90°, 60°, 45°, 30°), and shielding spacers of three different diameters (32 mm, 38mm and 50 mm). The adaptors are used to attach the 32 mm diameter source holder assembly to the desired spacer. Experiments with different combinations of these components (including different sources and spacer lengths) are carried out to determine the optimum parameters for borehole assaying using the SGG method.

significant decrease in count rate in the low energy window W10, but no change in W3. W10 is affected by both density and Z effect while W3 is only affected by density. Therefore a ratio of counts in W3 to the counts in W10 can be used to obtain information on changes in Z.

The SGG ratio log is a ratio of counts in W3 to counts in W10 (i.e. W3/W10). This ratio increases when the probe passes through zones containing high Z materials. Experimentation is continuing to determine the optimum energy windows to use for this spectral ratio, as well as to optimize all of the other parameters mentioned. In particular the characteristics of the most common Canadian mineral exploration boreholes are taken into consideration (e.g. BQ; 60 mm diameter, water-filled).

Preliminary field testing indicates that the SGG method is a promising technique for development of quantitative borehole assaying for Canadian mining.

3. FIELD TESTS IN MINERAL DEPOSITS

A series of experiments has been conducted varying all of the above parameters including the energy windows. The SGG probe has been field tested using some of the experimental configurations, in boreholes intersecting mineralization of different types. The high Z of lead in lead deposits is easily detectable and semi-quantitative assay logs have been produced. Barite associated with gold mineralization has also been detected and sphalerite-rich zones have been delineated in a zinc mining area. Three examples illustrating SGG logs recorded in a lead deposit, zinc deposit and a gold deposit are presented in Figures 4, 5, and 6 respectively, and are described below.

3.1 Yava Sandstone Lead Deposit, Nova Scotia

This deposit located in Nova Scotia consists of galena in sandstones, a relatively simple geology and mineralogy. The lead in galena with its high atomic number ($Z = 82$) causes the spectral ratio values in the SGG log to increase in proportion to the lead content. This is clearly demonstrated in the log in Figure 4.

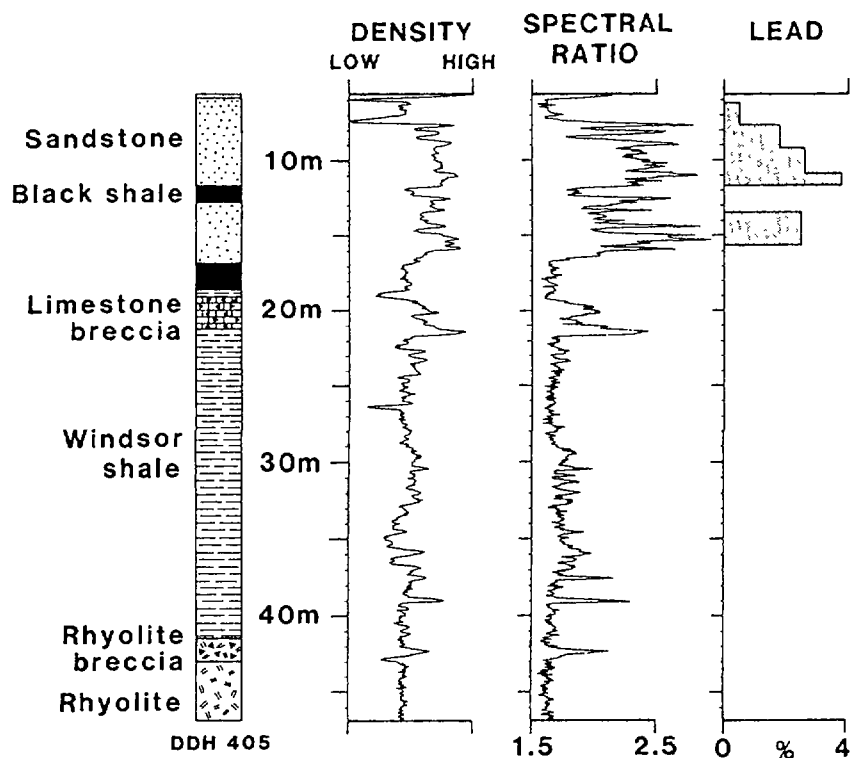


Figure 4: The spectral ratio log and a density log recorded in the Yava sandstone lead (galena) deposit in Nova Scotia. The lead assays from drill core shown in histogram form, show excellent correlation with the high values of the spectral ratio. The density log is not as sensitive to changes in lead content. Narrow zones of high ratio values are also lead-rich zones which were not assayed since they were not considered to be of economic significance.

The lead assays from drill core, plotted in histogram form in the figure show that the SGG log can be considered a semi-quantitative assay log. Note the lead concentration is less than 4%. A qualitative density log is also shown in figure 4 for comparison.

3.2 Zinc Deposit, Daniels Harbour, Newfoundland

This deposit consists primarily of sphalerite in limestone, another relatively simple geological setting. Although the atomic number of zinc is only 30, average grades of considerably less than 8% Zn are clearly defined by the high spectral ratio values shown in the SGG log (figure 5).

3.3 Gold deposits, Hemlo area, Ontario

An SGG log from a borehole in this area is shown in figure 6, along with a qualitative density log. The gold is not directly detectable but the barite and pyrite with which it is associated is easily detected. Optimizing the choice of energy windows for barium ($Z = 56$) and iron ($Z = 26$) may make it possible to determine the location and width of the gold-mineralized barite-rich zones within the broader pyritized zones.

4. QUANTITATIVE ASSAYING WITH THE SGG METHOD

Experiments are underway to quantify the relationship between the spectral ratio and lead content at the Yava lead deposit. A combination of detailed assays in drill core and model boreholes with different ore grades is being used. Additional work with barite and pyrite in model boreholes will also be carried out.

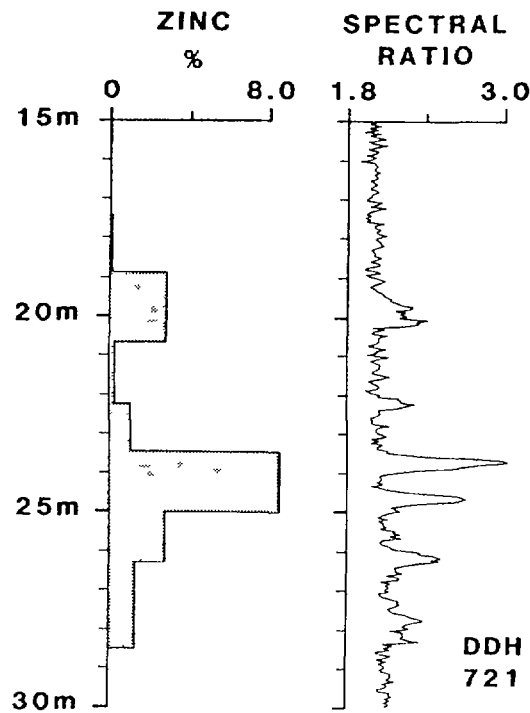


Figure 5 The spectral ratio log recorded in a zinc (sphalerite) deposit at Daniels Harbour, Newfoundland. Because of the large samples, the zinc assays of drill core do not show the zinc distribution as well as the SGG log

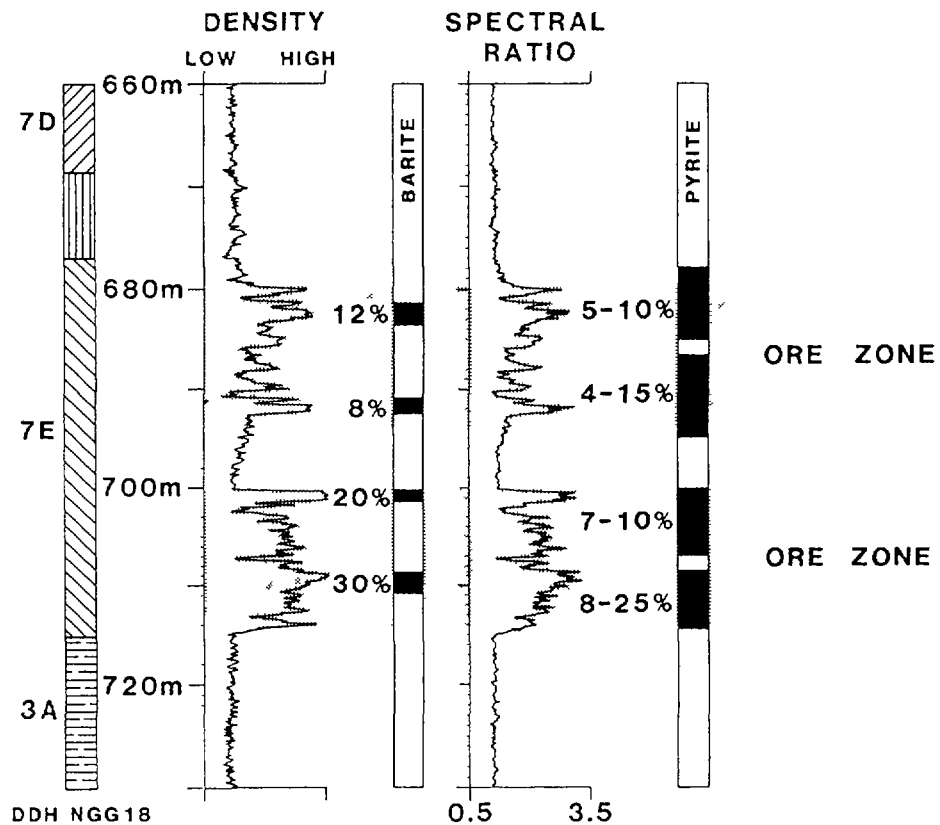


Figure 6 The spectral ratio log and density log recorded in a gold mineralized zone in the area of the Hemlo gold deposits, Ontario. The gold is associated with barite-rich zones within a broader pyritized zone. The high spectral ratio values delineate the ore zones but the barite is not distinguishable from the pyrite. Here the heavy mineral content is sufficiently high to affect the density log in the same way

Besides optimizing energy windows for measuring the desired elements, it is likely that the probe configuration for each deposit can be optimized for the particular geologic setting to provide the most accurate results.

5. REFERENCES

- [1] KILLEEN, P.G., Gamma ray spectrometric methods in uranium exploration - application and interpretation; in Geophysics and Geochemistry in the Search for Metallic Ores, (HOOD, P.J., Ed.), Geol. Surv. Can., Economic Geology Report 31, (1979), 163-229.
- [2] CZUBEK, J.A., Physical possibilities of gamma-gamma logging; in Radioisotope Instruments in Industry and Geophysics, (Proc. of Warsaw Symp., Oct. 1965) IAEA, Vienna, (1966), Vol. 2, 249-275.
- [3] CHARBUCINSKI, J., EISLER, P.L., MATHEW, P.J. and WYLIE, A.W., "Use of backscattered gamma radiation for determining grade of iron ores in blast holes and development drill holes", (Proc. Australas. Inst. Min. Metall., No. 262), (1977), 29-37.

QUANTITATIVE NUCLEAR BOREHOLE LOGGING BASED ON NEUTRON EXCITED GAMMA REACTIONS

M. BORSARU, P.L. EISLER, J. CHARBUCINSKI
Division of Mineral Engineering,
Commonwealth Scientific and Industrial
Research Organization,
Port Melbourne, Victoria,
Australia

Abstract

The application of the spectrometric neutron-gamma method for coal ash and soil salinity quantitative determinations has been described. The results of field tests for ash-in-coal determinations carried out in dry and water-filled boreholes of eight Australian black coal deposits are discussed. The borehole logging system-SIROLOG, now commercially available is described. The latest version of SIROLOG neutron-gamma probe achieved values of rms deviation better than 2% ash in most tests, both in water-filled and dry boreholes and for coals of ash content in the range 3 to 50%. The laboratory measurements and the preliminary field tests for quantitative logging of salinity in soils are described. A spectrometric neutron-gamma method using a 252-Cf source and a BGO detector was applied. Major constraints affecting salinity logging were identified. The most important of these were simulated in laboratory tests and evaluated.

1. INTRODUCTION

At CSIRO, the Borehole Logging Group, which is in the Division of Mineral Engineering, has for some years conducted research and carried out technology development in borehole logging based on nuclear geophysics. The group has contributed to the basic methodologies developed for the natural gamma, gamma-gamma, and neutron excited gamma-ray spectrometric logging techniques.

For those borehole logging methods based on the neutron excited gamma reactions, the group's past research was applied to the quantitative analysis of ore grades in nickel, coal, mineralised beach sands, and manganese ore deposits. Prompt neutron-gamma techniques, based on the use of radioisotopic sources (Am-Be and 252-Cf), were applied and tested for suitability in all these situations. However, neutron activation analysis methods were also applied successfully in the coal and manganese deposits. Also, it is worth noting that the group successfully tested pulsed neutron generator methods in coal deposits, to differentiate spectrometrically between gamma rays generated in neutron inelastic, radiative capture and neutron activation reactions.

Recently, the group has been involved in research for the coal mining industry to develop improved prompt neutron-gamma methods for measuring the raw ash content in coal strata, and in water and soil conservation problems by researching methods of measuring chlorine concentrations in water bores.

In coal applications, the anticipated advantages of the neutron-gamma technique over that of spectrometric gamma-gamma logging (also developed by the CSIRO group) were its greater suitability in water-filled boreholes of varying width and turbidity. From theory, the neutron gamma technique is

also the more suitable for ash measurements in coals of variable chemical composition of the mineral matter. This technique is also relevant to the analysis of sintered coals if combined with the spectrometric gamma-gamma.

For salinity logging, neutron-gamma is the only nuclear geophysical approach which appears feasible at this stage. The work, as indicated below, is still at an early stage of progress.

Some laboratory measurements were commenced with disseminated gold samples, in artificial borehole models, using the neutron activation analysis method. However, this investigation is only at a preliminary stage.

The present paper therefore deals with the recent work carried out in coal and salinity applications.

2. PROMPT NEUTRON-GAMMA LOGGING FOR COAL ASH IN WATER-FILLED AND DRY BOREHOLES.

In the operations of the Australian coal industry, there has been a shift in the requirements for monitoring coal quality during recent years. These requirements have diminished in exploration and have grown in mine production.

Coal quality is measured by the raw ash content, calorific value, rank, moisture content, volatiles, and sulfur content. Determining all the parameters mentioned above, together with the elemental composition of the coal, would require core drilling and analysis of the cores in the laboratory. These processes are time-consuming and costly. In many applications it is sufficient to measure only thickness, depth, and raw ash content of the seam, which can be achieved with fast borehole geophysical methods in open holes.

Because of the deep penetration of neutrons and gamma rays into the coal matrix, nuclear techniques are appropriate for borehole logging applications. The volume of coal investigated by nuclear radiation is much larger than the core analysed from a cored borehole, and it therefore provides a more representative sample. The gamma-gamma technique is currently employed in the coal industry to evaluate the coal seam parameters mentioned above. The ash content of the coal is derived from the correlation between ash and density. Although a universal correlation between ash and density does not exist, good correlations were found for many individual coal formations in Africa and Australia [1,2]. Variations in the physical properties of coal, such as rank and porosity, also influence the correlation between density and ash content in core samples. Agostini [3] and Daniels et al. [4] described cases where the ash content predicted from gamma-gamma density logs differs substantially from that of the corresponding core.

Another shortcoming of ash determination based on gamma-gamma density logs is the sensitivity of the density measurement to variations in borehole diameter. This results in reduced accuracy in rough, cavernous holes.

The prompt neutron-gamma method is an alternative nuclear technique with potential in borehole logging for coal [5,6]. This technique was investigated more recently [7-9] and reported to be competitive in performance with the most accurate gamma-gamma methods. Borsaru et al. [10] described initial field tests of the prompt neutron-gamma method in the Surat Basin. Satisfactory accuracy for ash determination was achieved. The previous work was for water-filled boreholes only. Here we deal with the application of the prompt neutron-gamma method for measuring the raw ash content of black coal in both water-filled and dry boreholes. The method described forms part of the SIROLOG* technology being developed by CSIRO.

* Acronym for CSIRO LOG

The neutron flux distribution in dry boreholes differs markedly from that in water-filled boreholes, because of the thermalising effect of the hydrogen in the water. Therefore, it is invalid to extrapolate the coal ash measurements from water-filled to dry boreholes. This is important when considering the logging method for open cut mine-production situations, where most boreholes are dry, which contrasts with the situation for coal-exploration holes in Australia, where most holes are at least partly water-filled.

The logging method described here employs the neutron capture reaction. The compound nucleus formed in neutron capture decays almost instantaneously, emitting gamma radiation. Due to its high hydrogen content, coal is an excellent matrix for this technique. The neutrons emitted are thermalised by colliding with the hydrogen nuclei present in coal, and they subsequently interact with the nuclei in the coal matrix. Another advantage of the prompt neutron-gamma technique for coal is that the major gamma rays, produced by the main constituents of the mineral matter in coal (Al, Si, Fe, Ca, Ti, S), have energies above 3 MeV (Table I).

The deeply penetrating high-energy gamma radiation detected in a borehole logging probe emanates from a large volume of coal; hence the technique is not as sensitive to the rugosity and condition of the borehole as the gamma-gamma technique.

The ash content of a coal sample is the weight percentage of residue after combustion, it is closely related to the mineral content of coal. There also is a good correlation between the ash content of coal and the main constituents of ash: Al, Si, and Fe, or a combination of two of these elements [7,8,10]. An analysis of correlation between the ash content and combined SiO_2 and Fe_2O_3 concentrations in Australian black coals showed that a standard deviation of 1.4 percent ash [10] can be obtained by measuring SiO_2 and Fe_2O_3 only. On this basis, the prompt neutron-gamma method can measure the ash content of Australian black coals satisfactorily.

A more detailed discussion of the prompt neutron-gamma technique for coal ash application was described in our earlier paper [11] where such aspects as choice of neutron source and choice of gamma-ray detector were analysed.

2.1 EQUIPMENT

The electronic equipment comprising of separate electronic modules (amplifier, gain stabiliser, multichannel analyser) used in previous work [12, 13], was replaced in the present work by a single unit (SIROMCA) [14]. SIROMCA was designed for those applications in which a full energy spectrum is required. SIROMCA is based on a successive approximation ADC which divides the energy spectrum into 480 channels. SIROMCA contains a dual memory bank, one of which is used as a buffer for the rapid transfer of data to the computer for computation and for subsequent output of spectral parameters and ash prediction, while the other is in readiness to receive data from the ADC. This permits rapid transfer of the complete spectra, ensuring minimum loss of strata information as the probe traverses the borehole. A schematic diagram of the borehole logging system is shown in Fig. 1 and a schematic diagram of SIROMCA is shown in Fig. 2.

The logging probe is modular so that the source-to-detector distance can be varied (15, 23, and 33 cm). The probe is fabricated from aluminium alloy and has an external diameter of 70 mm and a wall thickness of 3.2 mm. Two types of scintillation detectors were used for the measurements: a 38×76 mm NaI(Tl) detector and a 51×51 mm BGO detector. The energy resolutions at 662 keV were 7.0 percent for the NaI(Tl) detector and 13.7 percent for the BGO detector. Both detectors were shielded against thermal

Table I. Neutron capture data for major components of ash.

Element (atomic mass)	Cross- section σ (barn)*	Major gamma rays (MeV)	Gamma-ray intensity (I) per 100 neutron radiative captures
Aluminium (26.98)	0.23	7.72	27.4
		7.69	4.2
Silicon (28.09)	0.16	7.2	7.8
		6.38	12.4
		4.93	62.7
		3.54	68.0
Iron (55.85)	2.55	7.65	22.1
		7.63	27.2
Titanium (47.90)	6.1	6.76	24.2
		6.56	4.7
		6.42	30.1
		4.88	5.2
		1.38	69
Calcium (40.08)	0.43	6.42	38.9
		4.42	14.9
		1.94	72.5
Sulfur (32.06)	0.52	5.42	59.1
		4.87	11.5
		3.22	27.1
		2.93	22.3
		2.38	44.5
		0.84	75.5

* Thermal neutron capture.

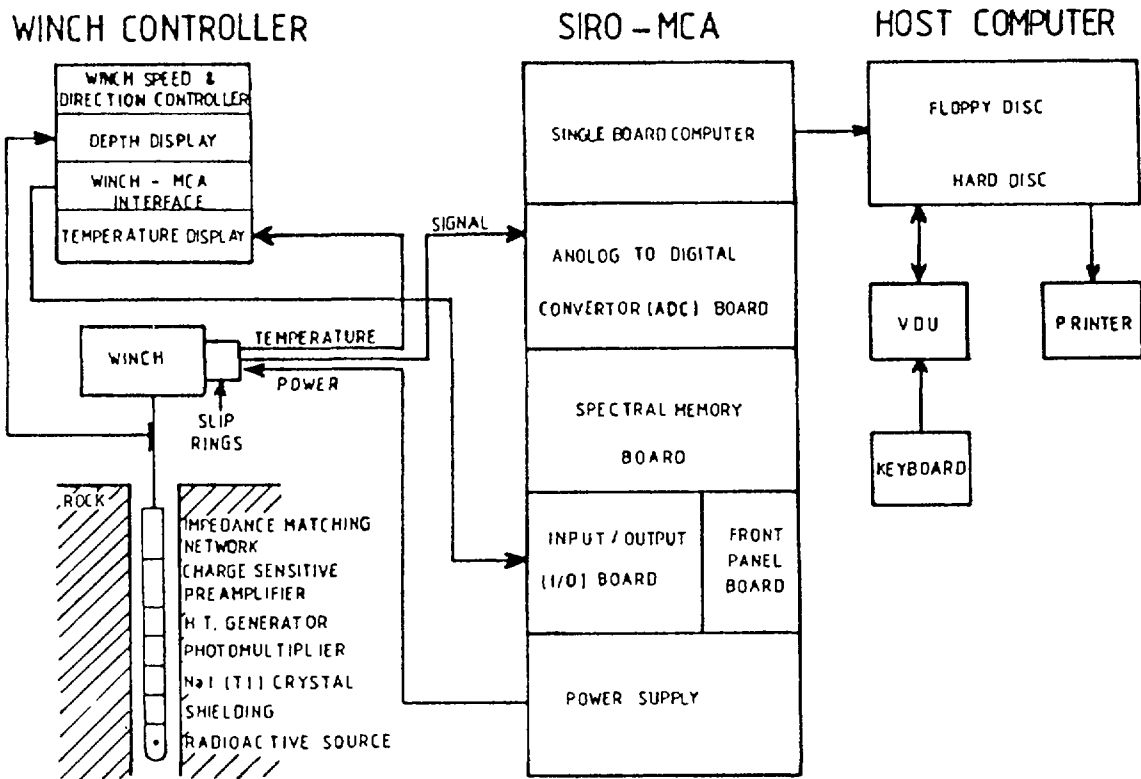


FIG. 1. Schematic of nuclear geophysical borehole logging system

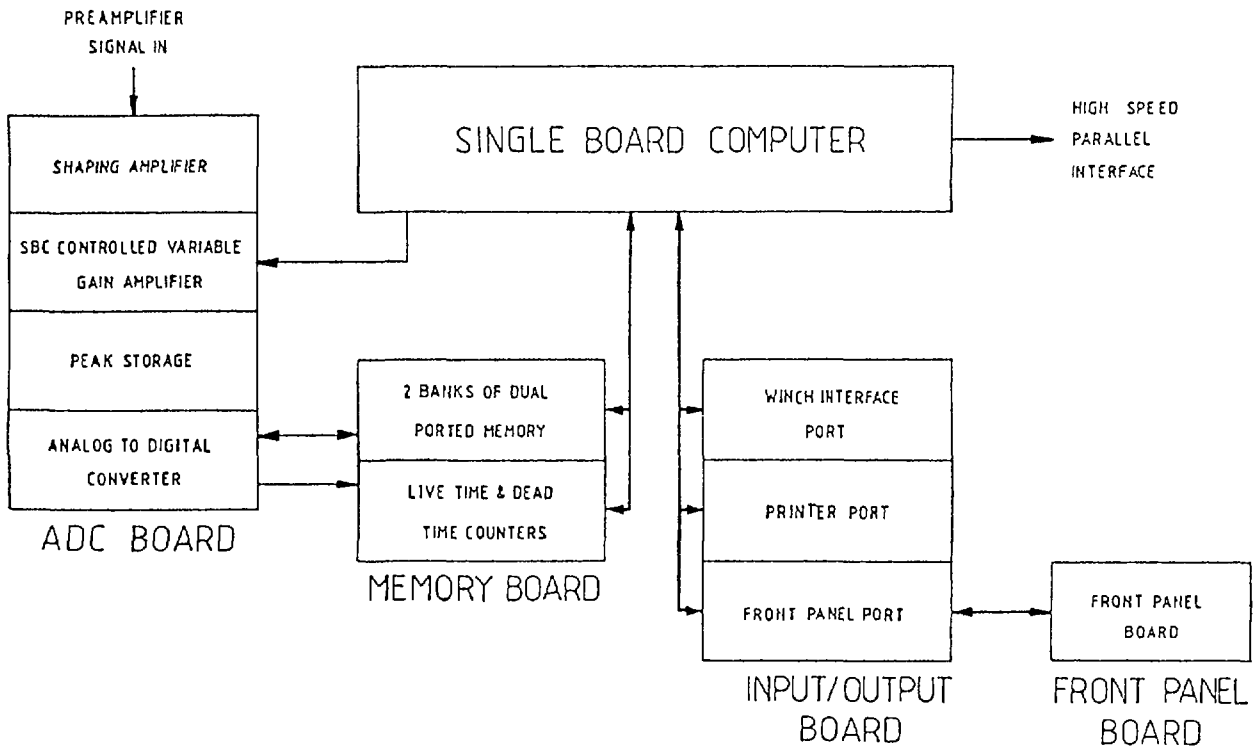


FIG. 2. SIROMCA block diagram

neutrons by a thin coating ($\approx 16 \text{ mg/cm}^2$) of 10-B. The intensity of the 478 keV gamma-ray peak due to neutron capture by 10-B provides a measure of the thermal neutron flux around the detector. The strength of the 252-Cf neutron source was 0.7 or 2.5 μg , depending upon the source-to-detector distance in the probe. The detector, located above the source, was shielded from the primary gamma radiation of the 252-Cf source by Bi and Pb. The logging probe was centralised by two flat, star-shaped centralisers made of flexible plastic (Lurethane), one located above the detector and the other located below the neutron source. The gain of the electronic equipment was automatically stabilised by using the 2.22 MeV capture gamma-ray peak of hydrogen. Gain stabilisation is especially important with the BGO detector because of its extreme sensitivity to temperature variations.

2.2 FIELD TESTS

The field tests of the neutron-gamma logging method were carried out in eight areas of eastern Australia in both cored and open boreholes. Three of these areas were in the Hunter Valley of New South Wales, two of the areas were in the Surat Basin of southern Queensland and the remaining three areas were in the Bowen Basin of central Queensland. The nominal diameter of the holes was 96 mm, but the real diameter, even in a given area, varied from 96 to about 175 mm.

Typical neutron-gamma spectra in a coal seam are shown in Fig. 3. The three gamma-ray spectra were collected when logging an $\approx 2 \text{ m}$ thick coal stratum at a logging speed of $\approx .008 \text{ m/s}$ with the same logging probe equipped with a $51 \times 51 \text{ mm}$ BGO detector. The peaks visible in the spectra are from boron (0.48 MeV), hydrogen (2.22 MeV), and silicon (3.54 and 4.93 MeV). The resolution of the BGO detector and the counting statistics are insufficient to observe clearly identifiable peaks corresponding to Fe, Al,

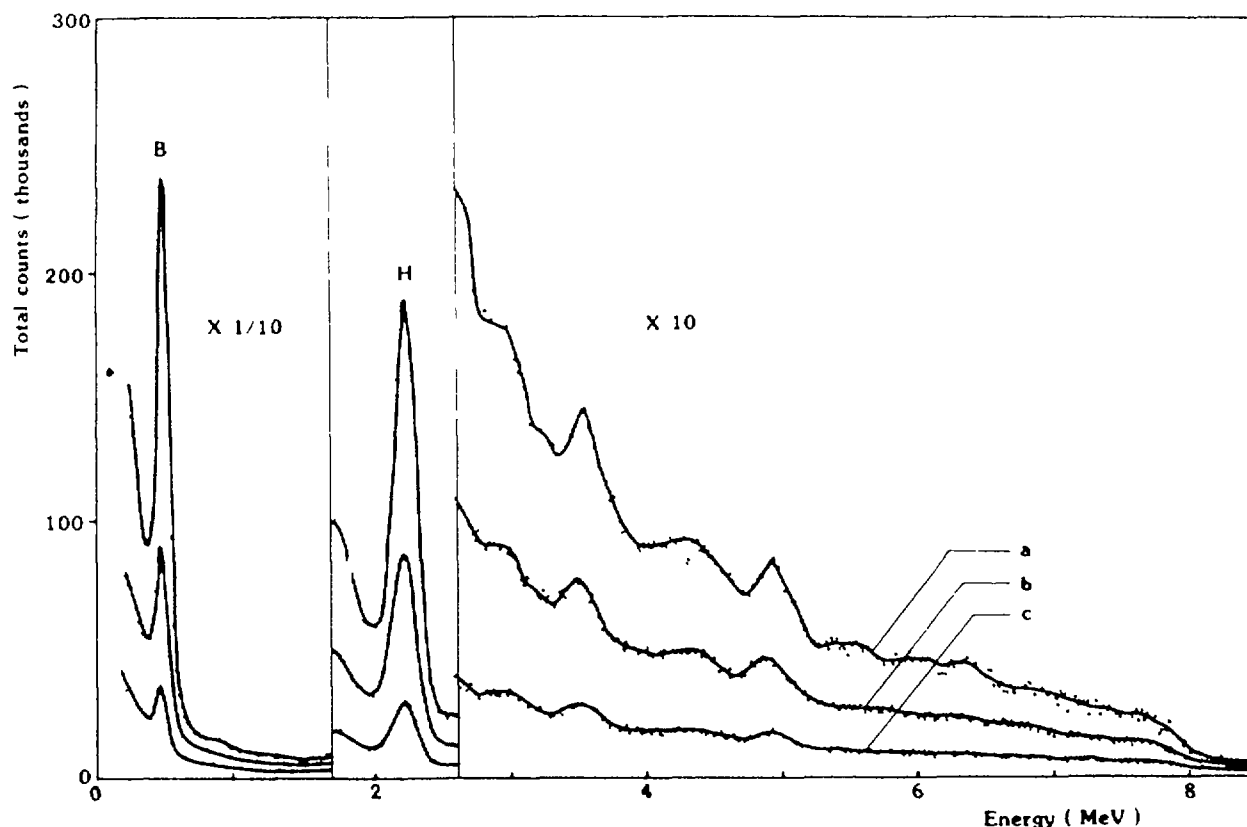


FIG. 3. Typical neutron-capture spectra recorded in coal for three source-detector separations: (a) 15 cm; (b) 23 cm; (c) 33 cm.

Ca, and Ti. Although individual concentrations cannot be measured, it is possible to set windows in the spectrum which correspond to combinations of these elements. These windows are indicated by horizontal lines in Fig. 4, which shows schematically the distribution of the major neutron capture gamma rays corresponding to the ash constituents (Al, Si, Fe, Ti, S and Ca), and also to H and B which are used to monitor the neutron flux. The heights of the vertical lines shown in Figure 4 are the products of the neutron capture cross-section and the relative intensities (photons/100 neutrons).

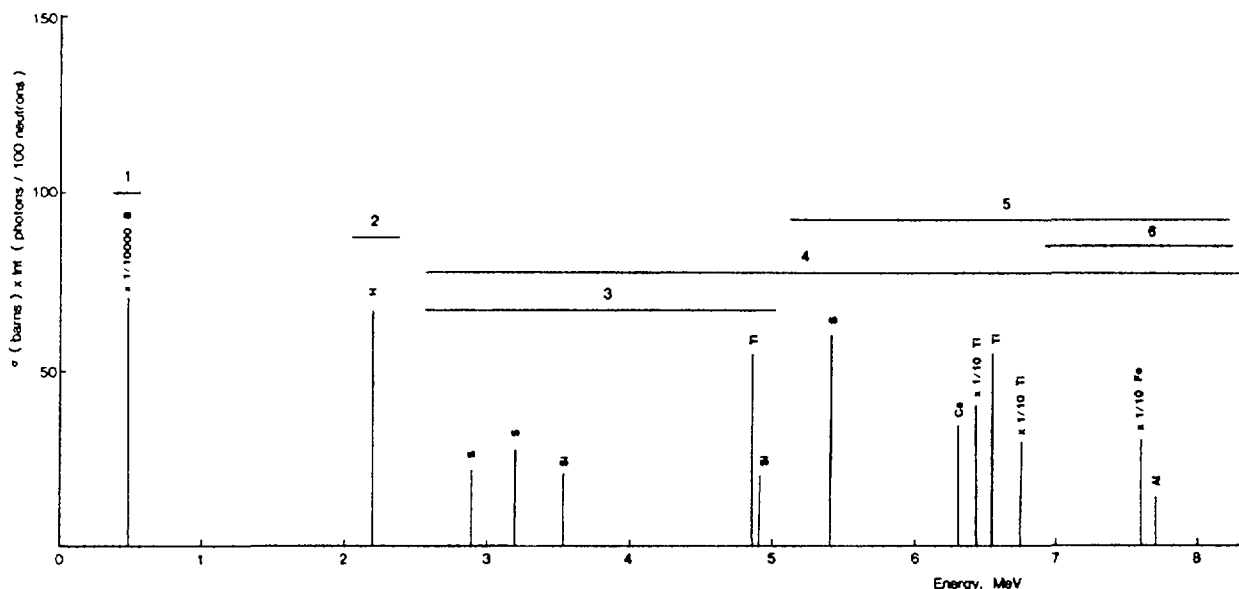


FIG. 4. The energy distribution and relative intensities of the neutron-capture gamma rays of B, H, and the common constituents of ash.

Measurement of ash in coal by the prompt neutron-gamma method entailed setting windows in the gamma-ray spectrum and fitting a linear regression model of the form:

$$\text{percent ash} = a_0 + a_1 X_1 + \dots + a_n X_n,$$

where a_0, a_1, \dots, a_n are constants and X_1, X_2, \dots, X_n are variables.

The variables were the gamma-ray count rates in various energy windows and also the spectral ratios between the count rates measured in the same selected windows.

The results and discussion of field tests, carried out in dry and water-filled boreholes, are presented separately because the space-energy distributions of the neutron flux differ markedly under these borehole conditions.

2.2.1 Logging in Water-Filled Boreholes

In planning the series of field trials for the prompt neutron-gamma technique, the first objective was to confirm that quantitative measurements of coal ash were feasible.

At the time of the first field trial, at deposit A in the Hunter Valley, the detector chosen for the prompt neutron-gamma probe was a premium grade 38×76 NaI(Tl) detector. For the calibration, 19 different

strata were used as observations for the regression analysis. The thickness of the strata varied from 50 cm (a single ply) to 260 cm (a stratum consisting of coal and stone bands). Values of ash content were obtained from chemical analysis of core samples. The rms deviation between the assays obtained from prompt neutron-gamma logging and the laboratory analyses was 2 percent ash, confirming that the technique was feasible.

The aim of the next two field trials was to investigate ways of improving the accuracy of measuring ash. At Deposits A and B in the Surat Basin, the NaI(Tl) detector previously used in the Hunter Valley was replaced by a 51 x 51 mm BGO detector. The greater efficiency of the detector is advantageous for measuring the gamma-ray lines above 3 MeV, which characterise the mineral constituents of the coal.

At Deposit A, the value of the rms deviation using 25 strata as observations was 1.4 percent ash. The precision of measurement, calculated from the results of duplicate logs in 23 strata, was 0.6 percent ash (1σ). Similar duplicate logs were carried out in other deposits where the method was tested, and values obtained for the precision of measurements were similar (0.5-0.8 percent ash) to those of Deposit A.

Two further modifications of the probe were considered: to apply shielding against slow neutrons on the outside of the probe, and to vary the source-detector separation. In the measurements described, the detector and the photomultiplier were shielded with a thin layer of 10-B. Measurements previously carried out in the laboratory using a water tank had shown that the background spectrum at high energies was reduced by about half when external neutron shielding was used on the probe. The intent of this external shielding was to reduce the flux of gamma rays excited by neutron reactions in the probe housing, the bismuth shield, and the various electronic components. The external coating of 10-B (15 mg/cm^2) was applied by painting the probe barrel with a mixture of 10-B and Araldite 488E epoxy resin (1:3 proportion). The shielding was mechanically strong and did not crack during logging operations.

The improved shielding arrangement was field tested at Deposit B in the Hunter Valley. Using the same configuration as in the Surat Basin, the value of the rms deviation obtained using external neutron shielding was 1.8% ash, whereas without this shielding it was 2.6% ash.

Having established that external neutron shielding gives the better rms deviation, further trials were undertaken using this probe with two other source-detector separations, 15 and 33 cm. The results from this field trial (Deposit B of the Hunter Valley) show that the best probe configuration consists of a BGO detector, a short source-detector spacing of 15 cm, and external thermal neutron shielding (10-B) for the barrel of the probe. Such a configuration gives both the best vertical resolution for seam delineation and the best accuracy of ash prediction.

The same configuration was used for subsequent trials in two coal formations in the Bowen Basin. In the first trial (Bowen A), data were collected in two deposits approximately 40 km apart in the German Creek formation. The data from these deposits were combined to provide sufficient observations for a regression analysis. In the second trial data were collected in two deposits in the Rangal formation (Bowen B). These deposits were also approximately 40 km apart.

Table II summarizes the results obtained in all of the field trials described. The values of rms deviation quoted are not solely dependent upon the inherent accuracy of the prompt neutron-gamma technique. They also include errors due to the initial sampling of the core material for chemical analysis, the chemical analysis itself, and geostatistical variations in the deposits. Sampling errors can be quite significant, and the fact that we had no control over sampling in this work may account for some of the large variation in the rms deviations obtained at the different deposits.

Table II. Summary of ash determination in various Australian black coal deposits by the neutron capture method. (water-filled boreholes)

Location	Number of observations	Range of ash (%)	Mean value and standard deviation of ash (%)	Scintillator	Source-to-detector distance (cm)	Strength of the 252-Cf neutron source (μg)	Number of variables in regression equation	rms deviation (%)
Hunter Valley A	19	15.9-47.5	30.8 \pm 10.4	NaI(Tl)	18	2.5	2	2.0
Surat A	25	7.0-24.8	12.4 \pm 3.8	BGO	23	2.5	3	1.4
Surat A and B	35	7.0-31.0	16.2 \pm 7.3	BGO	23	2.5	3	2.6
Hunter Valley B	27	7.7-50.3	26.8 \pm 12.6	BGO	23	2.5	1	2.6
Hunter Valley B	27	7.7-50.3	26.8 \pm 12.6	BGO*	23	2.5	1	1.8
Hunter Valley B	27	7.7-50.3	26.8 \pm 12.6	BGO*	33	2.5	3	2.3
Hunter Valley B	27	7.7-50.3	26.8 \pm 12.6	BGO*	15	0.7	1	1.8
Hunter Valley B	27	7.7-50.3	26.8 \pm 12.6	NaI(Tl)	19	2.5	1	2.5
Bowen Basin A	28	7-38.6	21.3 \pm 6	BGO*	15	0.7	3	1.7
Bowen Basin B	25	11.2-44.7	26.5 \pm 12.4	BGO*	15	0.7	2	2.8

* The outside of the logging probe was painted with 10-B in the area where the BGO detector was located in addition to the inner shielding.

2.2.2 Logging in Dry Boreholes

The neutron capture technique in dry boreholes was tested in two deposits, Bowen C and Hunter Valley C, of black coal located in Queensland and New South Wales respectively.

In Deposit Bowen C, the test was carried out with two source-to-detector distances: 23 cm and 15 cm. Nine dry-cored holes were logged with a source-to-detector distance of 23 cm and four boreholes were logged with a source-to-detector distance of 15 cm. Fig. 5 is a cross plot of the calibration data for the chemical assays and the neutron capture predictions of the 23 cm source-to-detector distance probe using a regression equation of the form:

$$\% \text{ ash} = -12.02 + 58.380 R \quad (1)$$

where R, the parameter derived from the capture spectrum, is the ratio between the number of gamma rays recorded in the energy windows 2.6-5.2 MeV and 2.0-2.4 MeV. Thus, the ratio R can be interpreted as a normalisation of the count rate in the 2.6-5.2 MeV energy window with respect to that of the 2.22 MeV hydrogen peak. This normalisation helps to correct for the perturbation of the neutron flux due to variations in the bulk density, hydrogen content and elemental composition of the coal, and the physical condition of the borehole. The rms deviation (between log and laboratory assays) for ash determination using the regression equation given above was 1.6% ash, where the ash content of the coal seams varied from 8 to 46% ash. A similar value of rms deviation (1.7% ash) was obtained using the probe with a 15 cm source-to-detector distance. The results confirmed that neutron capture is a useful technique for coal ash measurement and coal seam delineation in dry boreholes.

Six cored and five open boreholes were logged in the second Deposit (Hunter Valley C). Logging in this area was carried out with the 15 cm source-to-detector distance probe only. The probe was calibrated using 24 core assays from five of the six cored holes. The ash content in the seams used for calibration varied from 5 to 26% ash. The rms deviation value of

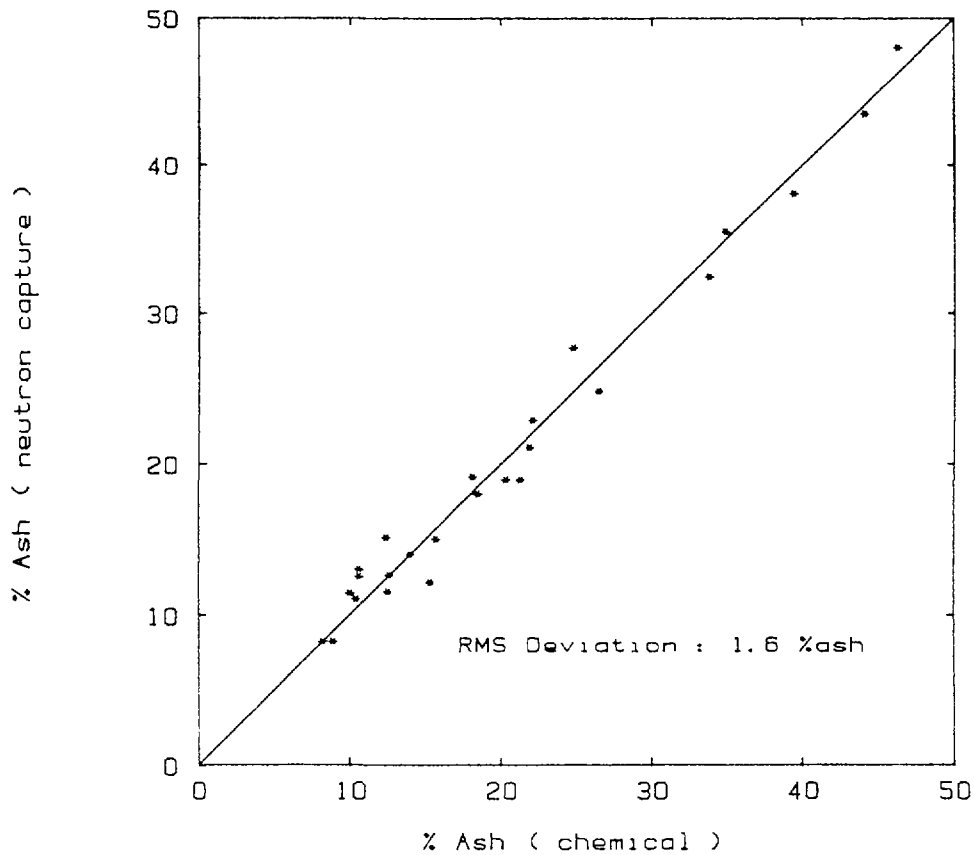


FIG. 5. Cross plot of the calibration data for Deposit Bowen C.

1.5% ash was very similar to that obtained in the Bowen C. Deposit. The calibration equation was later used to predict the ash content of the coal seams in both the cored and open boreholes. The calibration equation was

$$\% \text{ ash} = -18.96 + 74.499 R \quad (2)$$

where R is the same parameter as defined above.

In order to assess the validity of ash prediction by the neutron capture technique, we logged all the cored and open boreholes in this deposit with the spectrometric gamma-gamma probe. Samples for chemical analysis cannot be taken with adequate accuracy from open holes and therefore a comparison of these two logging techniques for ash prediction is extremely useful. The gamma-gamma probe was calibrated in the same cored holes and for the same chemically assayed coal seams, as were used for the calibration of the neutron-gamma method. The gamma-gamma logging was carried out with a centralised probe having a source-to-detector distance of 19 cm. The primary gamma-ray source was 37 MBq ¹³⁷Cs.

Fig. 6 shows the comparison of ash prediction between the neutron-gamma and gamma-gamma probes in both the cored and open dry boreholes. The coal seams used for the comparison were different from the seams used for the probe calibration. A similar comparison for water-filled sections of these holes is presented in Table III.

The rms deviation between ash predictions by the neutron-gamma and gamma-gamma techniques is 1.6% ash. Such a standard deviation, which is consistent with those for the neutron-gamma (1.5% and 1.7%) described above, indicates that the two techniques applied in dry boreholes have comparable performance for quantitative ash measurements.

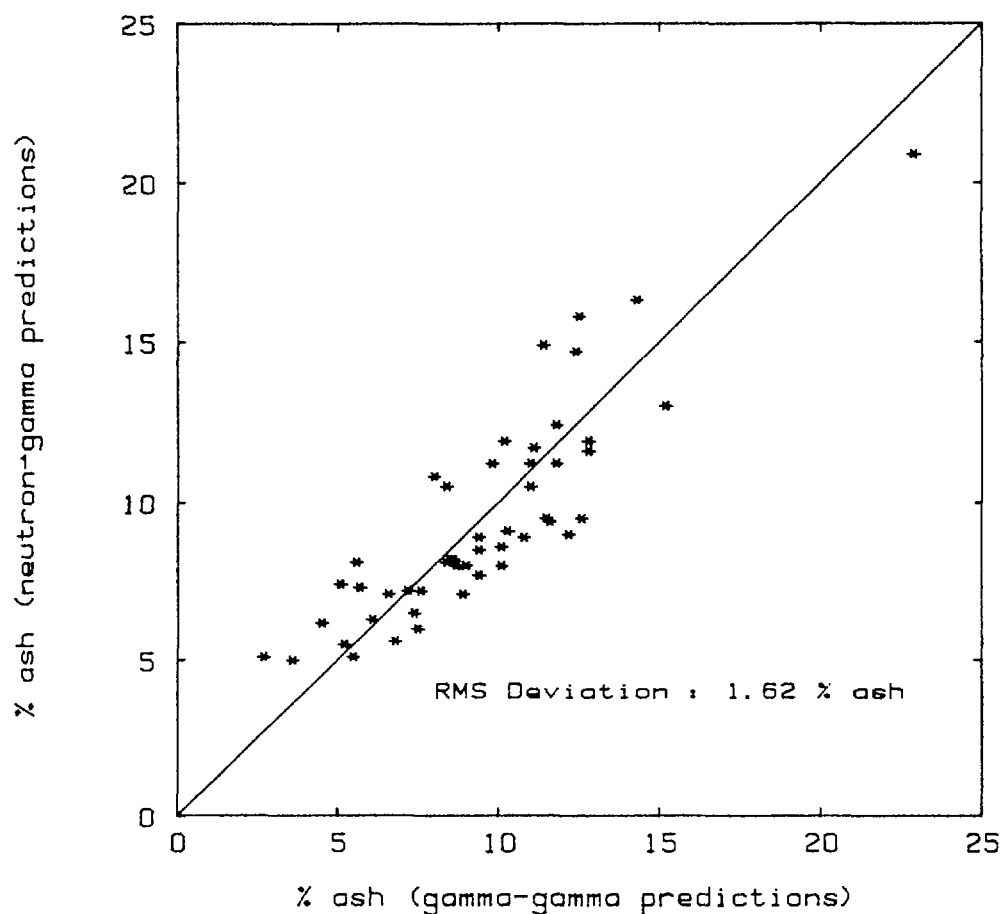


FIG. 6. Comparison of ash prediction between the neutron-gamma and spectrometric gamma-gamma probes (Deposit Hunter Valley C).

Twelve observations from cored holes were available for verification of the calibration equation (2). Unfortunately, the only samples which were available for the comparison, were in a narrow range of ash variation (5-13%). Nevertheless, the rms deviation value of 1.2% ash, that was obtained, proves the suitability of the neutron-gamma method for ash determination in dry boreholes.

The possibility of establishing a single calibration for both black coal deposits (Hunter Valley C and Bowen C), which were more than 1500 km apart, was examined. In dry boreholes, most of the thermalisation of neutrons takes place in the coal only, while in water-filled holes, variations in borehole diameter contribute to changes in the thermalised neutron flux. Variations in the thermal neutron flux in dry boreholes, therefore, are related to the properties of the coal, mainly its hydrogen content, which makes the method less dependent on borehole diameter than in water-filled boreholes. Fig. 7, which shows the ratio R as a function of ash content in the two deposits, indicates that these two deposits can be characterised by a single calibration equation. The rms deviation of 1.4% ash thus obtained compares favourably with the values of rms deviation obtained in each deposit taken separately. The limitations of such a universal calibration can only be established by testing in more deposits.

3. NEUTRON-GAMMA LOGGING FOR SALINITY DETERMINATION

One of the most serious problems confronting the world's socio-economic future is the degradation of its arable soils. In dry arable

Table III. Comparison of ash predictions from gamma-gamma and neutron-gamma logs and laboratory core assays.

Depth (m)	Gamma-gamma	Neutron-capture	Core assay
% ASH			
<u>Cored hole 1</u>			
83.95-90.45	7.9	7.2	7.1
91.05-92.05	18.8	19.6	18.9
<u>Cored hole 2</u>			
86.55-88.30	5.3	6.4	8.6
91.20-97.10	9.2	7.4	7.8
98.55-99.05	18.1	18.3	
<u>Cored hole 3</u>			
53.85-59.30	7.1	7.3	9.2
<u>Cored hole 4</u>			
67.40-69.35	3.7	6.5	6.6
70.70-77.45	7.1	7.8	8.4
<u>Cored hole 6</u>			
93.35- 95.30	6.2	8.0	8.8
96.20- 97.00	5.5	10.0	10.2
98.35-103.00	8.6	10.0	8.8
103.45-104.55	12.8	16.2	13.1
<u>Open hole 2</u>			
82.50-84.30	6.1	6.6	
85.20-86.05	6.9	8.3	
87.15-91.80	7.6	7.3	
94.80-95.50	11.6	9.3	
<u>Open hole 5</u>			
70.40-72.35	5.1	5.9	
73.75-80.00	9.0	8.3	

* All holes were water-filled.

lands, one of the most important factors in soil degradation is soil salination. This process afflicts much of Australia's hitherto productive land in two forms, dry and wet land salination. The salt problems were largely precipitated by the excessive removal of native trees, irrigation, poor water management and engineering design. In the irrigation areas of the Murray-Darling Basin, which is the main productive zone of south eastern Australia, the dry land salination effect alone currently costs \$40 million annually in lost production. But this degradation effect is advancing so rapidly that lost production values may increase by 60% within a decade. Costly wet land salination is also occurring in both this region and in south-western Australia.

It is in the control and prevention of further salination that bore-hole logging measurements of chlorine levels in water bores have a potentially useful role. They could assist understanding and mapping the transport of salt, both across land forms and through the strata. Non nuclear

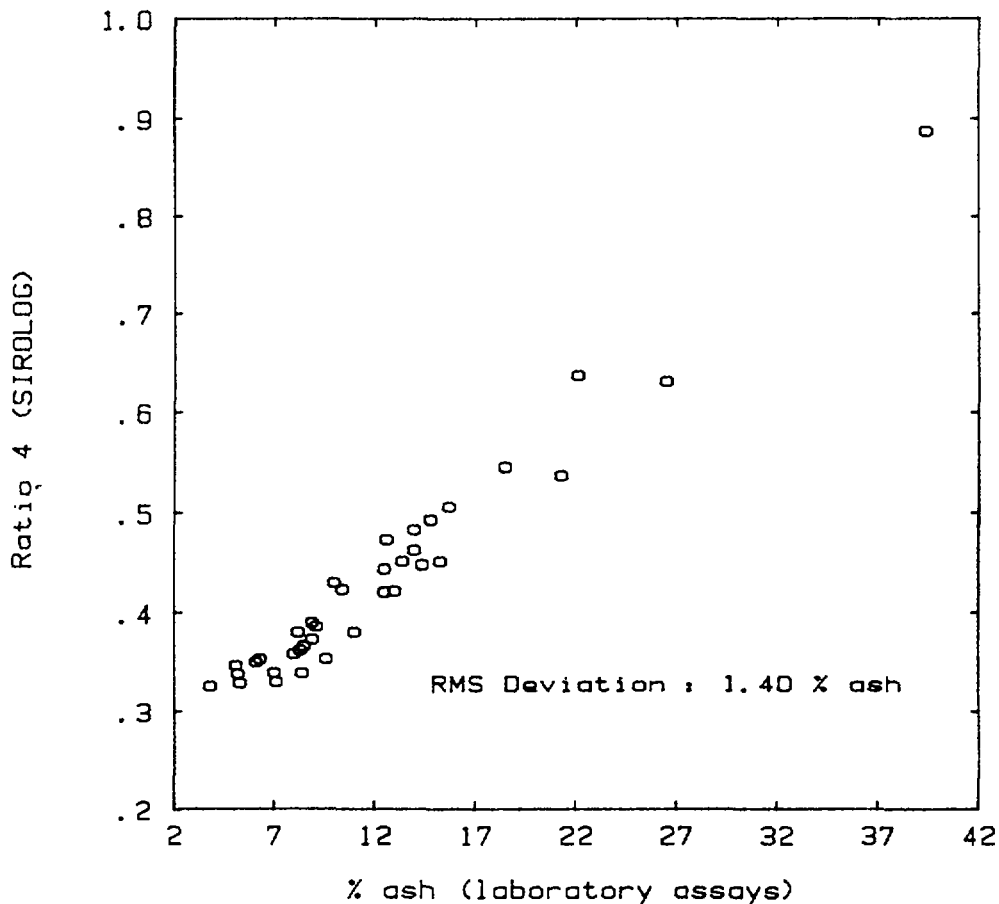


FIG. 7. Single parameter calibration (Ratio 4 vs % ash) for two deposits - Hunter Valley C and Bowen C.

techniques (e.g. resistivity and electromagnetic induction) are already used successfully in qualitative measurements for low and medium levels of chlorine content. However, the response of these instruments is virtually saturated for NaCl concentrations of more than 30,000 ppm. It is worth noting that in some dry lands, NaCl concentrations in the soil are known to approach 200,000 ppm. Also, the response of these instruments is neither linear with concentration, nor is it independent of lithology. It is on these grounds that we considered that research was warranted into the application of neutron-gamma logging for this problem.

Field measurements were carried out in the initial stages of the project, firstly, to determine the feasibility of the method in this application and, secondly, to identify the constraints affecting it. It should be noted that, at best, the available data on NaCl concentration-profiles in the water bores used was semiquantitative. In some cases the data were incomplete. Because these field measurements were only of an exploratory nature, they were followed up at the Port Melbourne Laboratory by definitive rig measurements carried out under controlled conditions.

3.1 CHLORINE LOGGING

Chlorine logging is a well established technique in the oil industry. This technique can, under appropriate circumstances, directly distinguish between oil and water saturation behind the casing, due to a significant difference in chlorine content between formation water and oil. For more than 20 years [15], chlorine logging has been based on pulsed neutron logging devices, which use several different gating systems.

The Neutron Lifetime Log - NLL [16] and Thermal Decay Time Log - TDT™ [17, 18] have been highly successful in differentiating high salinity formation waters from hydrocarbons behind casings on both a qualitative and a quantitative basis.

The pulsed neutron logging techniques, however, because of their hardware complexity and related costs, could not be proposed as the first choice for a method of salinity determination in the agricultural industry. The proposed technique would have to be relatively simple and requiring low cost instrumentation. This would entail the use of a radioisotopic neutron source. Chlorine logging based on the use of isotopic neutron sources (plutonium - beryllium) was also practised in the oil industry [19, 20], but it was applied semi-quantitatively.

3.2 FIELD TRIALS FOR CHLORINE LOGGING

Field tests were carried out in four different area of the state of Victoria (in south-eastern Australia) to determine firstly, whether quantitative chlorine logging in water bores was possible and secondly, how various factors in the analysis affect measurement sensitivity. These factors were casing type, range of NaCl concentration and probe configuration. The casings used in these investigations were tubes fabricated from ABS, iron and PVC. Samples of water from the boreholes, at various depths, ranged in concentration from 2000 to 150,000 ppm. However, most of the information received was both semi-quantitative, incomplete as regards the existence of submerged aquifers intersecting the water bores, and unreliable with respect to the depths of occurrence of the aquifers.

The present paper discusses measurement results from only two of the four areas - Lake Cullen and Girgarre. These areas were chosen for discussion because the available geological and chemical data were regarded as more reliable and complete than those from the other areas. In the Girgarre bore (referred to as Tatura 4370.5. in the figures and in subsequent discussion), the NaCl content of the water ranged from 2,000 to about 10,000 ppm, and generally increased with depth. The hole casing was ABS (polyethylene) and its depth was about 45 m. The Lake Cullen bore used an iron casing and was logged to a depth of about 220 m. The NaCl concentration of samples taken at four different levels in the bore ranged from 25,000 to 50,000 ppm. The internal diameters of the pipes were 127 mm for the ABS pipe and 102 mm for the iron pipe.

The results used in the following discussion were those obtained using only one configuration of the probe. This was a 38 × 76 mm BGO detector, a 5 µg 252-Cf neutron source and a source-detector separation of 150 mm. The detector was shielded with a coating of 10-B, that was opaque to thermal neutrons.

3.2.1 Results and Discussion

Figures 8 and 9 show the logs obtained for the iron cased Lake Cullen Bore. The first of the figures simply shows a chart output of the raw logging data averaged over each one-metre interval of borehole. The data shown are the count rate recorded in an energy window from 5.4 to 9.4 MeV. The second shows a parameter calculated from the same log, namely the ratio of the count rates in the 5.4 to 7.4 MeV window to that of the window encompassing the 0.478 MeV boron line used for monitoring the neutron flux at the detector. This ratio was chosen because it is less sensitive to variations in neutron flux than the raw count rate parameter. Possible causes for neutron flux variation are cavities behind the casing, variations of bulk density and variations in the content of hydrogen, chlorine and strong neutron absorbers. The increases in value of the ratio in

```

*****
#
# Date on file is 30-OCT-86
# Start time is 15:14:30
# End time is 18:28:57
# Operator is Je
# Client is dlrc
# Hole description lake cullenJ
# Record length is 950
# Number of records is 2130
# Lines per record is 400
# Data format is unformatted
# Technique is Bonton gamma
# Detector is 1.5x3 bgo
# Source is 50 ug Cf 1970
# Geometry is 10 cm spacing
#
*****

```

Data file - lclJ

Listing file - lllJ.lclJ.1

Plot information must be held in file /1970/11780

**** 3 point smooth ****

Var 1 : 270 - 470 Minimum : 2600.0 Maximum : 3600.0

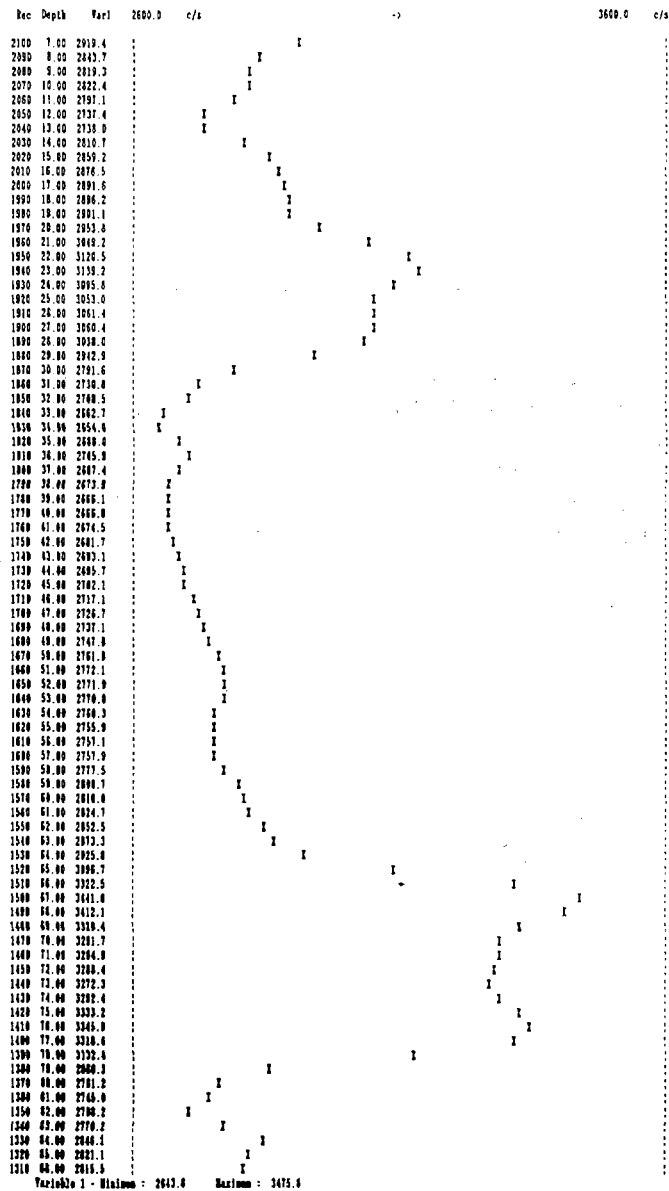


FIG. 8. Chart output of the salinity log (Lake Cullen).

SALINITY LOG - Hole Lake Cullen 3.1

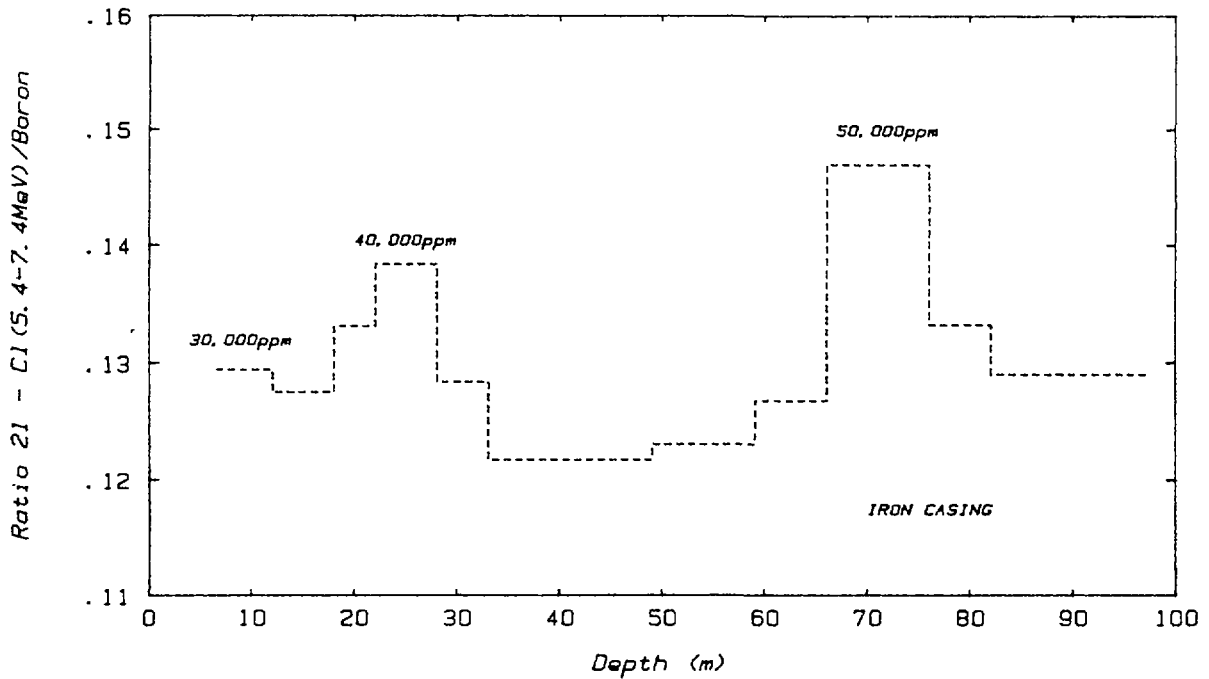


FIG. 9. Salinity parameter (Ratio 21) vs bore-depth.

Fig. 9 occurred where aquifers were located during the drilling, and these increases were commensurate with laboratory data obtained on NaCl concentrations in the water samples.

The variations with depth of a similar parameter are shown in Fig. 10 and 11 for the Tatura (4370.5) ABS lined hole. In this case, the parameter is the ratio of count rates in the 5.3-6.4 MeV region and the boron peak (net). The numerator is largely sensitive to Cl, although it also has iron and minor silicon components. Fig. 10 shows that the salinity level generally increased from top to bottom in the hole. Some decreases in the salinity level occurred where some aquifers were known to intersect the strata. The aquifers occurred in the strata from 5 to 9 metres (2,000 ppm) and from 17 to 23 metres (5,000 ppm). Laboratory assays for the NaCl concentration then progressively increased for water samples taken at increasing depths beyond the 26 metre depth level. Both Fig. 10 and 11 are consistent with the sample analyses carried out. Fig. 11 is important, because it shows the variation with depth of the ratio of count rates in the 5.3 to 6.4 MeV and 2.5 to 5.3 MeV windows. The denominator is sensitive to Si, but also contains spectral contributions from Cl and, to a lesser extent, Fe and Si.

The field measurements showed that salinity variations can be monitored in holes cased with iron and ABS material, but the measurement sensitivity is much greater for the latter type of casing.

3.3 LABORATORY MEASUREMENTS

The electronic equipment and the logging probe used for both the laboratory measurements and the field tests were described in an earlier section of this paper. For the laboratory salinity measurements, however, two sizes of BGO detector were used (38 x 76 mm and 51 x 51 mm), as well as a stronger 252-Cf neutron source ($\approx 5 \mu\text{g}$). Five 200 litre drums were used for the borehole-rig models of soil (rock) containing different amounts of NaCl. A sealed ABS pipe of 140 mm internal diameter was located at the

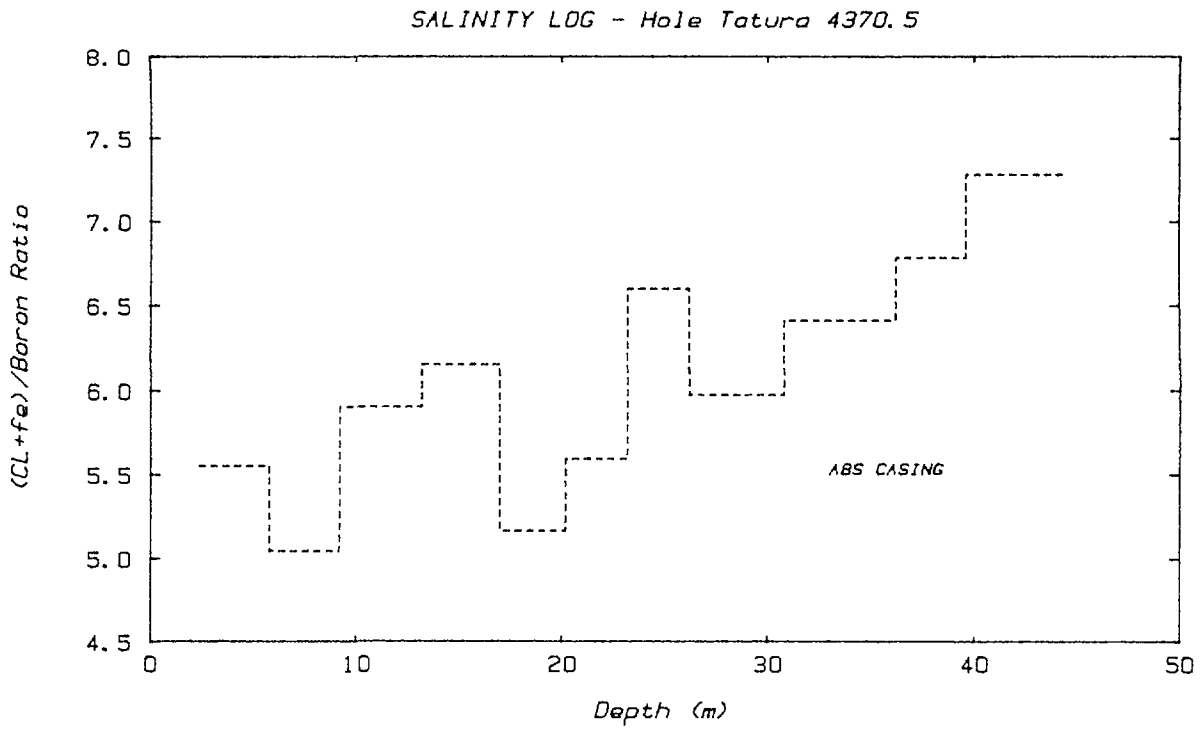


FIG. 10. Normalised chlorine sensitive parameter vs bore-depth.

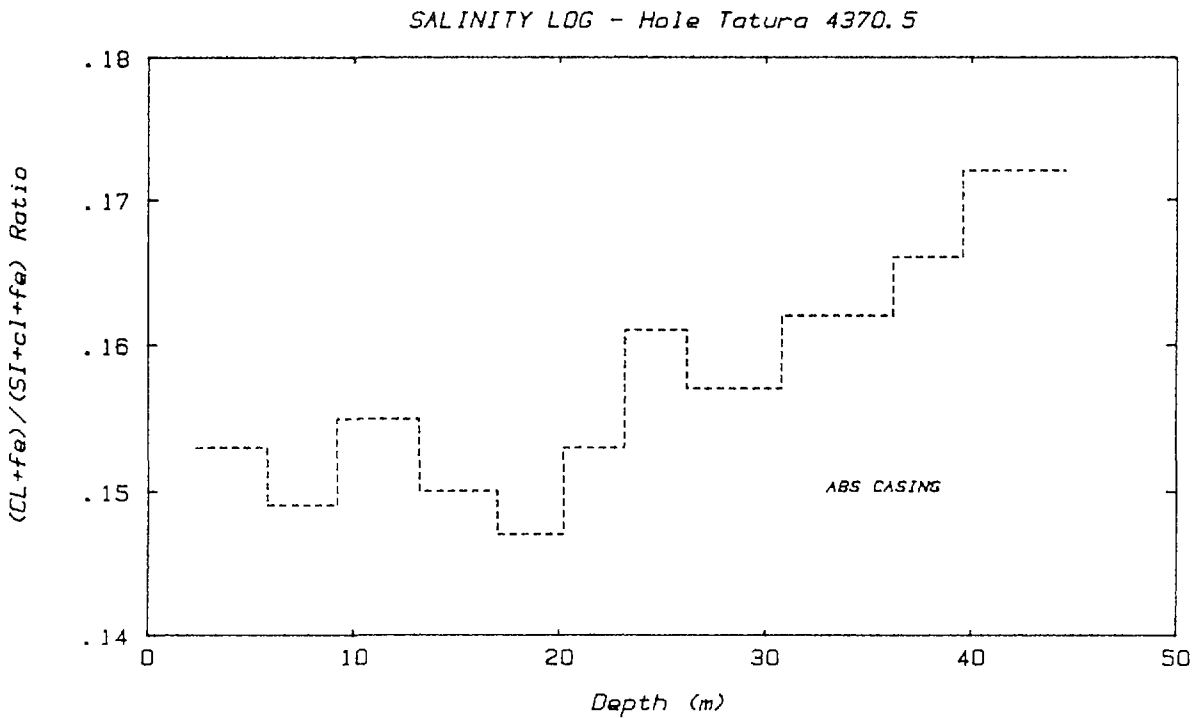


FIG. 11. Ratio of chlorine sensitive and silicon sensitive parameters vs bore-depth.

centre of each drum. Later, the drums were filled with a clean sand. The porosity was roughly the same for all five models and equal to 30%. One model was saturated with fresh water, and the remaining four models were also saturated with aqueous NaCl solutions with concentrations of 5,000, 15,000, 30,000 and 50,000 ppm. While the 200 litre drum did not represent an infinite medium for neutron transport, their volume was regarded as a satisfactory approximation.

In addition to the ABS pipe, three lengths of PVC pipe and two lengths of iron pipe were used. The thicknesses of the pipes selected were those which are most common in bore casings. The external diameter of these pipes was selected so that they would fit neatly inside the ABS pipes permanently installed in each model. ABS was selected for the host pipe because it would contribute negligibly to the spectral energy windows used for chlorine determination. By sealing the ABS pipes at one end, it was possible to have the borehole fluid with a different salinity content to that of the surrounding matrix, which is common on the land.

3.3.1 Results and Discussion

All results discussed here are for the case of a borehole filled with fresh water. This is less favourable for salinity measurements than where the borehole fluid salinity level is the same as in the surrounding soils or rocks.

Fig. 12 shows the high energy region of three neutron-gamma spectra recorded with a 38 × 76 mm BGO detector for 600s (live). These spectra were obtained for each casing material using unsalinated water for both the borehole fluid and the saturated sand matrix. Consequently, they are the background spectra for the casing materials used.

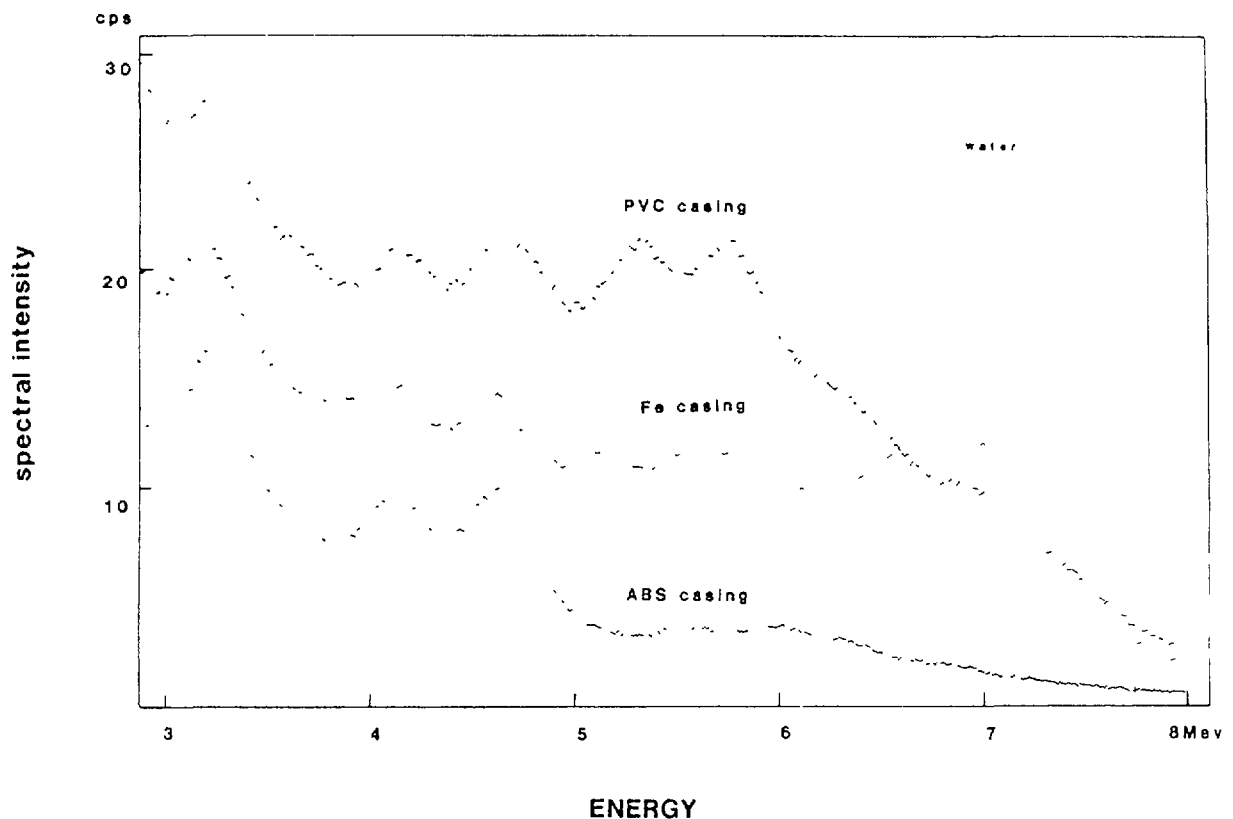


FIG. 12. Neutron-gamma spectra recorded in laboratory measurements for various casing materials.

Fig. 12 shows that the PVC and Fe casings contribute significantly to the background spectrum, particularly in the region from 5 to 9 MeV. These contributions are due to the chlorine and iron capture gamma-ray lines emitted from the PVC and iron casings respectively. The existence of a significant background in this energy range reduces the effectiveness of the neutron-gamma method for salinity determination. Consequently, this technique would have inferior sensitivity for salinity measurements in bores lined with either PVC or Fe casing.

Figs. 13, 14 and 15 indicate, as expected, much smaller signal to background ratios for chlorine detection with PVC and Fe casings than with the ABS casing. Fig. 16 shows the variation of a spectral ratio selected for its suitability in salinity determinations, with chlorine concentration, for different types of casing materials. The drum-models of 90 cm height were arranged in increasing order of NaCl concentration.

Consequently, increasing depth shown for the X-axis of the figure is consistent with increasing NaCl concentration in the sample. The ratios were normalised to that obtained for unsalinated water. These measurements were made with a 51×51 mm BGO detector and a source-to-detector distance of 15 cm. The advantage of using ABS casing is obvious. Nevertheless, even those bores cased with Fe and PVC still provide scope for quantitative salinity determination.

There is also another way of increasing the sensitivity of neutron-gamma logging for quantitative salinity measurements, namely that of increasing the source-detector separation. Figure 17 shows how the sensitivity changes when the source-to-detector distance is increased from 15 to 33 cm. However, the measured count rate in the energy window selected (5.4-6.3 MeV) decreases by almost an order of magnitude when the probe separation is increased in this way. This decreased count rate would have to be compensated either by using a stronger ^{252}Cf source, or by decreasing the logging speed.

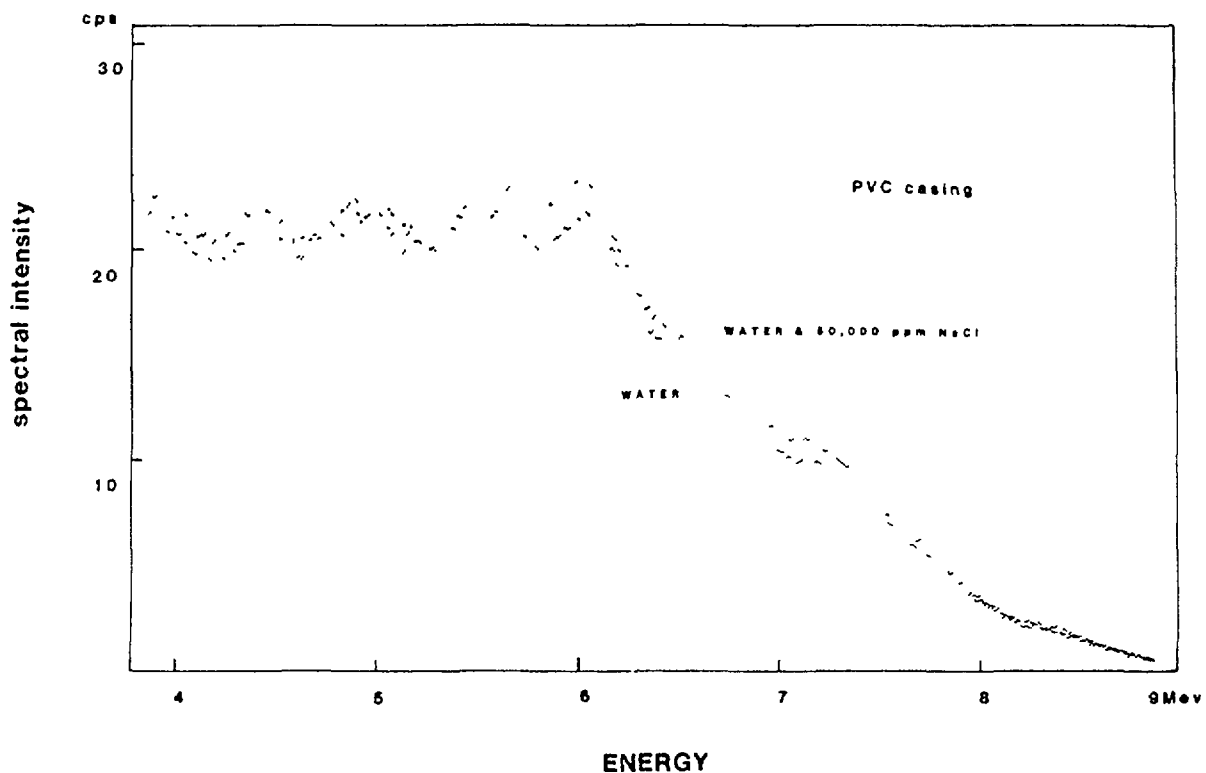


FIG. 13. Neutron-gamma spectra from two models of different salinity - PVC casing.

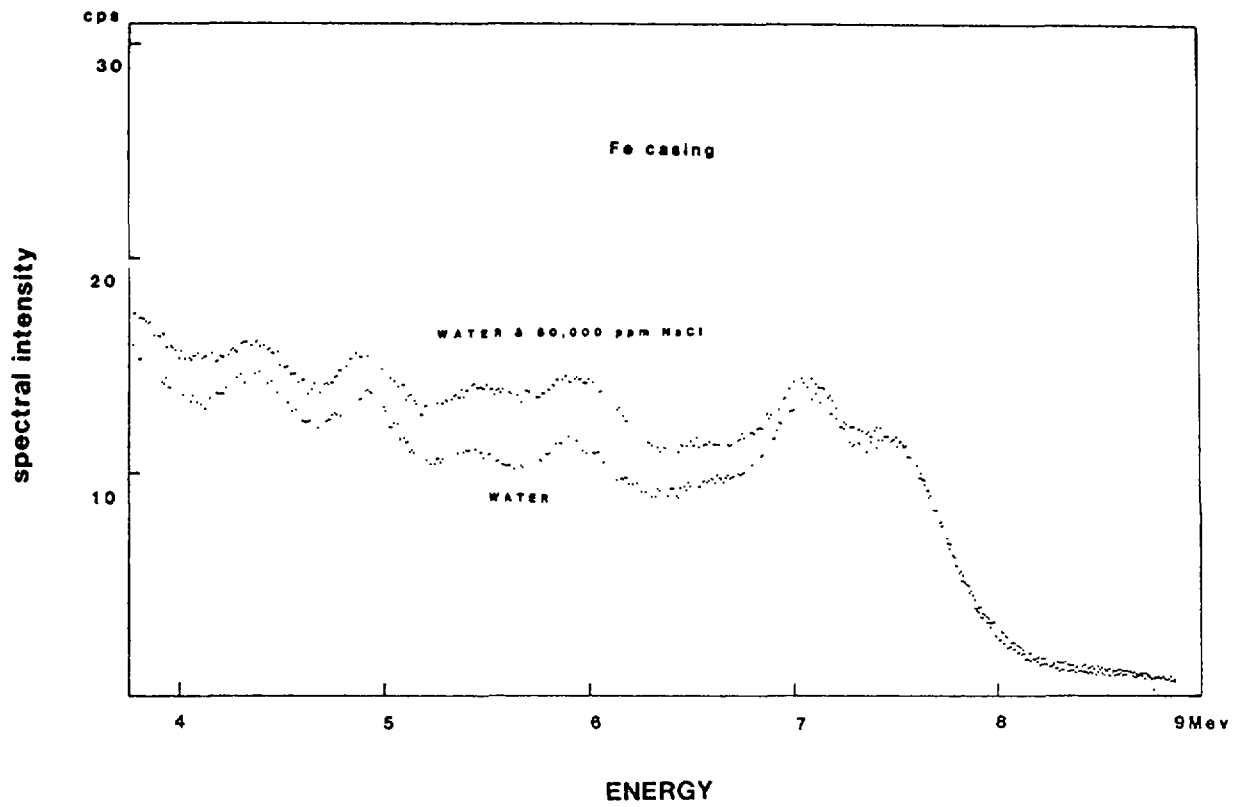


FIG. 14. Neutron-gamma spectra from two models of different salinity - Fe casing.

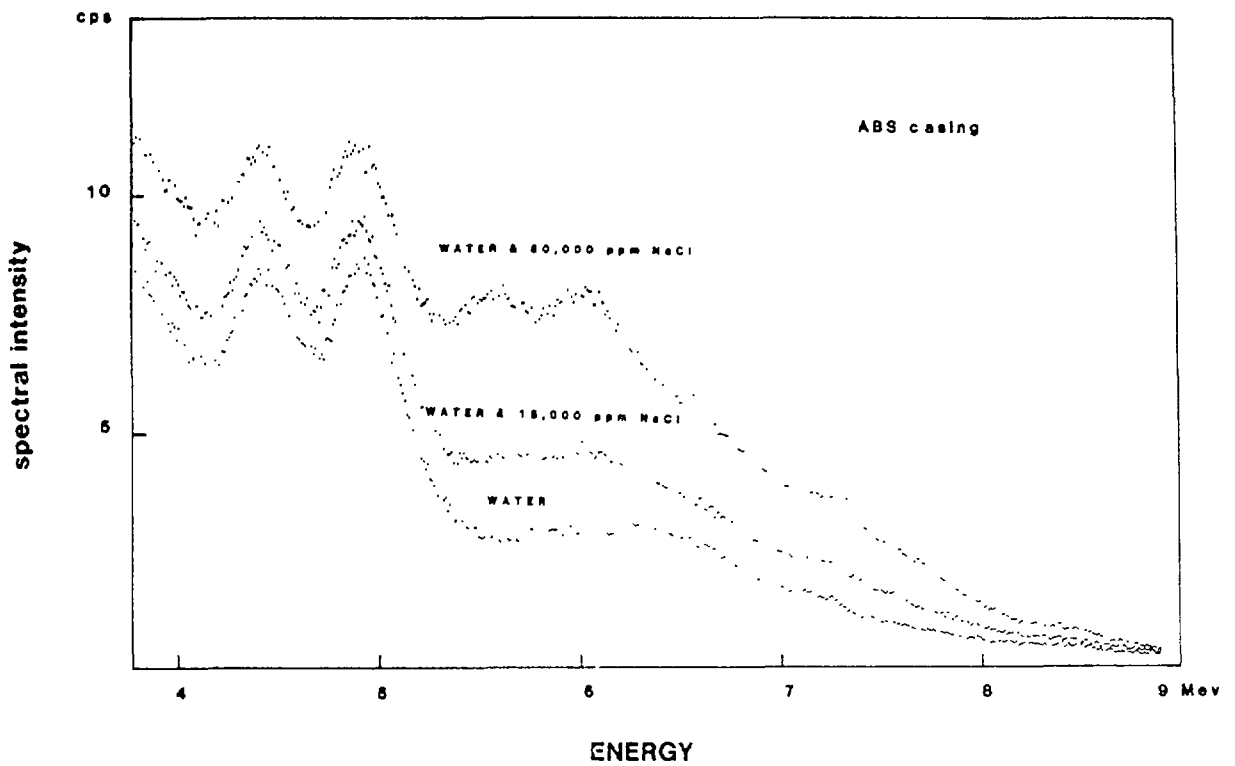


FIG. 15. Neutron-gamma spectra from three models of different salinity - ABS casing.

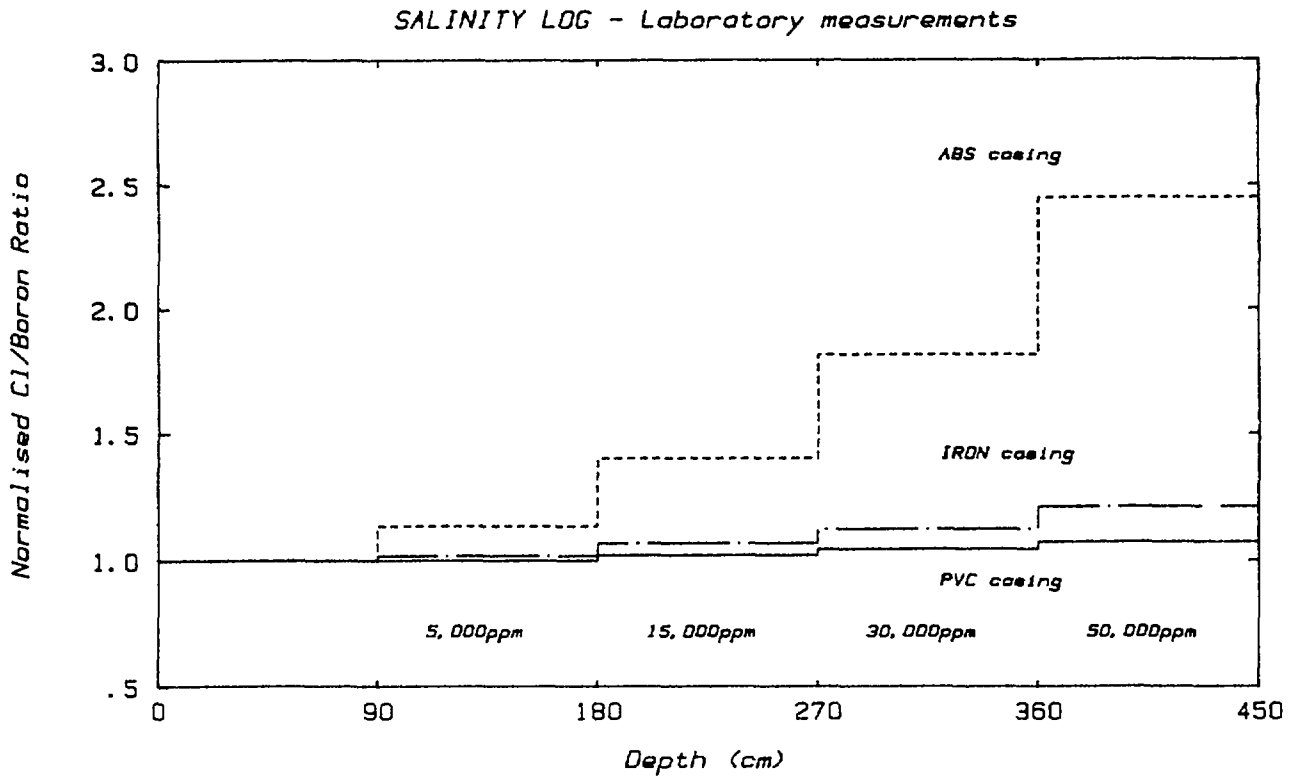


FIG. 16. Normalised chlorine sensitive parameter against NaCl content for three most common casing materials.

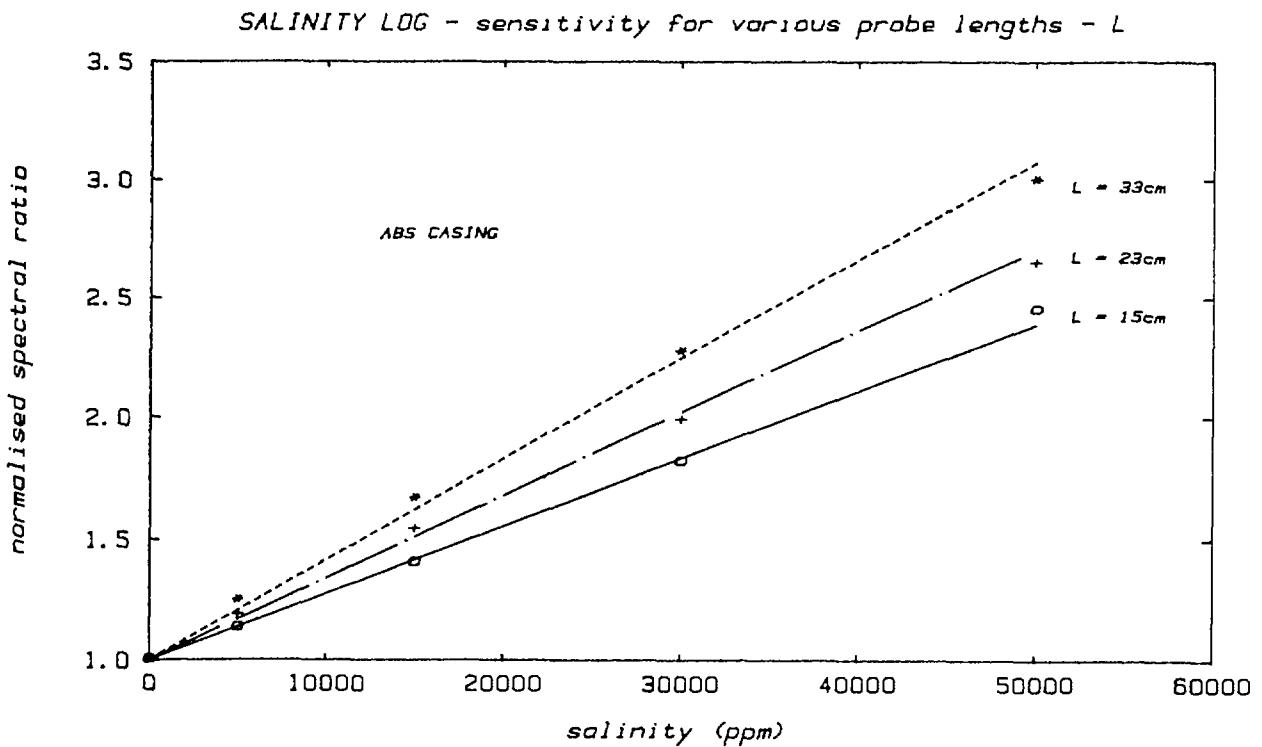


FIG. 17. Salinity measurement sensitivity for three source-detector separations.

The above figures reveal certain information which is relevant in successfully applying the neutron-capture method to salinity measurement. Firstly, the ABS casing should be used whenever possible. Secondly, the increase in sensitivity with source-detector separation requires a longer probe than the one used in the preliminary field trials, particularly when the casing material is iron or PVC.

4. CONCLUSIONS

The research into quantitative application of the spectrometric neutron-gamma method demonstrated its capability for accurate coal ash determination and also a potential for salinity measurements in water bores which are relevant to the agricultural industry.

The field tests for coal applications, were carried out in eight different deposits. They demonstrated that the prompt neutron-gamma method is a viable technique for the quantitative determination of ash in coal strata. From the results of the field trials, the probe configuration giving the best vertical resolution and the smallest rms deviation for ash determination was selected. This probe consists of a BGO detector, a short source-detector separation of 15 cm and thermal neutron shielding (10-B) applied to the exterior of the probe barrel.

The prompt neutron-gamma technique was successfully tested in both water-filled and dry boreholes. With the exception of one set of measurements, carried out in the Bowen Basin C Deposit, values of rms deviation better than 2% ash were achieved using the best probe configuration.

The logging system described is now commercially available and forms part of the SIROLOG technology developed by CSIRO.

The laboratory tests, supported by the preliminary field trials, indicated that the neutron-gamma logging technique based on the use of a BGO detector in a probe of short source to detector separation, is capable of measuring changes in NaCl content above 2,000 ppm in bores lined with polyethylene (ABS) casing. The sensitivity for this type of measurement is inferior in holes cased with iron. But in this application, logging is usefully sensitive, where NaCl contents vary in the range 20,000 to 50,000 ppm. The measurement is even less sensitive in PVC lined holes, but has potential for very saline conditions.

REFERENCES

- [1] LAVERS, B.A., SMITS, L.J.M., "Recent developments in coal petrophysics", Proc. SPWLA 17th Annual Logging Symposium (1976).
- [2] BROM, R.W.C. and DRIEDONKS, F., "Applications of petrophysical logging in the evaluation of coal deposits", the 22nd Annual Logging Symposium of SPWLA, 1981, Frans. Soc. Prof. Well Log Anal., (1981) paper KK.
- [3] AGOSTINI, A., Bull. Aust.Soc.Explor.Geophys.8 (1977) 26.
- [4] DANIELS, J.J. Scott, J.H., LIU, J., "Estimation of coal quality parameters from geophysical well logs", Proc. SPWLA 24th Annual Logging Logging Symposium (1983).

- [5] NARGOLWALLA, S.S., KUNG, A., LEGRADY, O.J., STREVER, J., CSILLAG, A., SEIGEL, H.O., "Nuclear Metalog grade logging in mineral deposits", Nuclear Techniques and Mineral Resources 1977 (Proc. Symp. Vienna, 1977), IAEA, Vienna (1977) 229.
- [6] SENFTLE, F.E., Min. Eng. (AIME) 30 6 (1978) 666.
- [7] MIKESELL, J.L., DOTSON, D.W., SENFTLE, F.E., Nucl. Instrum. Methods 215 (1983) 561.
- [8] CLAYTON, C.G., WORMALD, M.R., "Coal analysis by nuclear methods", Nuclear Geophysics - Selected Papers on Applications of Nuclear Techniques in Mineral Exploration, Mining and Process Control, Pergamon Press, Oxford (1983) 3.
- [9] WORMALD, M.R., CLAYTON, C.G., "In-situ analysis of coal by measurement of neutron-induced prompt γ -rays", *ibid.*, 71.
- [10] EISLER, P.L., BORSARU, M., YOUL, S.F., CHARBUCINSKI, J., Quantitative spectrometric borehole techniques for coal mining, Int. J. Nucl. Geophysics (1987), to be published.
- [11] CHARBUCINSKI, J., BORSARU, M., EISLER, P.L., YOUL, S.F., Geophysics, Vol 51, 5 (1986) 1110-1118.
- [12] BORSARU, M., CHARBUCINSKI, J., EISLER, P.L., YOUL, S.F. Geoprospection, 23 (1985) 503-518.
- [13] CHARBUCINSKI, J., BORSARU, M., EISLER, P.L., YOUL, S.F. "In situ borehole determination of ash content of coal using gamma-gamma and neutron-gamma techniques", (Proc. of an Advisory Group Meeting on Gamma, X-Ray and Neutron Techniques for the Coal Industry, IAEA, Vienna 1984) IAEA, Vienna (1986) 43-66.
- [14] WADDINGTON, P.J., HUPPERT, P., CERAVOLO, C., PHILLIPS, P.L. - to be published.
- [15] YOUMANS, A.H., HOPKINSON, C., BERGEN, R.A., OSKRY, H.L., J. Pet. Tech., 3, (1964) 319-328.
- [16] SERPAS, G.J., WICKMANN, P.A., FERTL, W.H., DEVRIES, M.R., RANDALL, R.R., "The dual detector neutron lifetime log - theory and practical applications", (Trans SPWLA 18th Annual Logging Symp, Houston, 1977), SPWLA, Houston (1977) paper CC.
- [17] WAHL, J.S., NELLIGAN, W.B., FRENTROP, A.H., JOHNSTONE, C.W., SCHWARTS, R.J., J. Pet. Tech., 9 (1970) 365-379.
- [18] HALL, J.E., JOHNSTONE, C.W., BALDWIN, J.L., JACOBSON, L.A., J. Pet. Tech., 1 (1982) 199-207.
- [19] STROUD, S.G., SCHALLER, H.E., J. Pet. Tech., 2 (1960) 37.
- [20] DEWAN, J.T., STONE, O.L., MORRIS, R.L., J. Pet. Tech., 6 (1961) 531-537.

ELEMENTAL CONCENTRATIONS FROM GAMMA RAY SPECTROSCOPY LOGS

J.S. SCHWEITZER, D.V. ELLIS, J.A. GRAU
Schlumberger-Doll Research,
Ridgefield, Connecticut

R.C. HERTZOG
Schlumberger Well Services,
Houston, Texas

United States of America

Abstract

A set of gamma-ray spectrometers have been combined in a single tool string to routinely obtain elemental concentrations for ten formation elements in a single logging run. The key to obtaining the elemental concentrations for the set of significant elements is a new technique for combining logging measurements using different types of nuclear reactions through a model based on both nuclear physics and geochemistry. The model has been validated by comparisons between logging and core analysis results for numerous wells.

1. Introduction

It has long been recognized that accurately determining elemental concentrations through logging measurements provides important data for evaluating oil, gas, and mineral reserves and for obtaining better insight into geological processes. Until recently, the problem of relating gamma-ray intensities to elemental concentrations has been extremely difficult and generally successful for only a few types of restricted environments. A recent development has been the construction of an analysis procedure that combines gamma-ray intensities obtained from natural activity, prompt thermal neutron capture reactions, and delayed activity to obtain elemental concentrations for ten elements that are significant for describing geological strata. This procedure is embodied in a model that combines both nuclear physics and geochemistry to describe the relationship between elemental concentrations in clastic sediments and all major unmeasured elements, to allow the proper normalization to be obtained for elemental measurements that cannot be calibrated in elemental concentrations. This technique can be implemented with a recently developed set of gamma-ray spectrometers¹ that can obtain all the elemental measurements in a single logging run, thus overcoming the problems associated with changing hole conditions when data are accumulated in separate logging runs.

The Geochemical Logging Tool (GLT[†]) includes measurements of natural activity for determining Th, U, and K concentrations, delayed activation measurements for determining Al concentrations, and measurements of prompt gamma rays following thermal neutron capture for determining Si, Ca, Fe, S, Gd, and Ti concentrations. The details of the spectrometers used to measure the gamma-ray spectra have been presented previously.¹ The conversion of gamma-ray intensities to elemental concentrations is obtained in one of two ways: through direct calibration, for Th, U, K, and Al, and through the geochemically-based closure model for the elements measured by prompt thermal neutron capture gamma rays. Recent research in geochemically derived properties from elemental concentrations in sedimentary environments²⁻⁶ provides quantitative analyses of rock properties that could be previously achieved only through detailed analyses on core samples. While the model was derived for the minerals contained in sedimentary environments, a recent application of this approach to crystalline rock⁷ also yielded excellent results for the elemental concentrations.

We first review the details of the closure model to understand the limitations on the accuracy of derived elemental concentrations imposed by the possible mineralogical variation in the rock. Then the results for the elemental concentrations determined from the spectroscopic measurements are presented and compared with some examples of elemental concentrations measured in core samples.

2. Geochemical Closure Model

Certain types of spectroscopic measurements in rock formations can be calibrated directly in weight percent of the measured element. The measurement of natural activity, which does not require a neutron source, is easiest to calibrate.⁸ When a neutron source is used, determining the neutron flux distribution in the rock is very difficult. However, if the neutron source is of known intensity, as is the case for measurements of delayed activity from thermal neutron capture reactions with a ²⁵²Cf source,¹ certain measurable or calculable parameters (neutron slowing-down length, L_s ; formation and borehole thermal neutron macroscopic cross sections, Σ_f and Σ_b ; and borehole size) can be used directly to transform the detected gamma-ray intensities into elemental concentrations. The analysis of prompt gamma rays following neutron capture has so far eluded a direct calibration in terms of elemental concentrations, especially when an inherently unstable accelerator source of 14-MeV neutrons is used. For these measurements a model is needed to convert the observed capture gamma-ray flux attributable to a particular element into a concentration for that element. Previous attempts⁹ at such an approach have had success in limited applications, such as the measurement of elemental concentrations in coal seams where all significant elements, except for oxygen, could be measured through thermal neutron

[†] Mark of Schlumberger

capture gamma-rays. Attempts to relate elements measured through different types of reactions¹⁰ have likewise been successful under only very limited mineralogical conditions. The model we use has met with significant success in clastic sediments.¹¹ The model is a combination of oxide and carbonate representations that relates the concentrations of measured elements to the concentrations of unmeasured elements and includes elements measured by natural radioactivity, thermal neutron capture, and thermal neutron-induced delayed activity. One key to the improved results comes from considering only elements that are contained in the rock matrix, excluding those that might be present in the pore fluid or in the borehole fluid.

The model is a simple closure relation and can be expressed mathematically as:

$$F \left\{ \sum_i X_i \frac{Y_i}{S_i} \right\} + X_K W_K + X_{Al} W_{Al} = 1 \quad (1)$$

where:

- F is the calibration factor to be determined at each depth from this equation,
- Y_i is the fraction of the measured prompt gamma rays that are attributed to element i ,
- S_i is the relative weight-fraction detection sensitivity for element i ,
- X_i is the ratio of the weight of the associated oxide or carbonate to the weight of element i ,
- W_{Al} is the weight fraction of aluminum determined from the activation measurement, and
- W_K is the weight fraction of potassium determined from natural activity.

The sensitivities, S_i , are measured in the laboratory and contain most of the nuclear physics involved in the relationship between the gamma-ray yields, Y_i , and the respective elemental concentrations. The yields, Y_i , are determined^{1,12} from a least-squares fit of the measured spectra with elemental standard spectra. Thus, if we are indeed measuring the elements needed to describe 100% of the rock minerals, then the only unknown, F , can be determined trivially from the above equation. The terms $F Y_i / S_i$ are then the weight percent of the elements determined through prompt gamma-ray, neutron capture measurements.

There are two components of the model which must be ascertained in each geological environment. Do the elements measured, together with their associated carbon and oxygen,

describe all the rock minerals? Are the assumed relationships between the measured elements and the unmeasured carbon and oxygen valid? Typical values of the oxide factors, X_i , associated with measured elements are shown in Table 1. In certain cases, such as for silicon, the X_i value of 2.139 is just the mass of S_iO_2 divided by the mass of S_i . In other cases, such as for Fe, the chosen value of 2.075 is significantly different from the 1.430 value that would be appropriate for Fe_2O_3 . This is due to the presumed association of bound water, in the form of hydroxyls, with the occurrence of Fe in the form of Fe_2O_3 . Fortunately, if Fe occurs as $FeCO_3$, which has no hydroxyls, the value of 2.075 is still appropriate. Thus, if the presence of minerals other than those of the model used in

Table I. Optimized oxide factors to be used to account for the unmeasured elements in the closure relationship.

Element	Oxide Factor
Si	2.139
Ca	2.497
Al	2.741
Ti	1.668
K	0.615
Fe	2.075
S	1.125

clastic sediments is known, they can be easily incorporated. Table 2 shows the accuracy with which the chosen values of X_i can account for the unmeasured elements contained in different minerals. For most minerals agreement is found to within $\pm 5\%$. Of the minerals that show worse agreement, pyrite can be treated separately by logic imposed on the Fe and S yields. Ca-feldspar does not fit well with the current version of the model because Ca is assumed to occur as $CaCO_3$ rather than CaO . Fortunately, however, Ca-feldspar is not common in the subsurface, and thus is not likely to cause large errors in the results. If there were 10% Ca-feldspar in the rock, for example, the elemental concentrations would be in error by only 3%.

The Mg-rich minerals dolomite and ankerite provide the only significant disagreement with the model. These minerals can be correctly evaluated by comparing a measurement of the photoelectric cross section with a calculation of the expected photoelectric cross section, P_e , based on the initially determined elemental concentrations. Since the closure model assumes that all significant elements of the rock are accounted for, macroscopic parameters that do not strongly depend on trace elements (as the thermal neutron cross section might) should be calculated correctly from the derived elemental concentrations.

Table II. Inherent closure calculation for common minerals. A mineral perfectly accounted for would have a value of 100.0.

Mineral	Closure Sum
Pyrite	156.7
Ca Feldspar	129.1
Muscovite	104.7
Glauconite	103.3
Illite	102.8
Montmorillinite	101.8
Chlorite	101.4
Sandstone	100.0
Limestone	100.0
Anhydrite	100.0
Siderite	100.0
K Feldspar	100.0
Kaolinite	100.0
Biotite	96.4
Na Feldspar	95.2
Ankerite	79.0
Dolomite	54.2

If the mass fraction of element i is Wt_i , then the P_e of the collection of elements is given by:

$$P_e = \sum_i Wt_i (Z_i/10)^{3.6} . \quad (2)$$

Implicit in the model used to determine GLT elemental concentrations is that only those elements associated with the rock matrix are measured. Thus the log value of $P_{e,log}$ must be corrected to reflect the value of the matrix alone, $P_{e,mat}$.

This can be easily done in the case of a porous, liquid-filled formation. To reconstruct a P_e using Equation (2), it is necessary to obtain weight fractions for the GLT-measured elements. This is done using the closure technique described above for determining the depth-dependent normalization factor F . The reconstructed matrix P_e is then computed as:

$$P_{e,mat}(recon) = \sum_i P_{e,i} Wt_i + P_{e,K} Wt_K + P_{e,Al} Wt_{Al} + 0.23 . \quad (3)$$

where the small contribution from oxygen is estimated by assuming $Wt_O = 0.52$. When little or no Mg is present, the calculated weight fractions will be accurate and the com-

parison of the reconstructed matrix P_e to the measured matrix P_e will be good. However if a substantial weight fraction of Mg is present, the closure relation will overestimate the normalization factor, causing all of the capture-measured weight fractions to be overestimated, and thus causing $P_{e,mat}(recon)$ to be overestimated.

Any discrepancy between the reconstructed and measured values of matrix P_e can be used to estimate the weight fraction of Mg and to eliminate the overestimate of the capture-measured elemental weight fractions. This is done by including a Mg term in the closure equation:

$$F' \sum_i X_i \frac{Y_i}{S_i} + X_{Mg} Wt_{Mg} + X_K Wt_K + X_{Al} Wt_{Al} = 1, \quad (4)$$

as well as in the matrix P_e equation:

$$F' \sum_i P_{e,i} \frac{Y_i}{S_i} + P_{e,Mg} Wt_{Mg} + P_{e,K} Wt_K + P_{e,Al} Wt_{Al} + 0.23 = P_{e,mat}(meas). \quad (5)$$

These two equations can be solved simultaneously for the two unknowns: Wt_{Mg} and F' , the new normalization factor.

This comparison provides a determination of the Mg concentration as well as the corrected values for the elements measured by neutron capture gamma rays, as can be seen in Figure 1. Through most of the region logged, there is minimal Mg, and the reconstructed and measured P_e curves are in good agreement. However, in the upper dolomite, above 350 feet, there is a significant difference between the two curves, allowing for the determination of Wt_{Mg} and the corrected capture-measurement normalization F' .

The validity of such a model can only be tested against core data. However, it is important to note several potential limitations: that core and log data may not be from the same depth, that core data may reflect small scale heterogeneities, and that the logging measurements sample a much larger volume than do the core samples. Nevertheless, the first question on the validity of the closure model can best be tested with elemental concentration data from laboratory analyses of cores. Almost 500 core samples are compared with the elemental concentrations and the model relationship for the associated unmeasured elements in Figure 2. Almost all data are in excellent agreement with the closure model, which confirms that this approach is satisfactory for describing the elements contained in sedimentary rocks.

3. Elemental Concentrations

The ultimate test of the closure model is to compare log-derived elemental concentrations with those measured in the laboratory on core samples obtained from the well. An example of such a comparison is shown in Figure 3, where the solid circles are the results of neutron activation analyses on core samples. In general, remarkably good agreement is obtained. The first four elements are calibrated directly, and the last five depend

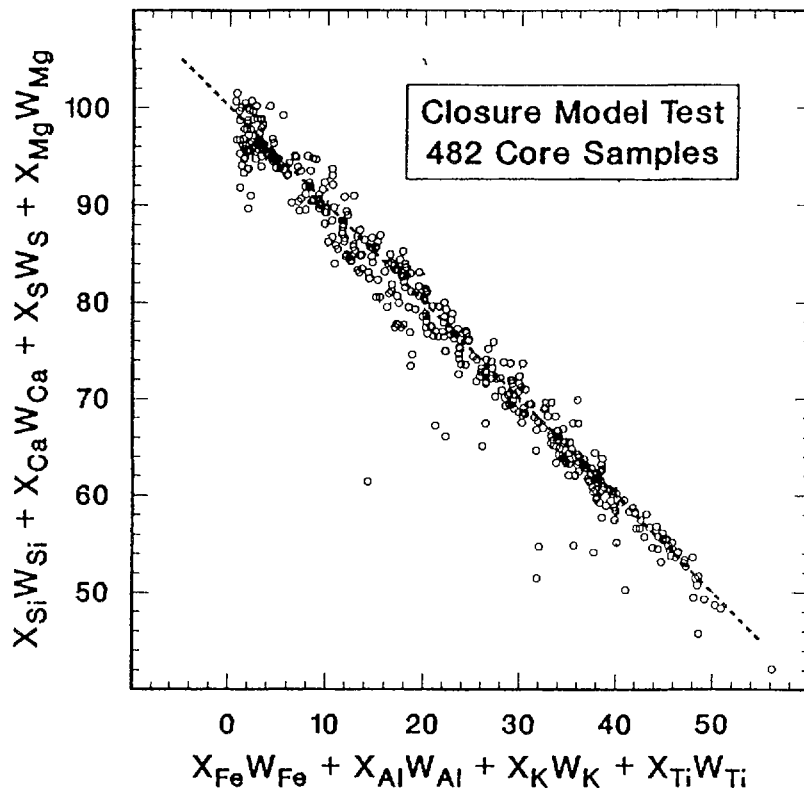


Figure 1. Comparison between the measured and calculated photoelectric cross section. Above 350 feet there is a disagreement due to the presence of dolomite. This difference can be used to derive the concentration of Mg.

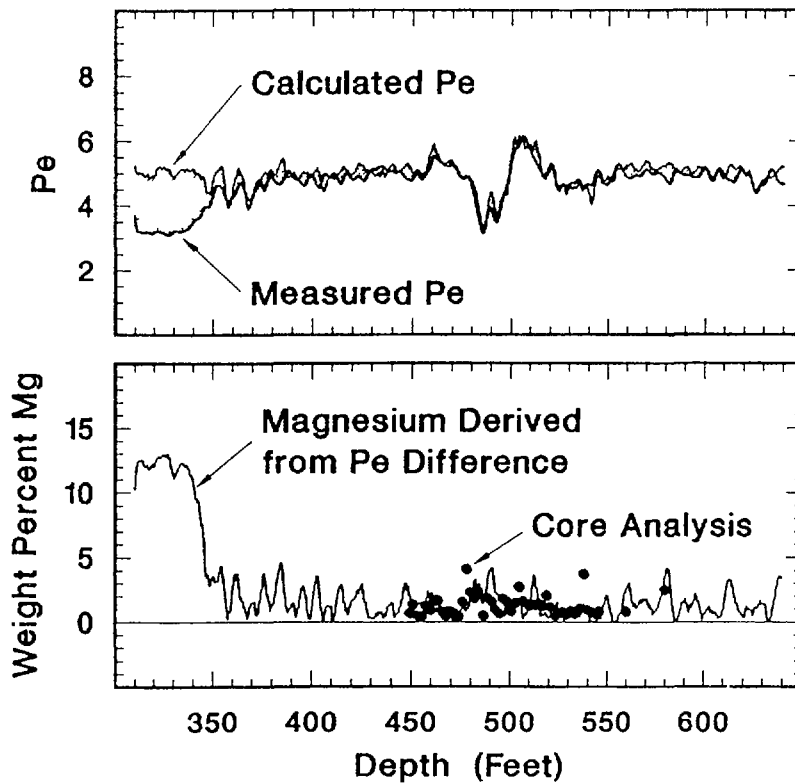


Figure 2. Comparison between the measured elemental concentrations and their associated unmeasured elements and the results from core analyses.

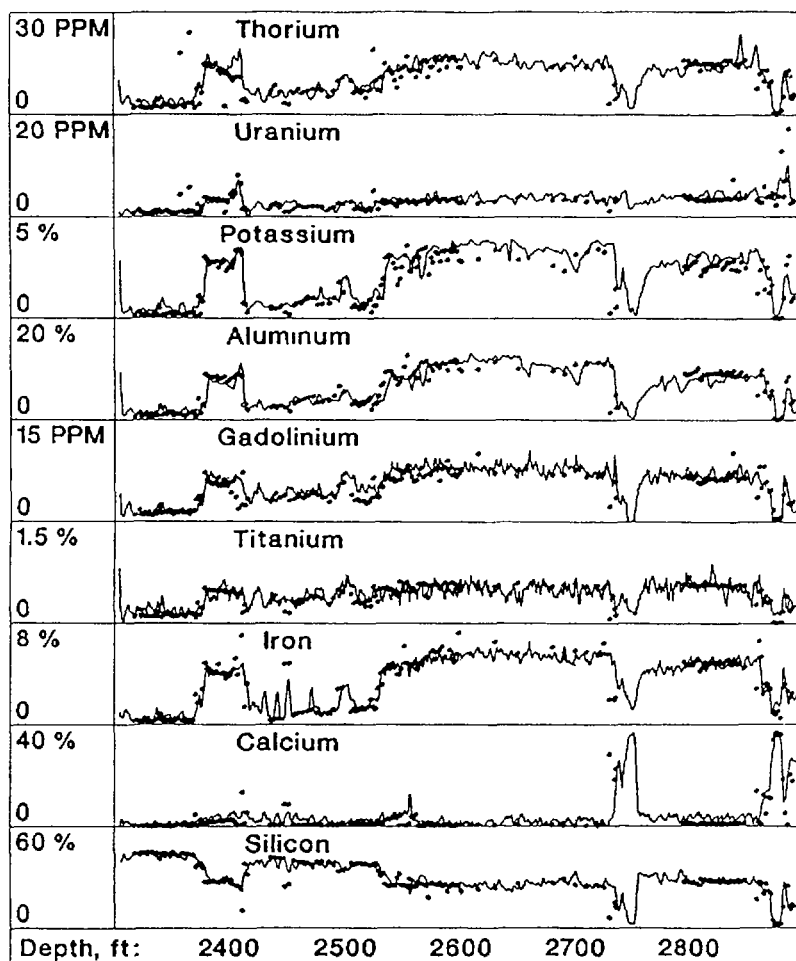


Figure 3. Comparison between elemental concentrations from logging measurements and the elemental concentrations determined from core analyses (solid circles).

on the calculated value for F . Sulfur is not shown as it was not present in this well. Similar comparisons have been performed on dozens of data sets from different wells with comparable agreement.

A striking example of the robustness of the model is provided by a recent example of a well drilled through crystalline rock,⁷ where the mineral suite is significantly different than that on which the model was based. Even though, in principle, there are known changes to the model that could optimize its accuracy in crystalline rock, no changes were made to the constants in the model. The results of the model are shown in Figure 4, where some cuttings analysis are also presented. The absolute elemental concentrations are in good agreement (though the validity of the cuttings analysis comparison is even more questionable than a core comparison). The robustness of the current approach is illustrated in the region near 1500 m, where there are substantial changes in the borehole size. These borehole size changes would lead to a dramatic change in the raw intensities of gamma rays measured through neutron capture reactions. The normalization factor, F (labeled GST calibration), changes by more than a factor of 2 to account for these

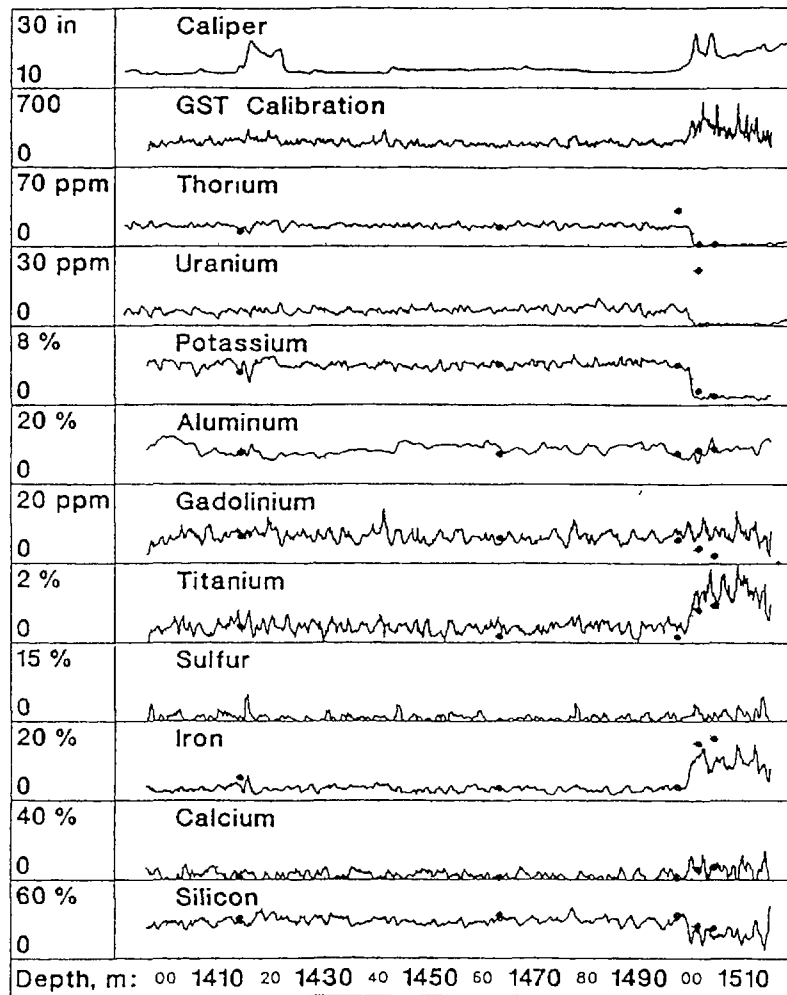


Figure 4. Comparison between elemental concentrations from logging measurements and the elemental concentrations determined from cuttings analyses (solid circles) for a well drilled through crystalline rock which has a set of minerals that fall outside the set for which the model was intended.

effects. The variation in elemental concentrations through this region are well described by the final results. Thus it appears that the calibration factor in our model successfully accounts for many of the large intensity variations caused by changes in the borehole environment.

A final concern for routine elemental analysis is the statistical precision and the overall accuracy of measured elemental concentrations. Statistical precision can be estimated by comparing the results obtained by repeat runs over the same section, as illustrated in Figure 5. The standard deviation between runs is quite acceptable, and it also includes additional scatter from factors such as slight depth mismatches between runs. The overall accuracy is harder to assess, but such an evaluation has been completed for the aluminum concentration,¹³ as summarized in Table 3. Although the accuracy and precision is not comparable to what can be achieved in the laboratory, it is more than adequate for most applications.

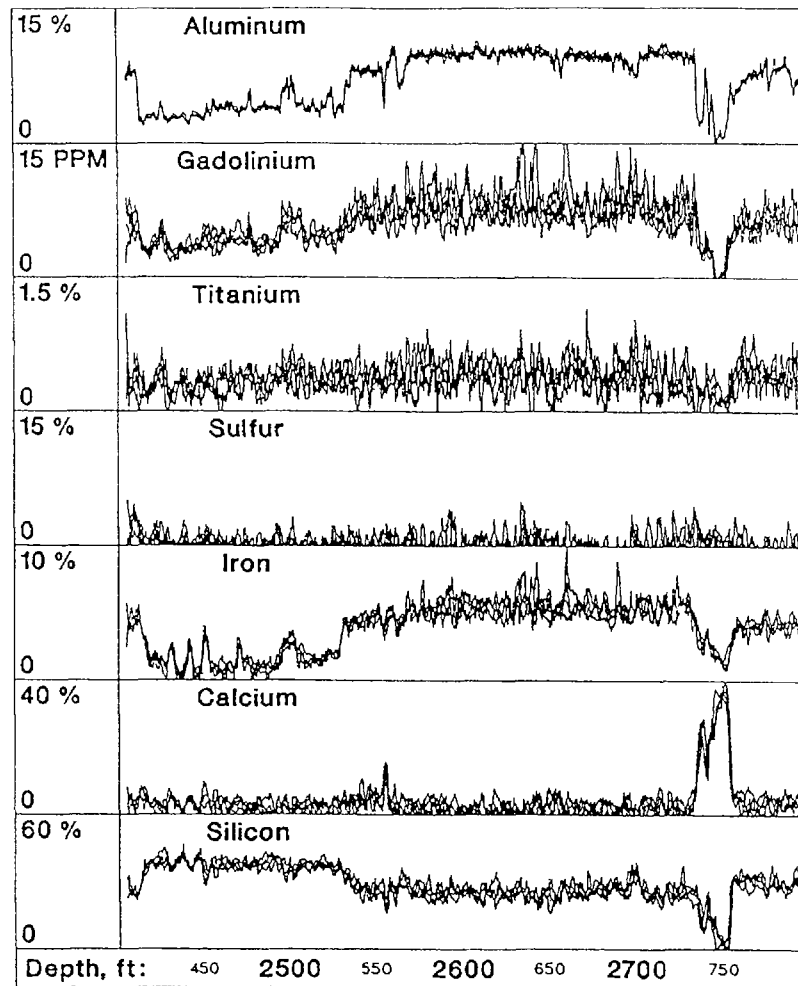


Figure 5. Comparison of the elemental concentration repeatability for many of the measured elements from four repeat runs over the same section.

Table III. Summary of all sources contributing to the accuracy and precision of the aluminum activation measurement.

Source of error	Accuracy	Precision
Laboratory Calibration	3.5%	—
Field Calibration	3.7%	—
Environmental Correction	9.4% (17.2%)*	2.6%
Contributing Factors:		
Normalizaton	5.3%	—
Slowing-down Length	5.3%	2.0%
Formation Sigma	4% (15+%)*	1.6%
Borehole Sigma	3.5%	0.4%
Caliper ($\pm 0.25''$)	2.0%	—
Density	—	0.5%
Count Rate Terms	5.0%	4.3%
Contributing Factors:		(15% Al)
Speed Correction	5.0%	0.3%
Relative Efficiency	0.3%	—
Counting Statistics	—	4.3 - 13.2%
		(15 - 1% Al)
Total from all Sources:	11.8% (18.8%)*	5.0%

* without borehole environmental corrections to Σ_F .

4. Conclusions

A geochemically-based closure model has been described that allows relative measurements of thermal neutron capture gamma-ray spectral contributions to be converted into absolute elemental concentrations in conjunction with directly calibrated measurements of Th, U, K, and Al. The results of this procedure have been successfully compared to the results from the laboratory analysis of numerous core samples. The measurements and analysis model have been tested on data from dozens of wells on three continents with excellent agreement, even in regions outside of the sedimentary environment for which the model was derived. It is now practical to consider that elemental concentrations can be directly obtained from logging measurements without large restrictions in the type of strata or borehole environment, and without the need for many external normalizations.

5. References

- [1] Hertzog, R., et al., "Geochemical Logging With Spectrometry Tools", SPE16792, (Tech. Symp. Soc. Petroleum Engineers, Dallas, 1987).
- [2] Herron, M.M., Mineralogy from geochemical well logging, *Clay and Clay Minerals* **34** (1986) 203.
- [3] Herron, M.M., Geochemical classification of terrigenous sands and shales from core or log data, submitted to *Jour. Sedimentary Petrology*.
- [4] Herron, M.M., Future applications of elemental concentrations from geophysical logging, *Nucl. Geophys.* **1** (1987) 197.
- [5] Herron, M.M., "Estimating the Intrinsic Permeability of Clastic Sediments from Geochemical Data", Paper HH, (SPWLA 28th Ann. Logging Symp., London, 1987).
- [6] Herron, M.M., Grau, J.A., "Clay and Framework Mineralogy, Cation Exchange Capacity, Matrix Density, and Porosity from Geochemical Well Logging in Kern County, California", (AAPG Ann. Convention, Los Angeles, 1987).
- [7] Grau, J.A., Ellis, D.V., Herron, M.M., Schweitzer, J.S., "Geochemical Logging in the Siljan Ring", (3rd Int. Symp. on Observation of the Continental Crust Through Drilling, Mora and Orsa, Sweden, 1987).
- [8] Serra, O., Baldwin, J., Quirein, J., "Theory, Interpretation, and Practical Applications of Natural Gamma-Ray Spectroscopy, Paper Q, (SPWLA 21st Ann. Logging Symp., Lafayette, La. 1980).
- [9] Senftle, F.E., Tanner, A.B., Philbin, P.W., Boynton, G.R., Schram, C.W., In-situ analysis of coal using a $^{252}\text{Cf-Ge(Li)}$ borehole sonde, *Mining Engineering (AIME)* **30** (1978) 666.
- [10] Clayton, C.G., Coleman, C.F., Analysis of neutron flux distributions generated by source of fast neutrons in a range of bituminous coals, *Int. Jour. Appl. Radiat. Isot.* **36** (1985) 757.

- [11] Grau, J.A., Herron, M.M., "Absolute Elemental Concentrations Estimated from Geochemical Well Logging Using Neutron-Induced Gamma-Ray Spectrometry and a Geological Model", (AAPG Ann. Convention, Los Angeles, 1987).
- [12] Grau, J.A., Schweitzer, J.S., Prompt γ -ray spectral analysis of well data obtained with NaI(Tl) and 14 MeV neutrons, Nucl. Geophys. 1, (1987) 157.
- [13] Schweitzer, J.S., Grau, J.A., Hertzog, R.C., "Precision and Accuracy of Short-Lived Activation Measurements for In Situ Geological Analyses", (2nd Int. Workshop on Activation Analysis With Short-Lived Nuclides, Vienna, 1987).

BOREHOLE CAPTURE GAMMA RAY SPECTROMETRY IN VERY DRY ROCK

F.E. SENFTLE, J.L. MIKESELL
US Geological Survey,
Reston, Virginia,
United States of America

Abstract

Using a simulated borehole geometry, prompt gamma-ray spectra have been recorded in four large salt samples, each having a small but different water concentration. Spectra were taken in both dry and water-filled boreholes using a ^{252}Cf neutron source. Analysis of the data shows a very high ratio of fast neutron fluence rate to thermal neutron fluence rate which decreases sharply with increasing concentrations of water. The high ratio is primarily the result of strong thermal neutron absorption by chlorine.

The high neutron fluence rate ratios found in dry salt suggest the possibility of significant contributions to the spectra by non-thermal neutron capture gamma-rays. Examination of the counts in the chlorine capture gamma-ray peaks showed no evidence of significant effects on the capture intensities by non-thermal neutron absorption even in dry boreholes and in the driest salt samples measured. This conclusion is supported by the lack of line broadening in the capture gamma-ray spectra. Rock with a macroscopic cross section as high as that of salt is rare; thus the depression of the thermal neutron fluence rate found in dry salt is an extreme case. There need be little concern that capture gamma-ray spectra taken in a borehole in common rocks will be altered by resonance or fast neutron absorption.

The thermal neutron fluence rate in relatively dry salt at a source-to-detector distance of 39 cm increases with small increments of formation water. Published data for common rocks indicate the opposite is true for higher concentrations of water. The apparent discrepancy is due to the movement of the cross-over point toward greater distances from the source as the water concentration becomes very low.

1. INTRODUCTION

Most borehole neutron-induced gamma-ray spectrometry measurements reported in the literature have been made in coal seams or in relatively shallow sedimentary ore deposits.¹⁻⁴ These matrices generally contain sufficient hydrogen to moderate the source neutrons to the energies needed for capture gamma-ray analysis. As nuclear spectrometry is applied to deeper deposits, drier formations are encountered which may present special neutron moderation problems. Unaltered igneous rocks often contain only 0.5 to 1 percent water⁵ whereas near-surface altered igneous and sedimentary rocks generally have considerably higher water concentrations. Capture gamma-ray spectrometry makes use of neutrons of thermal energies, and the fluence rate of thermal neutrons is reduced in dry rock because of its poor moderating characteristics.

Neutron fluence rate is a function of rock composition, source-to-detector distance, and the nuclear properties of the elements present. Sanders⁶ has presented an excellent review of the nuclear properties of rocks, and has given Monte Carlo calculations of the neutron and gamma-ray fluence rate distributions in rock matrices with and without moisture present. In order to produce well-moderated neutrons for use in thermal-neutron capture gamma-ray analyses, the rock sampled in a borehole should be composed of elements having high slowing-down powers and low thermal-neutron absorption cross sections. On the other hand, the quality of the spectrum produced is enhanced if the elements sought after have moderately high capture cross sections. As hydrogen is the only common element in rocks that can absorb large amounts of energy in a collision with a neutron, water needs to be present in sufficient abundance to produce thermal neutrons from the high-energy neutrons emitted by the neutron source. If there is not sufficient water present, as in deep unaltered non-porous rocks, the thermal neutron fluence rate will be low. This situation may be severely exacerbated by the

presence of even small concentrations of those elements having very high thermal neutron absorption cross-sections (neutron sinks or poisons).⁷ Where the rock moisture is very low and/or where elements which act as neutron poisons are present, the neutron energy distribution will be skewed toward those neutrons having epithermal and higher energies. The probability of these neutrons interacting with the matrix elements by radiative capture will be considerably lower than for thermal neutrons except at specific neutron energies, usually in the epithermal region, where resonance absorption may take place. The relative intensities of the gamma rays from resonance capture are often quite different than for gamma rays following thermal neutron capture^{8,9}. Except in the case of a few elements, resonance-capture gamma-ray intensities are not well known⁸⁻¹¹. Resonance capture and high-energy capture events exhibit themselves in the capture gamma-ray spectrum by their effects on the "primary" gamma rays, i.e. those transitions which originate at the initial capture state. Primary gamma-ray peaks will be broadened and shifted toward higher energies. If resonance capture and high-energy capture are significant, photopeak identification and quantitative elemental measurements become more difficult. Thus, in very dry rocks, there is a question of whether or not one can perform quantitative borehole elemental analyses at all. The same question was asked, but left unanswered, as far back as 1969 when capture gamma-ray analysis was considered as a method to be used on the dry lunar surface.¹²

In this work we examine the problem of high thermal neutron absorption and of low water concentration on the fast and thermal components of the neutron fluence rate. Large samples of very dry NaCl, a matrix with a poor slowing-down power (because of the low hydrogen concentration) and a high thermal neutron macroscopic absorption cross-section were used for the measurements. Chlorine has a neutron absorption cross-section of 33 barns, and with an abundance of about 60 weight percent in NaCl this element becomes an effective thermal-neutron sink. The neutron fluence rate data in dry salt

are compared with published fast and thermal fluence rate measurements in sand having low to medium concentrations of water.

2. EXPERIMENTAL METHOD

All of the measurements were made in simulated boreholes. Four steel casks, 1.22 m in diameter and 1.5 m high were used to hold the NaCl. A steel pipe (10 cm I.D.) was welded along the axis of each cask to simulate the borehole. The salt was loaded through a port at the top of each cask and sealed with a metal cover and rubber gasket to keep out moisture. The salt in each cask (~ 2200 kg) contained a relatively uniform water concentration and varied from 0.035 to 3.31 percent from one cask to another. The water in the two driest samples was as received from the mine. A small amount of $\text{Na}_2\text{CO}_3 \cdot 10 \text{H}_2\text{O}$ was thoroughly mixed with natural salt to prepare the two samples with the highest water concentrations. Sample preparation and analytical details were given in a previous publication¹³.

The gamma-ray spectral analyses were made by counting for 1 hour with a high-purity germanium detector cooled with melting propane and mounted in a borehole gamma-ray sonde. The details of the spectrometer, experimental procedure, and data reduction methods have been described elsewhere^{14,15}.

A two microgram ^{252}Cf neutron source (5×10^6 n/s) was mounted 39 cm below the center of the detector. A 12.5 cm solid aluminum spacer was used instead of the usual nylon spacer to avoid introducing any hydrogen into the experiment. Directly below the spacer the ^{252}Cf source was held in a second aluminum section.

Measurements were made in both water-filled and dry borehole conditions. Because the simulated borehole in each cask was open at the bottom, a thin-walled phenolic liner capped at the bottom end was inserted into the steel "boreholes" to hold the water for the water-filled borehole measurements. With the sonde centered in the hole the equivalent thickness of

water (water plus phenolic liner) around the sonde was 1.35 cm. For comparative purposes a spectrum was also taken with the sonde suspended in a large plastic vat of strong brine solution.

3. EXPERIMENTAL RESULTS

Prompt gamma-ray spectra due to neutron capture and inelastic neutron scattering were made in each of the salt samples using both dry and water-filled boreholes.

3.1 Gamma-rays from (n,n' γ) reactions:

Inelastic scattering peaks from copper and aluminum (in the sonde), and iron (in the cask), were seen in addition to those from the sodium and

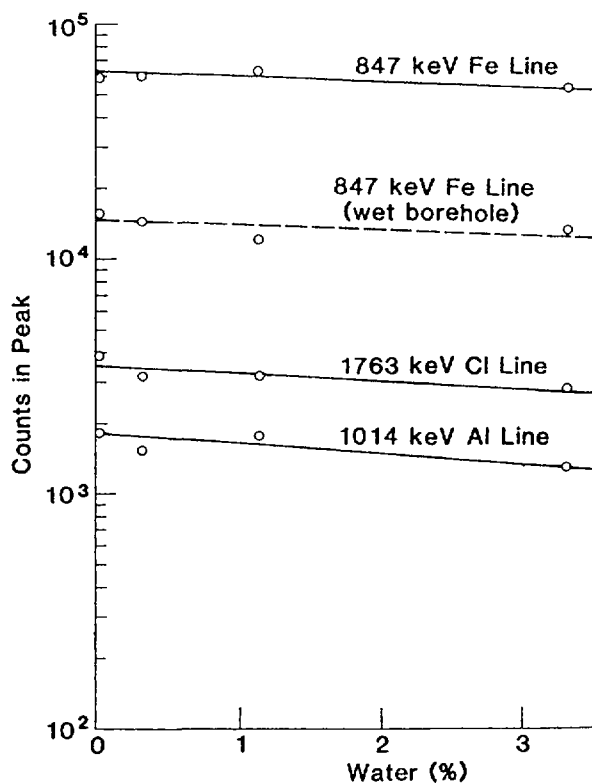


FIG. 1.

Counts in several of the gamma-ray peaks due to inelastic neutron scattering as a function of water concentration in salt. The spectral data were recorded in dry boreholes using a ^{252}Cf neutron source. For comparison the curve due to the $\text{Fe}(n,n'\gamma)\text{Fe}$ reaction in the water-filled boreholes is also shown (dashed line).

chlorine in the sample. The counts due to inelastic neutron scattering reactions were several times higher in the spectra recorded in the dry boreholes than in the spectra recorded in water-filled boreholes. Figure 1 shows that the counts in several of the gamma-ray peaks, due to inelastic neutron scattering and measured in dry boreholes, decreased very gradually with formation water concentration up to 3.3 percent water. The counts in the iron peak (dashed line in Figure 1) shows how a water-filled borehole reduces the counts in the peaks due to neutron inelastic scattering compared with the same peak (solid line) in the spectra using a dry borehole.

3.2 Capture gamma rays:

The prompt gamma-ray spectra taken in both the dry and water-filled boreholes are completely dominated by chlorine capture photopeaks. Essentially all of the peaks could be attributed either to capture by chlorine and iron or to inelastic scattering. The hydrogen peak was not observed in any of the spectra obtained in the dry boreholes. Table 1 is a list of the major chlorine photopeaks in four representative spectra made in dry boreholes in salt samples of different water concentrations. Most of the peaks had relatively few counts, and several peaks are too weak to see in the driest samples, but begin to appear as the water concentration increases. In general, the photopeak counting rates increase substantially with water concentration (see examples shown in Figure 2) because of increased thermalization of the source neutrons. The counts from a comparative spectrum taken in brine are higher in most cases than in any of the dry salt samples. None of the "primary" chlorine gamma-ray peaks exhibited any shift or broadening, indicating that high-energy capture was not an important contributor to the production of those gamma rays. However, because only shifts greater than about 2-3 keV could be detected, due to the resolution limit of the detector, this lack of broadening gives no information about the influence on the capture spectrum by neutrons having less than this energy.

TABLE 1

Counts in major chlorine photopeaks taken from spectra made in dry boreholes in NaCl samples containing different concentrations of H₂O. Data from brine are given for comparison.

E (keV)	Sample 1 0.035% H ₂ O	Sample 2 0.33% H ₂ O	Sample 3 1.13% H ₂ O	Sample 4 3.31% H ₂ O	Brine
788	660	1704	3905	9199	5568
1131	406	400	487	714	613
1165	433	1630	4136	9192	7381
1600	461	600	691	1040	1162
1950	422	956	2080	4372	4010
1959	-	-	675	1230	1231
2075	171	157	167	238	349
2311	-	98	146	216	272
2467	81	58	155	201	-
2676	-	-	75	303	465
2864	92	211	519	1146	1599
2975	62	78	144	316	349
2995	-	136	198	158	183
3062	110	86	297	691	823
3822	-	59	126	137	300
3981	-	-	-	122	170
4440	53	48	35	127	285
4980	22	74	156	390	527
5715	53	39	175	461	776
6111	115	370	995	2065	3723
6619	57	145	274	627	803
7414	32	77	202	466	967
7790	39	84	202	314	732
8578	12	18	59	106	185

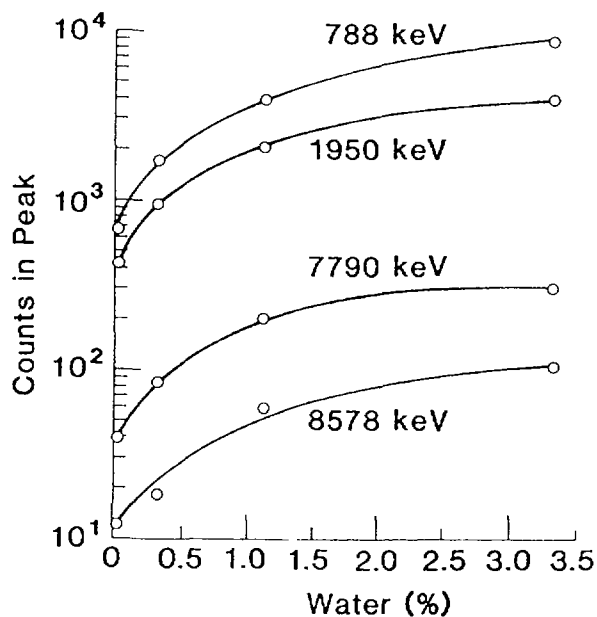


FIG. 2.

Counts in several capture gamma-ray peaks of chlorine as a function of water concentration in salt. Data were recorded in dry boreholes using a ^{252}Cf neutron source.

As the water concentration could not conveniently be increased beyond 3.3 percent in the salt samples, measurements were also made in water-filled boreholes to increase the degree of neutron thermalization further. Table 2 is a list of the major chlorine lines in the spectra for the salt samples taken in water-filled boreholes. The larger number of counts in the peaks reflects the increase in "effective" water in the samples. However, as the additional water is in the borehole rather than in the sample itself, the increase in counts is primarily due to neutrons slowed down in the borehole water and subsequently scattered back into the sample.

4. DISCUSSION OF EXPERIMENTAL RESULTS

Although they are related, the changes in the neutron fluence rate and the intensities of the capture gamma-ray lines will be discussed separately for clarity.

TABLE 2

Counts in major chlorine photopeaks taken from spectra made in water-filled boreholes in NaCl samples containing different concentrations of H₂O.

E (keV)	Sample 1 0.035% H ₂ O	Sample 2 0.33% H ₂ O	Sample 3 1.13% H ₂ O	Sample 4 3.31% H ₂ O
788	10338	11343	12052	16171
1131	950	777	992	1086
1165	10905	11610	12422	16874
1600	1013	1068	1237	1474
1950	4748	5011	5507	7503
1959	1790	1818	1716	2750
2075	174	203	192	303
2311	284	368	284	353
2467	281	385	281	585
2676	404	298	472	611
2864	1306	1245	1533	2124
2975	361	272	310	322
2995	140	121	179	272
3062	700	262	982	1271
3822	222	159	289	402
3981	233	187	195	259
4440	122	115	357	221
4980	120	133	244	381
5715	564	466	520	792
6111	2625	2469	2880	3665
6619	1383	1165	1440	1621
7414	552	639	644	798
7790	370	448	465	655
8578	94	118	118	176

4.1 Neutron fluence rate:

Both fast and thermal neutron reactions take place in the salt matrix, and it is possible to use the gamma ray counting rates produced by their respective reactions as an approximate measure of the fast and thermal neutron

fluence rates. Because the counting rate in the sodium inelastic scattering peak at 440 keV is proportional to the fast neutron fluence rate ($E_n > 459$ keV, the threshold of the $\text{Na}^{23}(n,n'\gamma)$ reaction) and the counting rate in the chlorine capture peak at 778 keV is proportional to the thermal fluence rate. The ratio of the counting rates is proportional to the ratio of the respective neutron fluence rates (we have ignored gamma-ray transport effects). By inserting the appropriate nuclear parameters taken from the literature^{16,17} into the ordinary prompt capture equation* and taking a ratio, one can estimate R, the ratio of the fast neutron fluence rate to the thermal neutron fluence rate. As the two gamma rays are relatively close in energy, we have assumed the efficiencies at the two gamma-ray energies are approximately the same and hence cancel. Thus,

$$\begin{aligned}
 R = \phi_{\text{fast}}/\phi_{\text{thermal}} &= (\sigma I/\sigma' I') (C_{\text{fast}}/C_{\text{thermal}}) \\
 &= 12.3 (C_{\text{fast}}/C_{\text{thermal}}) \quad (1)
 \end{aligned}$$

where C_{fast} and C_{thermal} are the measured counts in the 440 keV and 778 keV peaks respectively, and the primed symbols refer to the inelastic neutron scattering reaction. The 778 keV capture peak is primarily due to thermal neutron capture and the contribution to this peak by fast neutron capture is considered small or insignificant for reasons discussed below. Figure 3A is a plot of this ratio determined from the four salt spectra, showing that the ratio diminishes rapidly as the water concentration increases. In the very dry salt (0.035 percent water) the fast neutron fluence rate is nearly 1000 times greater than the thermal neutron fluence rate. Extrapolation of the curve indicates that even at 5 percent water the ratio R is about 50.

* $C = \sigma \phi N \epsilon I g$, where σ is the elemental cross section, ϕ is the neutron flux, N is the number of atoms of the element, ϵ is the counting efficiency, I is the capture gamma-ray intensity and g is a geometric factor.

4.2 Capture gamma rays:

The effects of epithermal capture and fast capture on the gamma ray spectrum will be seen best in situations where the fast neutron fluence rate is much higher than the thermal neutron fluence rate. The larger fluence rate ratio, R , in salt suggests that epithermal (particularly resonance absorption) neutron absorption may become an important contribution to the capture gamma-ray spectrum of salt, even though line broadening was not observed (see Section 3.2). Chlorine exhibits a number of epithermal resonances in its neutron capture cross section¹⁸. Resonance neutron absorption often yields gamma-rays with quite different relative intensities compared to those produced by thermal neutron absorption. Bird¹⁰ shows that the intrinsic intensities, I_{th} , of gamma rays produced by thermal neutron capture in chlorine are quite different from the intensities, I_f , for the same gamma ray produced by fast neutron capture. The ratio I_{th}/I_f varies not only with neutron energy, but also varies from one gamma ray energy to the next. The fact that the "primary" capture gamma rays exhibited no broadening in the dry salt spectra implies that fast neutron capture had no significant effect. This is reasonable, as the poisoning effects of salt cause the fast (neutron energies > 459 keV) fluence rate to be 1000 times greater than the thermal fluence rate, and the cross-section of chlorine at 459 keV is 10^6 times smaller than it is at thermal energies. Thus the number of fast neutrons actually captured is quite small, even in this extreme case. In non-poisoned rock the ratio R is much smaller than in dry salt, and thus the effects of fast neutron capture will be even less important.

The above discussion considers the effects of line broadening on the capture spectrum of neutrons having energies greater than 2-3 keV. However, there may be effects caused by neutrons with energies ranging from near-thermal to 2-3 keV. Bird¹⁰ has shown significant changes from the intrinsic thermal capture intensities of chlorine gamma rays when relatively low energy monoenergetic neutrons are used. The fact that the water in the borehole

increases the "effective" water in the salt allowed us to check the possibility of significant effects due to epithermal neutron absorption. For the stronger chlorine lines, Table 3 shows the ratios of the counts measured using water-filled boreholes to the counts in the same peaks measured in dry boreholes. These ratios are given for each of the salt samples. If epithermal neutron capture is not significant, then the ratio of the counting rate measured using water-filled boreholes to that measured using dry

TABLE 3

The ratio, C_w/C_d , of the measured counts for the strong capture gamma-ray peaks of chlorine in water-filled to those in a dry borehole in salt containing different amounts of water.

<u>E</u> <u>(keV)</u>	Sample 1 0.035% H ₂ O	Sample 2 0.33% H ₂ O	Sample 3 1.13% H ₂ O	Sample 4 3.31% H ₂ O
788	15.67	6.66	3.09	1.76
1131	2.34	1.94	2.04	1.52
1165	25.18	7.12	3.00	1.83
1600	2.20	1.78	1.79	1.42
1950	11.34	5.24	2.65	1.72
1959	-	-	2.54	2.23
2075	-	1.29	1.15	1.23
2311	-	3.75	2.42	1.63
2467	3.47	6.64	1.81	2.91
2676	-	-	6.29	2.01
2864	14.19	5.90	2.95	1.85
2975	5.82	3.49	2.15	1.02
2995	-	0.89	0.90	1.72
3062	6.36	3.05	3.31	1.84
3822	-	2.69	2.29	1.89
3981	9.32	-	-	2.12
4440	2.30	1.55	10.2	1.74
4980	7.73	1.80	1.56	0.98
5715	10.64	11.95	2.97	1.72
6111	22.83	6.67	2.89	1.77
6619	24.26	8.03	5.25	2.58
7413	17.25	7.23	3.19	1.71
7790	9.49	5.33	2.30	2.08
8578	7.83	6.55	2.00	2.26
<u>Standard deviation</u>	0.6779	0.6015	0.6574	0.240
<u>Mean</u>				

boreholes should be the same for each gamma ray in the spectrum. With only thermal neutron capture to consider, the ratio of the counting rates will be equal to the ratio of the thermal fluence rates with and without borehole water. If epithermal capture is important, then each gamma ray may exhibit a different ratio, because each gamma ray has its own intrinsic intensity for epithermal and for thermal neutron capture. As the water concentration increases from sample to sample, the counting rate ratio should be expected to approach one.

The ratios exhibited in Table 3 do approach one as the water concentrations increases but they also vary by as much as a factor of ten for different gamma rays in the same sample. However, we see the variations in this ratio for different gamma rays in the same spectrum not as an effect of epithermal capture, but as the effect of poor counting statistics. At the bottom of Table 3 are shown the percent standard deviation for the ratios in each sample. For each of the three driest samples the standard deviation is about the same. This shows that despite the large change in the thermal neutron fluence rate from sample to sample, the deviations in the ratio are not correlated with the water concentration, and hence are more likely to be caused by low counting rate. The spectrum made in the sample containing 3.31 percent water had the greatest number of counts in the peaks, and the standard deviation for this spectrum was substantially less as shown. Thus, even in a highly neutron-poisoned environment such as dry salt, one does not see persuasive evidence of effects due to epithermal neutron capture that would change the counting rate of one gamma ray relative to another.

The above conclusion is based on an examination of the capture spectrum of chlorine, an element which does not have a large resonance in its neutron capture cross section. One might encounter an element with a giant resonance in its cross section (such as Co, Mn, Cu, Au, Zr, Nb, Mo, Rh, Ag, or W) in the same matrix as a neutron poison. Under such unusual circumstances it is possible that effects due to resonance neutron capture may be seen.

4.3 Thermal neutron fluence rate

As the capture gamma rays measured in the salt are due primarily to thermal neutron capture we may interpret the gamma-ray curves in Figure 2 as being proportional to the thermal neutron fluence rate. At the source-to-detector distance at which the measurements were made (39 cm), these curves show the thermal neutron fluence rate increasing steadily as the water concentration goes from zero to 3.3 percent (see Figure 2) in both dry and water-filled boreholes. The data presented by other investigators^{19,20,21} would lead one to believe that at source-to-detector distances greater than about 20-25 cm (beyond the "cross-over region") the neutron fluence rate should decrease with water concentration. This interesting effect is only an apparent disparity and will be discussed below.

5. PREVIOUS WORK

To better understand the difference in behavior of neutrons in wet and in dry rocks it is pertinent to examine the experimental and theoretical work of other investigators.

5.1 The fast-to-thermal neutron fluence rate in sand

The neutron fluence rate ratios, R , that we have measured in dry salt are orders of magnitude higher than the ratios indicated for other matrices by Monte Carlo calculations or by experimental measurements. For instance, from the experimental work of Tomnovec and Mather²² one can calculate that for a source-to-detector distance of 38.1 cm the ratio R for dry topsoil (4.5 percent H_2O), for Nevada Test Site soil (2.7 percent H_2O) and for sand (1 percent H_2O) are 0.32, 0.30, and 0.58 respectively. Because of the large difference in the ratio R between salt and these materials it is of interest to compare our data in salt with the experimental data of Tomnovec and Mather²² in sand. They used cyclotron-accelerated 12 MeV protons impinging on a thick beryllium target situated 76.2 cm from the surface of the sample. The

neutrons emerged not from a point source in the sample but formed a nearly parallel beam incident on the surface of the sample. The incident neutron energy distribution was similar to that of a fission-neutron spectrum. The sample was a cylinder 55.2 cm in diameter and 77.5 cm long. The sample size was marginal, considering the long neutron slowing-down length in the driest samples, but from Tomnovec and Mather's discussion of the neutron fluence distribution within the sample, errors caused by the small sample size were less than about 20 percent. The sample size was probably large enough for a qualitative description of the neutron distribution, but inadequate for quantitative applications. Experimentally they measured the fast (> 2.5 MeV) neutron fluence rate and thermal (< 0.5 eV) neutron fluence rate in sand as a function of distance below the surface of the samples containing different amounts of simulated formation water (see Figure 6). From the data in their

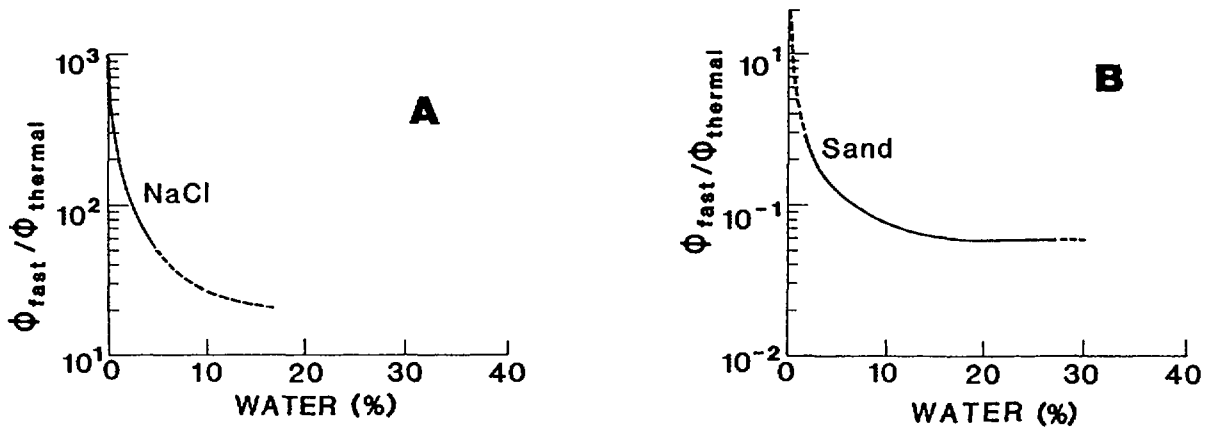


FIG. 3.

A - The ratio of the fast neutron fluence rate (> 459 keV) to the thermal fluence rate in salt from Equation 1, as a function of water concentration in dry boreholes using a ^{252}Cf neutron source (source-to-detector distance is 39 cm.). B - The ratio fast (> 2.5 MeV) to thermal neutron fluences experimentally determined by Tomnovec and Mather²²) for a depth of 38.1 cm in sand using a parallel beam of neutrons.

published curves we have constructed a plot of the neutron fluence rate ratio R as a function of water concentration for a source-to-detector distance of 38.1 cm, approximately the same distance as used in our experiments. The resulting curve (Figure 3B) is similar in shape to that which we obtained for dry salt (Figure 3A), but the neutron fluence rate ratios are much lower than in salt. The high ratios in salt are undoubtedly due to the reduction of the thermal fluence rate caused by the high thermal neutron absorption by chlorine.

5.2 Effect of water concentration (no borehole)

Using data from Tomnovec and Mather's thermal and fast neutron measurements in sand, we have made a plot of neutron fluence as a function of formation water for several source-to-detector distances (Figure 4). The thermal neutron fluence rate curve at 38.1 cm from the source for water concentrations of less than 10 percent increases with water in a manner similar to that of the capture gamma-ray counting rate for approximately the same distance in salt (see Figure 2). The curve for the fast neutron fluence rate measured at 38.1 cm in Figure 4 decreases very slightly with water concentration up to about 5 percent. This behavior is also consistent with our measurements in salt where the gamma-ray activity due to inelastically scattered neutrons decreased slightly with water concentration up to 3.31 percent water. In sand and also in salt the observed change in R with water at low water concentrations as shown in Figure 3A and 3B is due to the gradual decrease of the fast fluence rate with water content, while simultaneously the thermal fluence rate increases substantially. The data of Tomnovec and Mather²² show that the neutron fluence peaks, and then gradually decreases with water concentration. Sanders⁶ has used Monte-Carlo methods to calculate the behavior of 3 and 6 MeV capture gamma rays (californium neutron source) in a limestone matrix. His curves of gamma ray intensity versus porosity closely follow the experimental neutron fluence curves for low porosities shown in Figure 4.

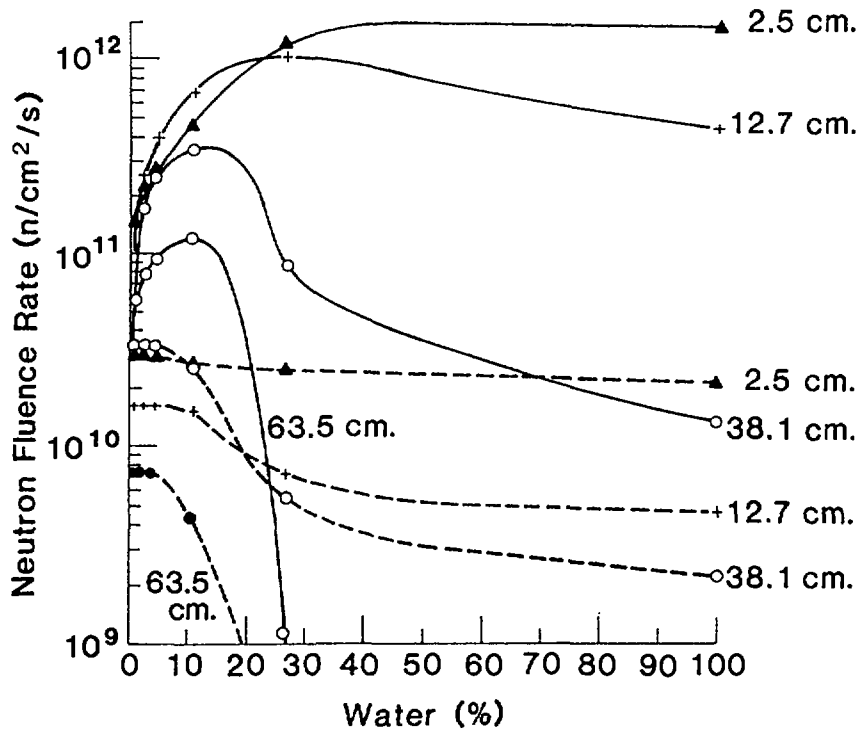


FIG. 4.

Thermal and fast neutron fluences in sand as a function of water concentration for several source-to-detector distances. Both the fast fluence (dashed lines) and thermal fluence (solid lines) show a change in shape as the surface-to-detector distance changes. Neutron source was a parallel beam at the sample surface (data from Tomnovec and Mather²²).

The thermal neutron fluence rate depends not only on the concentration of water but also on source-to-detector distance. At short source-to-detector distances moderation dominates over absorption by water and the thermal neutron fluence rate simply increases with water concentration toward a maximum value which is attained between 30 and 40 percent water. At longer source-to-detector distances the maximum is attained at somewhat lower water concentrations. At long source-to-detector distances, such as 38.1 cm, and for water concentrations above 20 percent, absorption of neutrons becomes dominant and the neutron fluence declines with increasing water concentration. At very low water concentrations, all of the thermal neutron curves of Figure 4 increase with water. This will be discussed further in Section 5.4.

The general behavior of these curves can be understood in terms of the slowing down length, L_s , of sand. Because of the relatively large value of L_s ($\approx 25-30$ cm) in dry sand²³, both high energy and thermal neutrons are disseminated throughout the rock, reaching out a meter or more from the source. Tittle²³ shows that the value of L_s drops rapidly with moisture until the saturated porosity reaches about 20 percent. At porosities of a few percent, small increases in moisture shorten L_s , increasing the number of thermal neutrons even out to large distances. For sand with any saturated porosity greater than 20 percent (about 10 percent water), the value of L_s is relatively constant and equal to 12-16 cm.²³ Thus, for any source-to-detector distance greater than this relatively constant value of L_s , one would expect to see the neutron fluence rate decline with porosity. For source-to detector distances shorter than the constant value of L_s , the neutron fluence rate increases with porosity.

5.3 Effect of Water Concentration (water filled borehole)

The above discussion is relevant to a continuous medium (no borehole) containing relatively small amounts of water. For practical reasons, most investigations involve water-filled boreholes. In a water-filled borehole a large number of neutrons are moderated by hydrogen in the borehole water. Thus, a cloud of thermal neutrons exists in the rock near the source irrespective of the water concentration in the rock matrix. The borehole water increases the "effective" water concentration and thus increases the thermal neutron fluence rate in a dry rock near the borehole in much the same way as true formation water. Because of the relatively high "effective" water concentration near the borehole, small changes in water concentration in the rock will not result in a significant change in the observed neutron fluence rate.

As water increases to high concentrations in the rock matrix, thermal neutrons are absorbed, and the thermal neutron fluence rate becomes attenuated

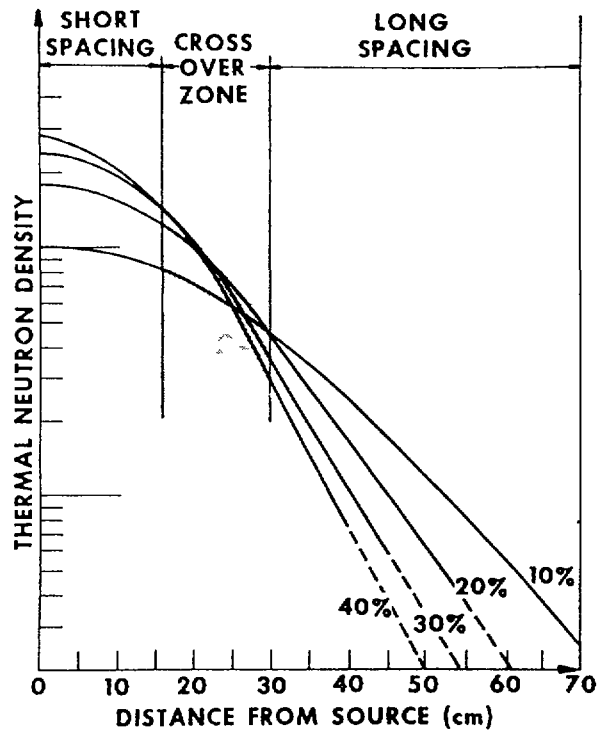


FIG. 5.

Calculated thermal neutron fluence rate as a function of distance from a Ra-Be neutron source in SiO_2 for water concentrations above 10 percent (From Tittman²⁰).

with distance. In a family of curves showing the change in fluence rate with distance (see Tittman's data in Figure 5), the curves for rocks with large water concentration will cross over those with less water concentration. In a water-filled borehole the cross-over region is a relatively narrow zone located about 15 to 30 cm from the borehole. At source-to-detector distances shorter than the distance to the cross-over region the thermal neutron fluence rate should increase with formation water. At distances greater than the distance to the cross-over region the neutron fluence rate should decrease with formation water.

5.4 The cross-over region (dry versus wet rocks)

In the measurements in salt reported here, the detector was at 39 cm, a distance well beyond the usual cross-over point, and it was observed that the thermal neutron fluence rate increased rather than decreased with formation

water (see Section 4.3). This effect was observed even in a water-filled borehole (see Table 2). These results suggest that the cross-over region lies beyond 39 cm in dry salt.

Figure 6 shows a plot from the paper by Tomnovec and Mather²². Their data show how the thermal neutron fluence rate varies with depth for several different water concentrations. (It should be pointed out that the broad maxima in these curves is a consequence of their use of a plane-wave beam of neutrons.) For water concentrations up to 11 percent, their curves do not cross, even out to distances of 62 cm (25 in). Thus, even at 62 cm the neutron fluence rate increases with water up to a water concentration of at least 11 percent. Our measurements in dry salt with a source-to-detector

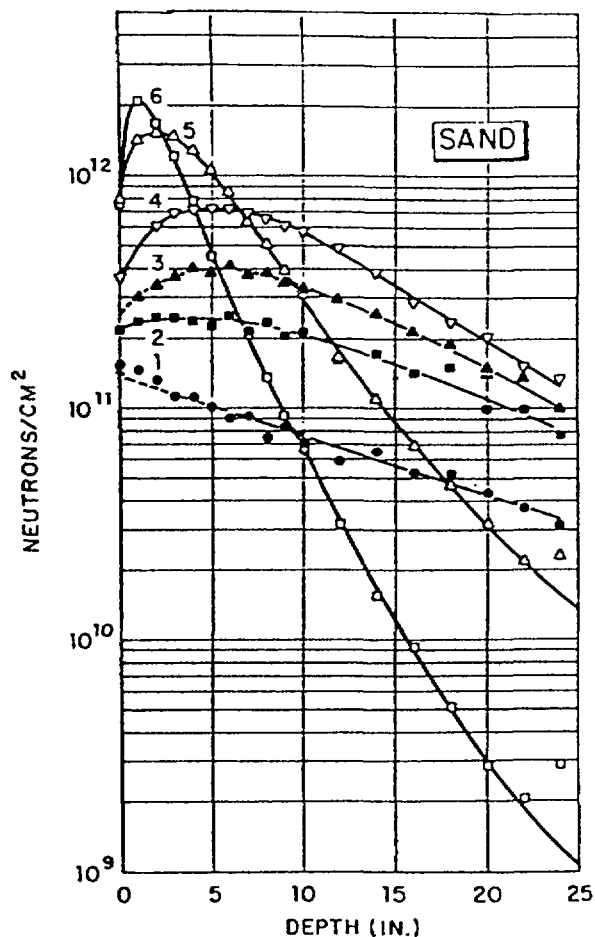


FIG. 6.

Experimental neutron fluence in sand as a function of penetration depth
(from Tomnovec and Mather²²).

distance of 39 cm agree with those of Tomnovec and Mather. The calculations of Filippov et al.²³ show the same general characteristics. We conclude that the "cross-over" region in dry sand is also at much larger distances than usually considered for rocks with large water concentrations.

Using a 3-group, 3-dimensional diffusion method developed by Mathis²⁵, Tittle²⁶ has calculated the thermal neutron fluence rate in quartz sandstone as a function of distance for saturated porosities from 0 to 35 percent. His calculations are for a point source of neutrons both in a water-filled borehole and also in a medium without a borehole. The calculation for the latter case should approximate the situation with a dry borehole. His calculations in water-filled boreholes show that the thermal neutron fluence rate for all porosities exhibits a narrow (16-18 cm) cross-over region. Although the slopes of his lines are somewhat different from those calculated by Tittman²¹, and others^{18,19} the results are generally compatible with the earlier computations and include data at lower water concentrations. In the continuous medium (no borehole) he shows that the cross-over point to be about 55 cm from the source in very dry sandstone. For high water concentrations the distance to the cross-over point decreases to about 18 cm. Our experiments in dry boreholes in salt and those of Tomnovec and Mather in sand confirm that the distance to the cross-over point is at considerably greater distances in dry rock than in wet rock. The reason why the neutron fluence rate increases with water in water-filled boreholes in dry salt is not clear.

6. EFFECT OF NEUTRON POISONS

Wormald and Clayton⁷ have calculated the concentrations in rock of some high-cross-section elements which would reduce the response of a neutron detector by 10 percent. For chlorine this is a concentration of only 0.044 percent. In our salt experiments the concentration of chlorine was 60 percent, making salt an extremely poisoned environment. Table 4 gives the concentrations of several common neutron poisons that would cause the same

Table 4

Percent concentration of potential "neutron poison" elements which will cause the same depression in the thermal neutron fluence rate as does the chlorine in salt.

Element	Concentration (percent)
B	0.8
Cd	25.1
Sm	1.5
Eu	1.8
Gd	1.8
Dy	9.8

degree of poisoning. In every case the concentration of the element is much higher than is likely to be found in nature. Thus, there is little likelihood that one will encounter a rock matrix as severely poisoned as is salt. We found no significant contribution of resonance neutron capture in those spectra made in salt and thus would not expect to see it in other poisoned matrices. However we would expect the counts in the spectra to be seriously reduced at much lower concentrations of neutron poisons because of the depressed thermal neutron fluence.

7. SUMMARY AND CONCLUSIONS

Using a simulated borehole geometry, gamma-ray measurements have been made in several large salt samples containing up to 3.3 percent water. Analysis of the results, and comparison with calculated and experimental results by others indicate that the fluence rate ratio R in salt is several orders of magnitude greater than that found for other rock types. The high ratio is primarily the result of thermal neutron absorption by chlorine in the salt.

The high ratio suggested that epithermal and fast neutron capture may make a significant contribution to the capture gamma-ray spectrum. However, further analysis of the gamma-ray counting rates showed that, even at a ratio of fast neutron fluence rate to thermal neutron fluence rate of 1000, thermal capture predominates. Concentrations of neutron poisons likely to be found in nature are too low to cause as great a depression in the thermal neutron fluence rate as does salt. However, when making capture gamma-ray spectra of those elements having giant resonances in their capture cross sections, one may need to exercise caution even for neutron fluence ratios of less than 1000. We conclude that non-thermal neutron capture need not be considered a serious problem in most borehole spectrometry applications.

At the source-to-detector distance used in our experiments (39 cm), the thermal neutron fluence rate was found to increase with water concentration. This appeared at first to be contrary to conventional notions about the location of the "cross-over" point, the distance at which neutron fluence rate becomes insensitive to changes in water concentration. Comparison with experimental and calculated neutron distributions published in the literature shows that for dry boreholes, the cross-over distance varies with water concentration and is substantially longer in dry rocks than in wet rocks. When water-filled boreholes are used the cross-over point is well-defined and is usually at short distances even in dry rocks, and this is also the case for rocks containing larger concentrations of water.

Because of the high ratio R , in a "poisoned" rock matrix epithermal and fast neutron capture will be enhanced. To determine if this enhancement is strong enough to alter the relative intensities of thermal neutron capture gamma rays, the spectra taken in salt samples containing very small water concentrations were examined. Analysis of the data indicate that even when R is 1000, the contribution by fast neutron capture did not significantly affect the relative intensities in an otherwise thermal capture spectrum. Massive dry salt is a more serious neutron poison than will be generally encountered

in nature. Thus, it is concluded that neutron poisons in normal concentrations, although they will depress the thermal neutron fluence rate, probably will not lead to a significant contribution from fast neutron capture gamma-ray events. The peaks in the spectrum due to neutron capture should have the same relative intensities that they would in a thermal neutron capture spectrum.

ACKNOWLEDGEMENTS

The authors wish to thank Dr. C. W. Tittle of Southern Methodist University, Dallas, Texas, and Dr. C. Eisenhower, U.S. National Bureau of Standards, for their stimulating discussions and helpful remarks. We also wish to thank our colleague A. B. Tanner for his helpful discussions.

REFERENCES

1. Wylie, A., Nuclear Assaying of Mining Boreholes, Elsevier Sci. Pub., New York (1984).
2. Senftle, F., In Short Course in Neutron Activation Analysis in the Geosciences, (Ed. G. K. Muecke), Mineralogical Association of Canada, Halifax, p. 211-244 (1980).
3. Clayton, C., and Wormald, M., 1983, Int. J. Appl. Isot. 34,3k (1983).
4. Senftle, F., Tanner, A., Philbin, P., Boynton, G., and Schram, W., p. 666-678 (1978).
5. Carmichael, R. (Ed.), Handbook of the physical properties of rocks, Vol. 1, CRC Press, Boca Raton, Florida, USA (1982).
6. Sanders, L. G., 1983, Int. J. Appl. Radiat. Isot. 34, p. 173-198, (1983).
7. Wormald, M. and Clayton, C., In Exploration for Uranium Deposits, Internat. Atom. Energy Agency, Vienna, IAEA-SM-208/35 p. 427-470 (1976).
8. Kenny, M., Austral. J. Phys. 24, 805-819 (1971).
9. Broomhall, G. J., Austral. J. Phys., 25, 9-19 (1972).

10. Bird, J., Allen, B., Bergqvist, I. and Biggerstaff, J., Compilation of keV-neutron gamma-ray spectra, Nucl. Data Tables II, Academic Press, p. 433-529 (1973).
11. Rae, E., Moyer, W., Fullwood, R., and Andrews, J., Phys. Rev. 155, p. 1301-1308 (1967).
12. Preskitt, C. A., John, J., and Reynolds, G. M., Trans. Am. Nucl. Soc. 12, p. 471 (1969).
13. Senftle, F., Mikesell, J., Doig, N., and Brown, F., Int. J. Appl. Radiat. Isot. 34, p. 389-396 (1983).
14. Tanner, A. B., Moxham, R. M., Senftle, F. E. and Baicker, J. A., Nucl. Instr. Methods, 7, pp. 1-7 (1972).
15. Senftle, F. E., Moxham, R. M., Tanner, A. B., Boynton, G. R., Philbin, P. W. and Baicker, J. A., Nucl. Instr. Methods, 138, pp. 371-380 (1976).
16. Erdman, G., Neutron Activation Tables, Verlag Chemie, New York (1976).
17. Magurno, B., Kinsey, R., and Scheffel, F., Nuclear Data Files, ENDF/B-5, Brookhaven National Lab New York (1982).
18. Macklin, R. L., Phys. Rev. C, 29, 1996-2000 (1984).
19. Allen, L. S., Tittle, C. W., Mills, W. R. and Caldwell, R. L., Geophysics 32(1) p. 60-68 (1967).
20. Rezvanov, R. A., Denisik, S. A., and Lebedev, V. E., Exploration Geophysics 51, p. 95-109 (1969).
21. Tittman, J., In Fundamentals of Logging: Lecture Series, Petroleum Engineering Conference, University of Kansas 115-136 (1956).
22. Tomnovec, F., and Mather, R., Rept. USNRDL-TR-413, U.S. Radiological Defense Laboratory, San Francisco, CA, (1960).
23. Tittle, W., Nucl. Geol. (in press) (1987).
24. Filippov, E. M., Vakhtin, B. S., and Novoselov, A. V., In Neutron-neutron and neutron-gamma methods in ore geophysics, (Ed. V. I. Baranov), Nauka, Novosibirsk, USSR., p. 212-213 (1972).

25. Mathis, G. L., Application of neutron diffusion theory to time-dependent and eccentric steady state neutron well logging, Ph.D. Thesis, Dept. of Physics, Southern Methodist University, Dallas, Texas, USA (1983).
26. Tittle, C. W., private communication (1987).

NUCLEAR QUANTITATIVE ANALYSIS OF P, Si, Ca, Mg, Fe, Al IN BOREHOLES ON A PHOSPHATE MINE

J.-L. PINAULT

Bureau de recherches géologiques et minières,
Orléans, France

Abstract

Neutron-gamma logging have been applied to determine the grade of ore in preproduction holes drilled into a layered phosphate deposit.

The probe was systematically passed down each boreholes with each of the two sources : Am/Be or Cf successively. The first source emits fast neutrons favouring measurement of phosphorus and magnesium (inelastic scattering) whereas the second is preferable for measurement of silicium, calcium, iron and aluminium. However the ore has a high water content which strongly modifies the energy (capture) distribution of the Am/Be source and allows simultaneous detection of all the elements by using only the Am/Be source. The probe was raised at a speed of 6 m/h. The sampling interval was about 50 cm. The calibration operation was made from analysis from homogeneous ore. The peak area due to capture of neutrons by hydrogen was only introduced into the model so as to take into account disturbances introduced by water. The relative errors are less than 10 % for the major components : P, Si, Ca.

In some instances, large differences were revealed between the "in situ" analysis and ore grade determination from cores because of ore heterogeneity. The analysis on cores are very erratic from one borehole to another while analysis by activation reveals regionalization phenomena due to its great representativity.

1. INTRODUCTION

The spectrometry of gamma radiation induced by capture or inelastic scattering of neutrons was often depicted as a powerful analytical tool for determining grade of ores in boreholes : [1], [3]. This report presents the results obtained in the Taiba phosphate mine in Senegal. This mine carries out now only reconnaissance boreholes on a frame 125 m wide, that don't lead to an accurate description of the pit because of the heterogeneity of the ore. The drilling cores are splitted into metric samples and the 40/12 000 μm fraction is assayed in the laboratory.

An improved knowledge of the pit could be obtained in preproduction drill holes with a more compact frame. For this purpose, the nuclear methods to characterize grade ores offer the following advantages :

- Economy on drilling costs : recovery of cores is no more required.
- Best representativity of the surroundings with respect to the important size of the analysed volume.
- Simultaneous analysis of P_2O_5 , CaO, MgO, SiO_2 , Fe_2O_3 , Al_2O_3 .
- Estimation of ore grade on the site.

2. GEOLOGY of the PHOSPHATE ore DEPOSITS

The Taiba mine is a calcium phosphate deposit. Upward, the stratigraphic column can be depicted as :

- A clayey wall (attapulgit),
- A 7 m thick phosphate layer (mean thickness),
- A 0.5 to 1.5 m thick clayey roof with montmorillonit,
- A 4 m thick lateritic phosphate layer with aluminium phosphate,
- A 4 m thick sandstone layer,
- A 15 to 25 m thick aeolian sand.

To be mined the phosphate ore has to satisfy the following conditions :

$$P_2O_5 \geq 20 \%$$

$$1.35 \leq \frac{CaO}{P_2O_5} \leq 1.55$$

$$\frac{Fe_2O_3 + Al_2O_3}{P_2O_5} \leq 0.20$$

The ore is excavated with draglines. A first operation excludes the major part of flints. Then, the 0/30 000 μm ore fraction is conveyed to the mill through an hydraulic pipe.

3. PRINCIPLES of NEUTRON - GAMMA LOGGING for PHOSPHORUS, MAGNESIUM, CALCIUM, SILICIUM, IRON and ALUMINIUM ASSAY

The more frequent neutron sources used for boreholes analysis are the 14 MeV generator (D-T reaction) and the isotopic sources : Cf^{252} (spontaneous fission, mean energy ~ 2 MeV) and Am/Be (α -n reaction, energy from 1 to 8 MeV).

The 14 MeV neutron generators are not suitable for determining grade of phosphorus : the yield of the inelastic scattering process leading to the excitation of the first P^{31} level (1.27 MeV) tends to zero when the energy of neutrons is above 5 MeV (excitation of the nucleus to the continuum).

By another way the radioisotope Al^{28} resulting from the $P^{31} (n, \alpha) Al^{28}$ reaction (half life = 2.24 mn) is not typical of phosphorus since it is also produced by the reaction on silicium : $Si^{28} (n, p) Al^{28}$.

Better results are obtained with an Am/Be source which allow the first level of P^{31} nucleus to be excited.

Neutrons released from Am/Be source are also able to excite the first level of Mg^{24} nucleus (1.37 MeV) with a high yield. However, magnesium is absent in the Taiba mine. So, we will not speak anymore of this element.

The elements Ca, Si, Fe, Al are analysed from their capture gamma rays, 6.42, 4.93, 7.64 and 7.72 MeV respectively. The highest yield is reached with the Cf source because, generally, the cross-sections are increasing when the energy of neutron is slowing down (well known $1/v$ law where v is the neutron velocity).

The average water content in the ore is more than 20 %. Thus, the energy distribution of neutrons in the formation is strongly disturbed and the Am/Be source allows to produce gamma rays from capture and inelastic scattering mechanism simultaneously.

4. INSTRUMENTATION

Neutron Activation Probe (NAP) and analyser

A schematic view of the NAP is shown in the figure 1. The main body is a cylinder made of carbon fibers. NAP is 82 mm in diameter and 120 cm long and can resist to 25 bars pressure. The probe contains neutron source, detector, pre-amplifier and signal output devices.

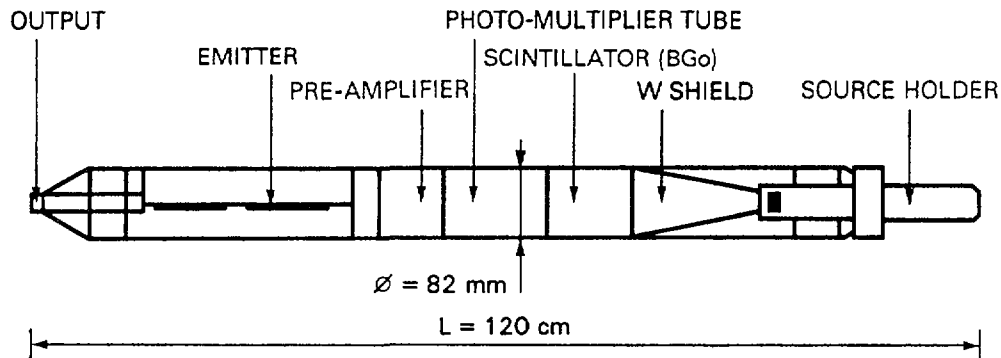


Figure 1 - Neutron activation probe.

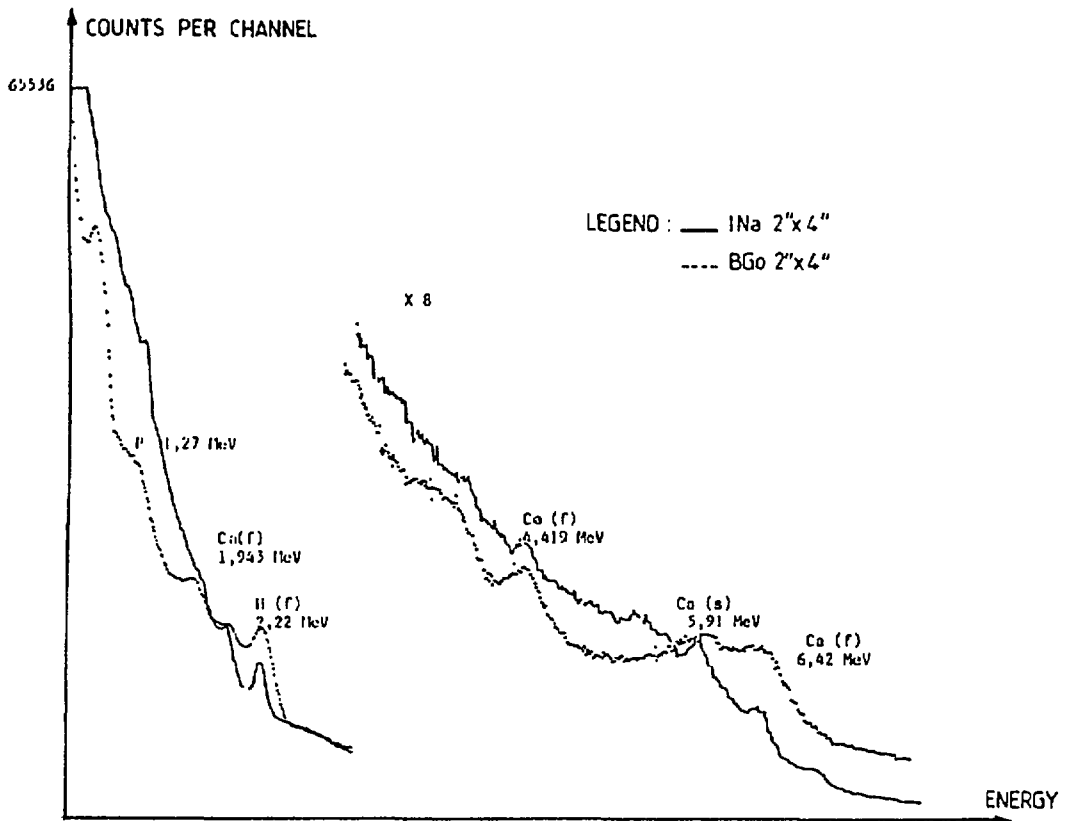
The source holder can accommodate two interchangeable neutron sources. A Cf ²⁵² (2 mCi) and an Am/Be (1 Ci) sources are available. A sintered W shield is placed between the source and the detector in order to absorb the fast neutrons. This shield allows to minimize the source-detector distance down to 15 cm leading with high efficiency for detection of prompt reactions occurring during neutron irradiation : capture or inelastic scattering.

The detector is a bismuth germanate (BGO) scintillator manufactured by Harshaw. The BGO detector is 2 inches x 4 inches in dimensions. A photomultiplier tube (PMT) is associated with the scintillator. The BGO-PMT assembly is protected from scattered thermal and epithermal neutrons by a sintered bore carbide shield (0.20 g/cm² of 10 B).

For low energy γ -rays peak, area/background ratio is higher for BGO than for INa of the same size, (Fig. 2). Moreover, double escape peaks remain very weak at high energies.

BGO resolution is less good than that of an INa detector. To overcome this problem we developed an efficient deconvolution algorithm. The scintillation phenomena of BGO depends of the temperature of the crystal. Thus probe calibration has to be done in the real conditions of use.

A power supply and an emitter unit used for the transfer of signals to a receiver unit are also included within the main body of the NAP. The receiver placed on the ground is connected to the NAP by a cable containing two wires for analog signals transmission without loss of resolution (differential mode). A 200 m



CAPTURE SPECTRUM. Cf SOURCE 1.6 μ g. SOURCE DETECTOR SPACING = 22cm - 1800s

Figure 2 - Spectrum of prompt gamma rays - Phosphate ore (Mataiva).

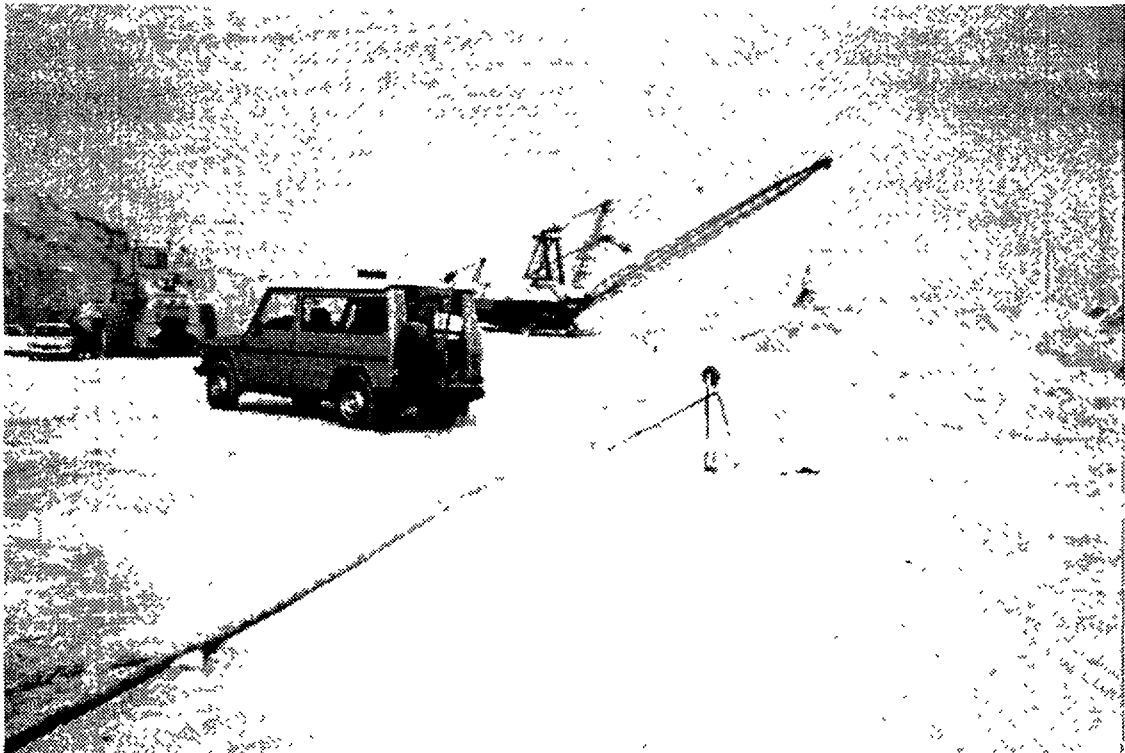


Figure 3 - The B.R.G.M. tool at Taiba (Sénégál).

length cable is used. Signals are amplified and their amplitudes are analysed by means of analog to digital converter and multichannel analyser linked to a micro-computer for data processing (Fig. 3).

5. SOFT for DATA ACQUISITION, PROCESSING and REDUCTION

Data acquisition

The NAP is raised continuously within the drill-hole and the signals are integrated as a function of time. The integration times require optimization based on the type of the nuclear reaction used for the analysis, concentrations to be analysed and matrix. The signals are then processed and expressed in terms of weight concentrations using a specific software as described below.

Data processing

An example of γ ray spectrum is shown in figure 2. It consists of small discrete monoenergetic peaks emerging from an intense continuum (background, BKG). A software was developed for BKG removal, peak overlap correction and intensity measurements of the characteristic peaks. The procedure used is based on digital filtering of the spectra. The experimental data are first corrected for the energy dependence of the resolution (peak width) by use of linear digital filter. The second step in data processing is BKG removal and estimation of peak intensity. A linear digital filter is applied to convert the original spectrum S to another called S' . Each peak P in S have a corresponding peak P' in S' with the peak height of P' (called H') equals the peak area of P (called A) : figure 4. Thus, the estimation of A from S' is easier. The B K G is then suppressed. Peak overlaps are more easily corrected in S' than in S .

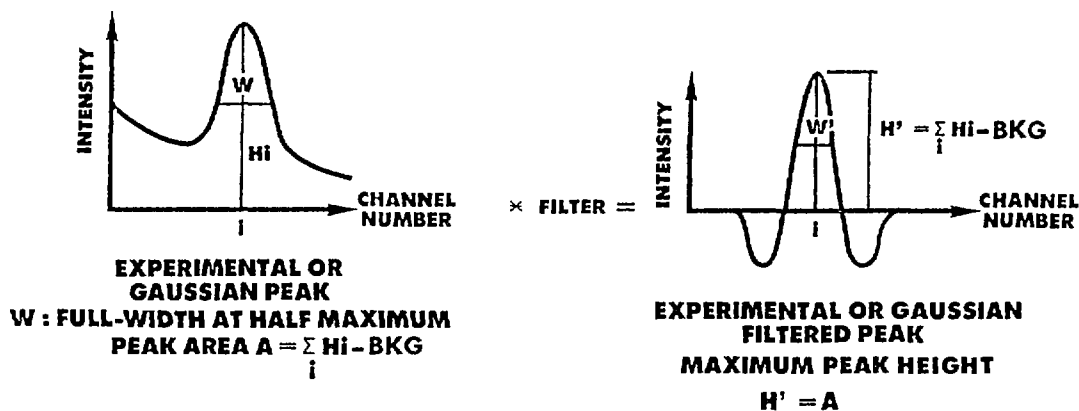


Figure 4 - Gamma-ray spectra processing linear digital filtering for background removal and peak height measurement.

The third step in data processing then concerns peak overlap correction as illustrated in figure 5. It consists in a product of square matrix $[\alpha_{ij}]^{-1}$ and vector $[H'_i]$ where $[\alpha_{ij}]$ is the "overlap matrix" (defined below).

The components of $[H'_i]$ are deduced from the S' spectrum for each analysed element i . The result of this product is the true intensity vector : $[I_i]$.

So, from the $[H'_i] = [\alpha_{ij}] \cdot [I_i]$ relation we infer $[I_i] = [\alpha_{ij}]^{-1} \cdot [H'_i]$ because $[\alpha_{ij}]$ is an inversible matrix.

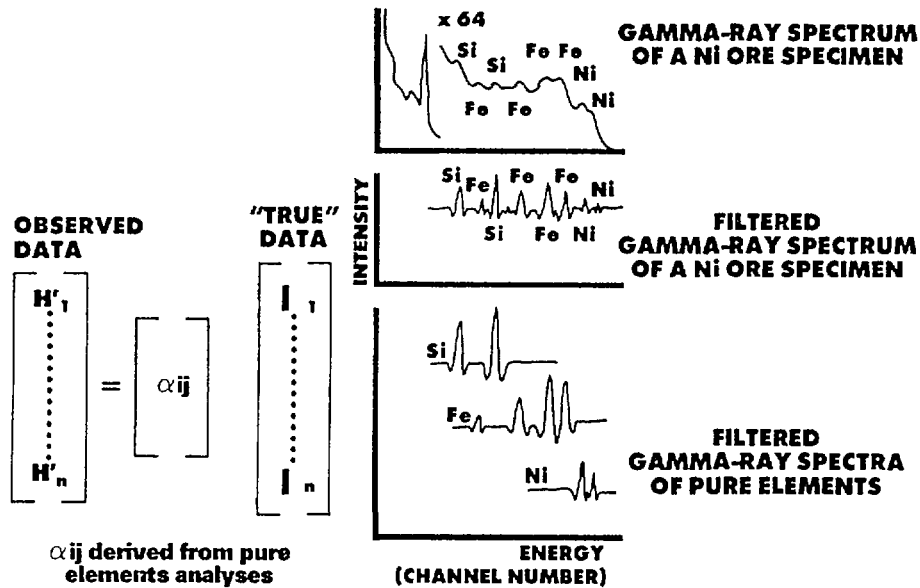


Figure 5 - Gamma-ray spectra processing: peak deconvolution.

The $[\alpha_{ij}]$ matrix is settled from pure element spectra : in this case the $[I_j]$ matrix is trivial i.e. all the components are zero, except the one corresponding to the pure element. Thus, the column j of the $[\alpha_{ij}]$ matrix expresses the contribution of the element, j , to the intensity of each analysed element. At last the $[\alpha_{ij}]$ matrix is normalized and inverted.

To be used this deconvolution method, requires that the shift and gain variations of the analogic electronic device must be corrected. To do so the characteristic peaks of boron (476 keV) and hydrogen (2.22 MeV) are used for calibration.

Data reduction to express ore grades from net intensities

A program was developed to express the intensities in term of weight concentrations of the elements detected according.

$$\frac{C_i}{I_i} = \exp \left\{ \beta_{oi} + \sum_{j=1}^n \beta_{ji} I_j \right\}$$

where C_i is the weight concentration of the analysed element i , I_i is the net intensity of the radiation characteristic of the element i , and β_{ji} are influence coefficients taking account for the contribution of the intensity I_j , of the element j , upon the intensity of element i .

The interelement effects result simultaneously from :

- Interactions between the incident neutrons and the formation.
- Interactions between the generated γ photons and the formation.

It has been shown experimentally and from Monte Carlo simulation that the effect resulting from neutron-matrix interactions represents the main contribution to non linearity of measured intensity versus concentration as expressed by the empirical relation above. In addition water present either in boreholes or in ore is the main constituent leading to the matrix effect. Measurement of γ -rays characte-

ristic of hydrogen allows to take the presence of water into account. In practice, the set of coefficients β_{ij} are derived from a least squares fitting procedure between experimental data obtained in a cored borehole (true intensities corresponding to each elements) and the analysis of cores in laboratory.

Application of Monte Carlo computation

To study the principal origin of disturbance affecting the intensities measured in boreholes due to matrix effects, we developed a Monte Carlo simulation program (MOCA) on a minicomputer, program easily transferable to a compatible P.C.).

Nuclear data are obtained from ENDL 84 (NEA Data Bank). This Monte Carlo program simulates neutron and gamma transport to the detector through the matrix.

The probe is reduced to its most significant components concerning neutrons and gamma rays phenomena (Fig. 6).

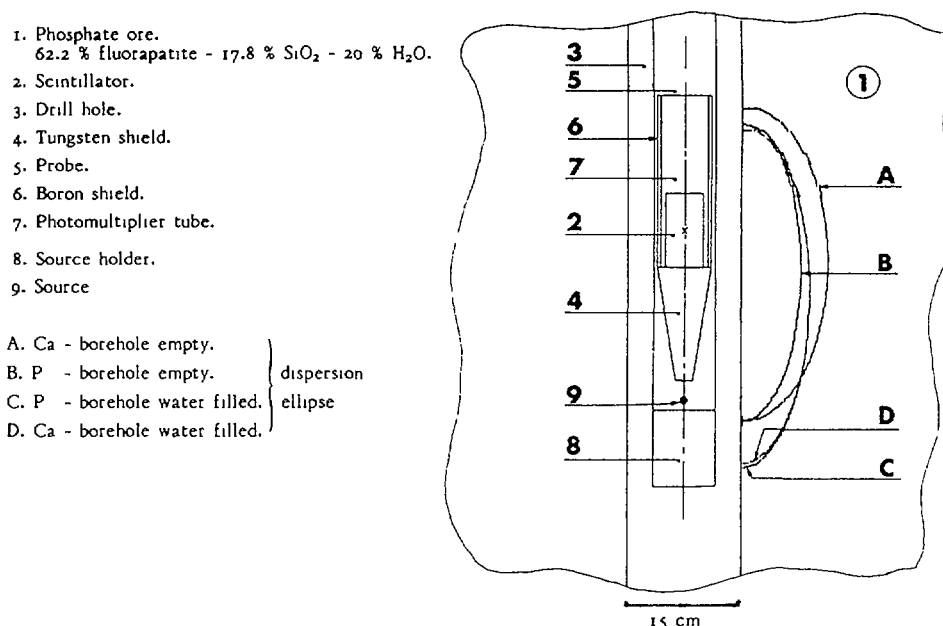


Figure 6 - Simplified probe for Monte Carlo simulation.

The MOCA program uses cylindrical co-ordinates (2 dimensions : radius R and depth Z).

Each surrounding component (probe's components, borehole, matrix) are represented by conics (cylinder, cone,...) either contiguous or fitted into each other limited or not by planes ($Z = CSte$).

All natural elements can be tabulated, from ENDL 84. Cross-sections are divided into 46 groups weighted by $1/E$ or by maxwellian distributions (in thermal class, 2 groups are needed to properly weight the cross section).

The gas model is used to describe thermal neutron behavior. To obtain a relative accuracy of a few percents, computation time may vary between 15 mn for reactions with threshold as inelastic scattering, (n, 2n) reaction,... and several hours for capture reactions in weakly hydrogenous matrix (cost time is cheap !).

Monte Carlo calculation gives estimation of both probability that one photon intercepts the detector and moments of first and second order of R and Z simultaneously. Thus, the dispersion ellipse from which 86,5 % of the total activity is detected, can be determined.

Preliminary results obtained from computation are presented (Fig. 6, 7). These examples only account for phosphorus (from inelastic scattering) and calcium (from capture) in a phosphate ore (80 % fluorapatite, 20 % flint). Water content varies between 10 % and 30 %. The borehole is assumed to be either empty or water filled. The probe is equipped with an Am/Be source and a BGO detector. The MOCA program provides a good appreciation of the matrix influence and of the effective involved volume. Water content has a strong effect on activity either for inelastic scattering or capture induced γ -rays. For the first type the activity decreases when the water content increases while it is in opposite direction in the second type because of the slow down effect of hydrogen (inelastic scattering is a reaction with threshold whereas the capture cross sections are predominant for thermal groups).

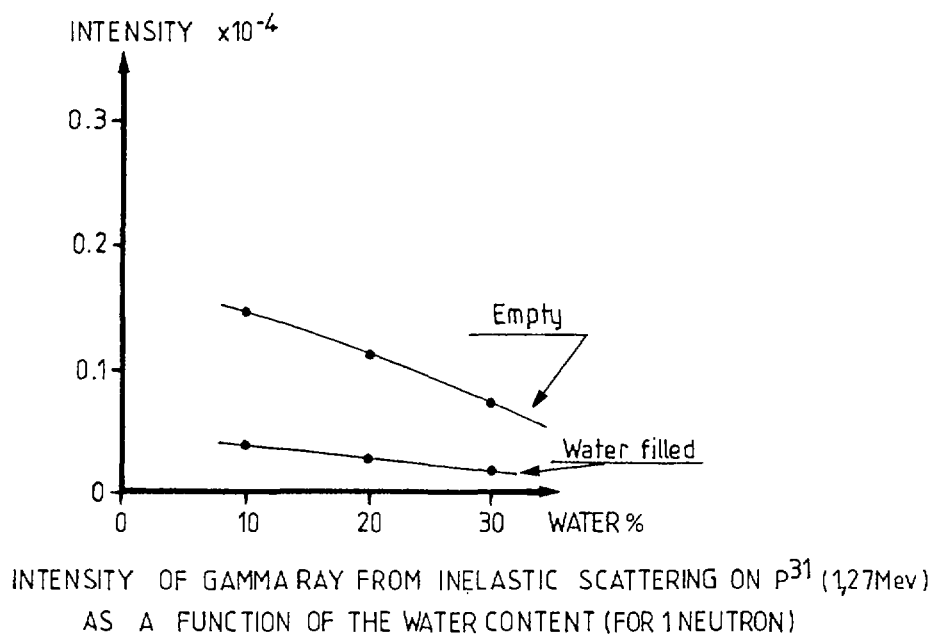


Figure 7 - A Monte Carlo simulation - borehole is empty or water filled.

When the borehole is water filled, the intensity resulting from inelastic scattering collapses. More unexpected is the increase of the analysed volume, owing to the filter effect of water on the neutron spectrum of the Am/Be source. At the worst (inelastic scattering of P in dry formation) the analysed volume is at least 5 times more important than the core volume. In case of Ca, Si, Fe, Al (capture), the analysed volume is increased by a factor of 10 with respect to the volume of the core. This effect is an asset for the use of nuclear techniques in borehole analysis, mainly in the heterogeneous ores as in phosphate mines.

6. RESULTS and DISCUSSION

The aim of this work was the analysis of P_2O_5 , SiO_2 , CaO , Al_2O_3 , Fe_2O_3 both in dry and water-filled boreholes.

Six cored boreholes (ST 1 to ST 6) 15 m apart were drilled from the drag-line platform. Cable drilled, with a diameter of 5" 1/2, the cores were recovered

at metre intervals and analysed in the laboratory after a splitting corresponding to the probe's sampling steps (~ 50 cm).

The boreholes pass through a more-or-less phosphate-bearing sandstone barren (aluminium phosphate) then through homogeneous P_2O_5 -rich ore and finally heterogeneous ore containing mainly flints over a thickness of about 5 m. The footwall is found at about 10 m depth. For production to proceed, the groundwater level was lowered to footwall by continuous pumping. Accordingly six boreholes were kept water free.

Later on, two boreholes (ST 7 and ST 8) 15 m apart and water-filled were drilled from the truck platform, before stripping the sandstone which is of about 9 m thickness. The ore is situated between the 9th and 15th m levels beneath the watertable, because of the distance of these boreholes from the ore face.

The probe was systematically passed down each borehole with both sources : Am/Be or Cf. The first source emits fast neutrons favouring measurement of phosphate while the second is preferable for measurement of silicon, calcium, iron and aluminium. However, the ore has a high water content which strongly modifies the spectrum of the Am/Be source and allows simultaneous detection of P_2O_5 , SiO_2 , CaO , Fe_2O_3 and Al_2O_3 by using only the Am/Be source.

The probe was raised at a speed of 6 m/h. Time acquisition was set at 5 minutes to get a sampling interval of 50 cm.

Calibration procedure was made using analysis of cores. For this purpose sampling was done in accordance with the integration steps of the probe, then the whole core was analysed in the laboratory by chemical methods.

Thirty samples taken in boreholes ST 2, ST 3, ST 5 and ST 8 were available. The first three holes were dry and the fourth was water filled. It was not possible to analyse phosphorus in the latter because of the water between the probe and the core wall (more than 3 cm, which is too much). Detection of phosphorus is restricted to dry boreholes. This doesn't lead to the condemnation of the method because the preproduction boreholes are near the ore face and thus the phosphate ore is generally above the level of the watertable. Analysis of elements detected from their capture gamma rays is sensitive enough.

A first study gave only about ten points correlated with the core analysis because of the ore heterogeneity. This population was used to draw the calibration curve. The peak area due to capture of neutrons by hydrogen was introduced in the model to take into account only the disturbances introduced by water which can be found both in the ore and in the borehole.

The relative errors are about 10 % (Fig. 8) including :

- Uncertainty related to analyses of cores when recovery is poor.
- Differences between analysis of cores and analysis related to activation of a volume surrounding the borehole. These two techniques can't give exactly the same results on the pseudo-homogeneous samples selected for calibration.

When calibration procedure is completed, the intensities acquired on the various boreholes are expressed as concentrations.

In some instances, large differences were revealed between the two analytical techniques, mainly because of ore heterogeneity. While the analysis on cores are very erratic from one borehole to another, analysis by activation reveals

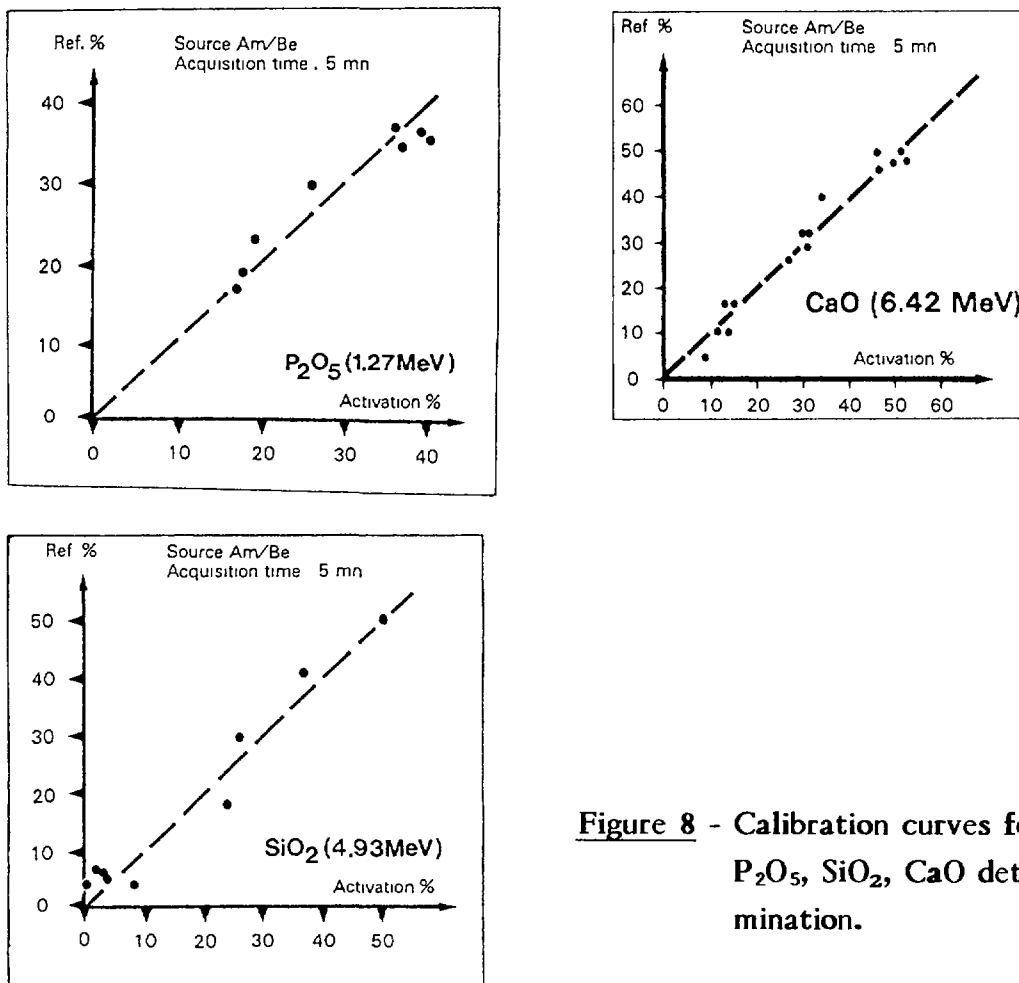


Figure 8 - Calibration curves for P_2O_5 , SiO_2 , CaO determination.

regionalization phenomena due to its better representativity : e.g. layering structure of silica in ore said to be heterogeneous and indicating a slight slope (Fig. 9).

7. DEVELOPMENT PROSPECTS and CONCLUSIONS

Activation analysis, by lowering drilling costs and giving better representativity, must provide a valuable aid in geostatistics for estimation of ore contents, either for deposit evaluation or contribution to selective exploitation (preproduction).

Several applications are interesting from the mining profession (non exhaustive list !):

- Nickel ore (Ni, Fe, Mg, Si).
- Bauxite and iron ores are more favourable cases than the Taiba phosphate because the mines have already preproduction problems and because there is no ore treatment before marketing. A good knowledge of the deposit is thus necessary to selectively extract ore including low contents of penalizing components.

Our feeling is that procedures indicated below are necessary to prove the well founded interest of "in-situ" analyses in preproduction holes :

- Selecting position of boreholes with aid of previous geostatistical studies.

① Ore with iron and aluminium (barren)

② P_2O_5 rich ore

③ Ore containing mainly flints

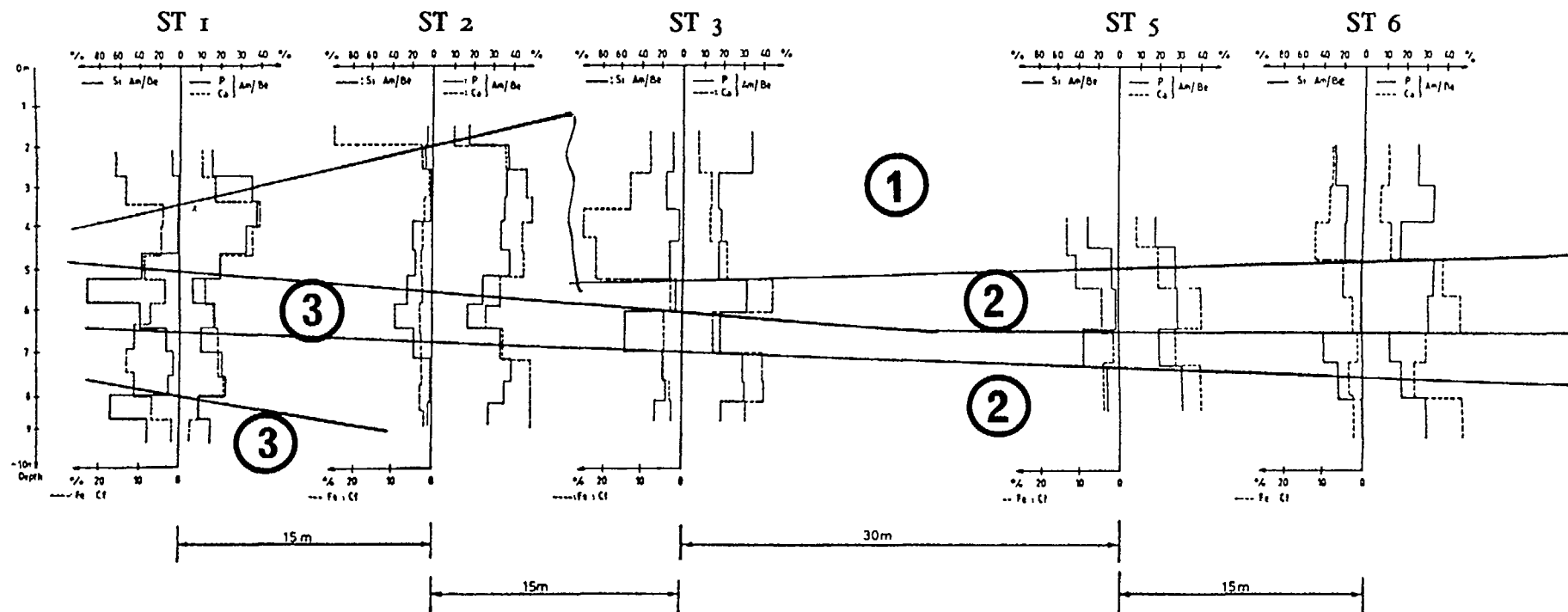


Figure 9 - Transversal section (parallel to the face) obtained from neutron activation in dry boreholes ST 1 to ST 6 (ST 4 not accessible).

- Calibrating "in-situ" the probe from core analyses.
- Interpretation of results by geostatistical methods to give three dimensional information.
- Comparison with contents previsions from known ore crushing.

The large volume participating in the reaction facilitates quantitative evaluation of deposits often difficult to get from analysis of cores alone. Its simple and quick implementation (about one hour for exploration of a 10 m borehole with a sampling interval of 1 m for phosphates) considerably decreases costs related to preproduction operations, provided that drilling techniques (percussion in this case) are adapted. A synchronism must be established between drilling and analysis because this analysis must be realized immediately after completion of the borehole to guarantee its quality (installation of casing should be prohibitive).

Simultaneous analysis of many important elements must establish unambiguously facies differentiation.

The experiments carried out at Taiba should also be undertaken on a mine where preproduction operations are used to get valuable results for geostatistical interpretation. This step must be overcome to get approval of people involved in the field.

Acknowledgement

This work was supported by EEC Grant MSM - 030 F (RS) and by B.R.G.M.

We wish to acknowledge the assistance and cooperation of the staff of the Société Sénégalaise des Phosphates de Taiba throughout this investigation.

REFERENCES

- [1] Nuclear Techniques and Mineral Resources 1977 (Proc. Symp. Vienna, 1977). IAEA, Vienna (1977).
- [2] "Nuclear Methods in Mineral Exploration and Production", developments in economic geology, Vol. 7 (MORSE, J.G., Ed.), Elsevier Scientific publishing company (1977).
- [3] "Nuclear Geophysics". Selected papers on applications of nuclear techniques in mineral exploration, mining and process control(CLAYTON, C.G., Ed.), Pergamon Press (1983).

**ANALYSIS OF BORON, SAMARIUM AND GADOLINIUM
IN ROCK SAMPLES BY NEUTRON CAPTURE
GAMMA RAY SPECTROMETRY**

C.W. TITTLE
Department of Physics,
Southern Methodist University,
Dallas, Texas

M.D. GLASCOCK
Research Reactor Facility,
University of Missouri,
Columbia, Missouri

United States of America

Abstract

Prompt gamma neutron activation analysis (PGNAA) is useful for determining many of the elements found in sedimentary rocks. It is particularly suitable for the trace elements boron, samarium and gadolinium. The sensitivity of detection can be of the order of 0.1 part per million with an adequate neutron source. Twenty-five sedimentary rock samples were analyzed in the PGNAA facility at the University of Missouri Research Reactor. The materials included Ottawa sand, Berea sandstone, Royer dolomite and several other formations of interest in the petroleum industry. Results of the analyses are presented. Correlations of gadolinium and samarium and of boron with the sum of samarium and gadolinium are given.

1. INTRODUCTION

Availability of an adequate neutron source can make prompt neutron-gamma spectrometry (PGNAA, meaning prompt gamma neutron activation analysis) a useful tool for analyzing rock samples for certain elements. The equipment required is relatively expensive and complicated [1]; thus, other analytical methods will often be more suitable for many elements. Nonetheless, the method has been employed rather extensively for elemental analyses of rocks and soils [1] [2] [3] [4] [5] [6]. The cited references may be consulted for more extensive lists of references.

In the case of the trace elements boron, samarium and gadolinium, PGNAA seems particularly suitable because of the good sensitivity exhibited. These elements are of especial interest in neutron well logging because they are strong absorbers of thermal neutrons.

The PGNAA facility at the University of Missouri Research Reactor Facility (MURR) has been described in detail [7]. It features a filtered external thermal neutron beam from a

horizontal port of the 10-MW research reactor. The flux at the sample location is 5×10^8 neutrons/cm²/sec. The gamma rays are analyzed by a germanium spectrometer. At the time of the measurements reported here, the detector element was 18 per cent Ge(Li), since replaced by 25 per cent intrinsic germanium.

We had a particular interest in looking at Ottawa sand, Berea sandstone and Royer dolomite, materials that have several uses in the petroleum industry. Ottawa sand (produced by Ottawa Silica Company, Ottawa, Illinois) has been widely used in the construction of model wells for nuclear well log calibration. Berea sandstone (available from Cleveland Quarries, Amherst, Ohio) is a standard reference material for core analysis and has also seen some application in model wells. Royer dolomite (supplied by Delta Mining Company, Mill Creek, Oklahoma) has been used in model wells, though its major uses are in glass manufacture and as a mineral additive in animal feed.

2. RESULTS WITH OTTAWA SAND

Ottawa sand is a nearly pure quartz sand; clay is washed out before drying and packaging. Ten samples were analyzed. Four came from different batches of Standard Sand, 20-30 mesh, ASTM Designation C-190. The fifth sample was a finer "Crystal" sand. The last five samples came from a completely separate batch. The results are given in Table I, where the entries are in parts per million. Very little boron was detected in Ottawa sand. The limit of sensitivity was about 0.2 ppm with about a four-hour count for the first five samples. A longer count gave a sensitivity of 0.1 ppm for the last five samples. The sensitivity to Sm or Gd was estimated to be 0.1 ppm or better. The measurements show a reasonable degree of homogeneity among the ten samples. In the case of all three elements, interferences from other elements were minimal. The gamma-ray energies used were the Doppler-broadened 477 keV line for B, 334 keV for Sm and 182 keV for Gd. There is potential interference to B from a 472-keV line of Na, but there was no sodium in the Ottawa sand samples.

Table I

OTTAWA SAND

No.	1	2	3	4	5	6	7	8	9	10
B	<0.2	<0.2	<0.2	<0.2	<0.2	<0.1	<0.1	<0.1	0.12	0.34
Sm	0.26	0.23	0.17	0.26	0.22	0.30	0.22	0.28	0.39	0.39
Gd	0.21	0.18	0.19	0.17	0.14	0.22	0.20	0.20	0.31	0.32

3. BEREA SANDSTONE

The five samples of Berea sandstone came from various batches of the material. The results are given in Table II. The variations shown for boron are largely real; the probable error does not exceed 2 ppm. These variations are undoubtedly related to changes in clay content. The variations indicated for Sm and Gd are within the error of measurement.

Table II
BEREA SANDSTONE

Sample No.	1	2	3	4	5
B, ppm	18.6	12.9	14.5	13.9	17.3
Sm, ppm	1.4	1.4	1.4	1.2	1.6
Gd, ppm	1.0	1.0	1.1	1.0	1.2

4. ROYER DOLOMITE

Royer dolomite, a clean carbonate rock from Oklahoma, is highly dolomitized. Six samples of this rock were analyzed. The first came from one batch; the last five came from a different batch. The results are shown in Table III. It can be seen that the different batches had rather different boron and samarium contents.

TABLE III
ROYER DOLOMITE

Sample No.	1	2	3	4	5	6
B, ppm	0.8	2.68	2.65	2.50	2.83	2.15
Sm, ppm	0.18	0.46	0.38	0.29	0.55	0.30
Gd, ppm	0.17	0.22	0.16	0.15	0.13	0.17

5. OTHER GEOLOGICAL MATERIALS

The measurements given for Ottawa sand, Berea sandstone and the last five Royer dolomite samples have not previously been reported. The last five Ottawa sand samples of Table I and the last five Royer dolomite samples of Table III were part of the samples distributed by the IAEA in the absorption cross section standardization program [8]. Several other rocks have been measured [6] in the same PGNA facility, however, as shown in Table IV; the first Royer dolomite sample was reported there as well. Austin chalk is a fairly clean limestone from Texas. Viola limestone is an oil-bearing Oklahoma formation; it contains appreciable amounts of clay and quartz.

Table IV

OTHER GEOLOGICAL MATERIALS

	Austin Chalk	Viola Limestone	Shale No. 1	Shale No. 2
B, ppm	8.5	21.1	80.4	61.5
Sm, ppm	0.40	1.17	5.99	1.79
Gd, ppm	0.39	1.01	4.92	1.58

6. DISCUSSION

The tables show at a glance that the Gd content is related to the Sm content, as is verified by Fig. 1, which shows what is essentially a proportionality:

$$Gd = -0.0482 + 0.8264 Sm$$

with standard error of 0.11 ppm and a correlation coefficient of 0.996. To avoid overcrowding of the plotted points, the Ottawa sand samples were treated as two points, each being the average of five. There is, in these samples, also a fair linear correlation between boron and the sum of Sm and Gd with a standard error of 1.10 ppm and a correlation coefficient of 0.906:

$$Sm + Gd = 0.3994 + 0.1025 B.$$

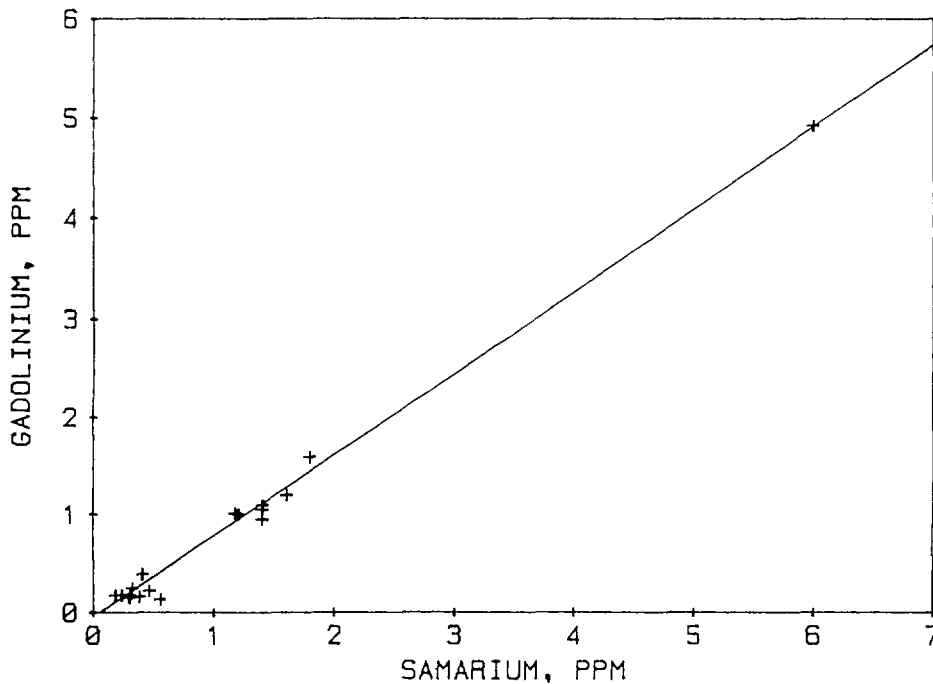


FIG. 1. CORRELATION OF SAMARIUM AND GADOLINIUM IN 17 ROCK SAMPLES

See Fig. 2. There is little doubt that the correlations reflect the relationship of these trace elements to the clay and feldspar fractions of the rocks.

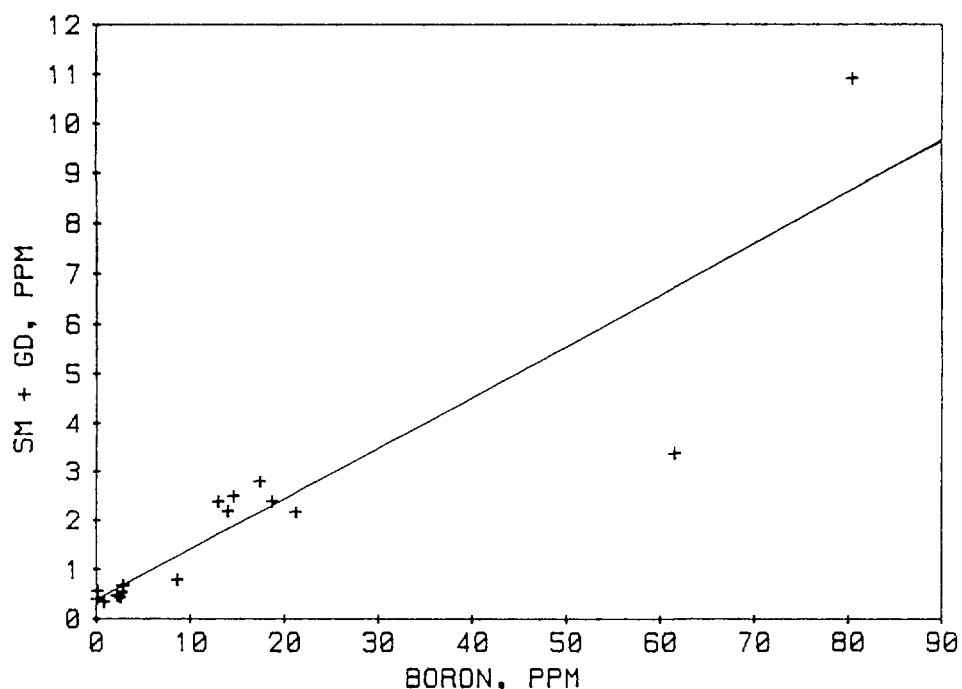


FIG. 2. CORRELATION OF BORON AND SM + GD IN 17 ROCK SAMPLES

7. CONCLUSION

Prompt neutron-gamma spectrometry is an effective analytical method for determining boron, samarium and gadolinium in rocks to levels well below 1 part per million. Ottawa sand, Berea sandstone and Royer dolomite, three geological materials that have application in the petroleum industry, are given as examples. The expected correlation between samarium and gadolinium is exhibited in these samples, supplemented by previous measurements of carbonate rocks and shales. There is also a fairly pronounced relationship of boron to samarium and gadolinium.

8. ACKNOWLEDGMENT

The authors express their appreciation to Gearhart Industries, Inc., for support of this project.

9. REFERENCES

- [1] CHRIEN, R.E., KANE, W.R., (Eds.), Neutron Capture Gamma Ray Spectroscopy, Plenum Press, New York (1979).
- [2] GLASCOCK, M.D., Practical Applications of Neutron-Capture Reactions and Prompt Gamma Rays, Inst. Phys. Conf. Ser. No. 62, Chapter 4. Paper presented at 4th (neutron, gamma) Int. Symp., Grenoble, 7-11 September 1981.
- [3] JAMES, W.D., GRAHAM, C.C., GLASCOCK, M.D., HANNA, A.G., Water-Leachable Boron from Coal Ashes, Environ. Sci. Technol. 16 (1982) 195.

- [4] EVANS, L.G., LAPIDES, J.R., TROMBKA, J. I., JENSEN, D.H.,
In Situ Elemental Analysis Using Neutron-Capture Gamma-
Ray Spectroscopy, Nucl. Instr. and Meth. 193 (1982) 353.
- [5] GRAHAM, C.C., GLASCOCK, M.D., CARNI, J.J., VOGT, J.R.,
SPALDING, T.G., Determination of Elements in National
Bureau of Standards' Geological Standard Reference
Materials by Neutron Activation Analysis, Anal. Chem. 54
(1982) 1623.
- [6] GLASCOCK, M.D., COVENEY, R.M. Jr, TITTLE, C.W., GARTNER,
M.L., MURPHY, R.D., Geochemical Applications for Prompt
Gamma Neutron Activation, Nucl. Instr. and Meth. in
Physics Research B10/11 (1985) 1042.
- [7] HANNA, A.G., BRUGGER, R.M., GLASCOCK, M.D., The Prompt
Gamma Neutron Activation Analysis Facility at MURR, Nucl.
Instr. and Meth. 188 (1981) 619.
- [8] CZUBEK, J.A., DROZDOWICZ, K., GABAŃSKA, B., IGIELSKI, A.,
KRYNICKA-DROZDOWICZ, E., Ottawa Sand, Royer Dolomite and
Dunite Sand as Reference Samples for the Thermal Neutron
Absorption Cross-Section, Nuclear Geophysics 1 4 (1987)
291.

**THE MONTE CARLO LIBRARY LEAST-SQUARES ANALYSIS
PRINCIPLE FOR BOREHOLE NUCLEAR WELL LOGGING
ELEMENTAL ANALYZERS**

K. VERGHESE, R.P. GARDNER, M. MICKAEL,
C.M. SHYU, T. HE
Department of Nuclear Engineering,
North Carolina State University,
Raleigh, North Carolina,
United States of America

Abstract

Monte Carlo simulation is an ideal way to generate the spectral response of well logging tools which are based on the (n, γ) technique. The primary use of Monte Carlo models in the past has been in the calibration of tools and log interpretation. Recently, it has been recognized that Monte Carlo simulation can also be used directly for the analysis of elemental composition. This new analysis principle combines the power of Monte Carlo for accurate simulation of the spectrum of each of the elements that are present in the formation with the linear library least-squares method for the determination of elemental amounts. The methodology of Monte Carlo - Library Least Squares Analysis is based on the following procedure: (1) for an assumed composition of the formation, generate the complete spectral response by Monte Carlo, (2) within the program, keep track of the individual spectral responses for each element, (3) using the library least-squares analysis method, calculate the elemental amounts in the formation using the measured spectrum of that formation and the individual elemental spectra from the Monte Carlo simulation as the library standards, and (4) if the elemental amounts calculated in step 3 are not close enough to those assumed in step 1, repeat steps 1 through 3 using an assumed composition that is closer to the that of the formation. Preliminary results from the application of this method to X-ray and neutron capture gamma-ray spectra show considerable promise and can be adapted for elemental composition analysis using spectral nuclear logging tools .

1. INTRODUCTION

Monte Carlo simulation is becoming a very important tool for modelling the responses of well-logging sondes. The literature on this subject is rather vast, but a recent survey by Butler [1] discusses many of the references on Monte Carlo simulation using general purpose codes which were originally written for nuclear reactor shielding computations and later adapted for nuclear well-logging simulation. As Butler points out, the use of general purpose reactor codes for nuclear logging applications requires considerable skill and artistry. Based on prior experience with general purpose reactor shielding codes, several years ago the authors decided to discard their use in simulating nuclear analyzer problems and started developing specific purpose Monte Carlo codes. The motivation for developing specific purpose codes is well-documented by the authors [2,3]. The specific purpose codes are generally more efficient and easier to use than

the general purpose codes because the Monte Carlo methodology is optimized for the particular types of problems that such codes are designed for. Laboratory benchmark tests of the spectra that are generated by these Monte Carlo codes show excellent agreement with experiments [4,5]. This gives credence to the concept of simulating spectral responses of nuclear analyzer systems very accurately and efficiently and using them for the design and calibration of analyzer systems.

Recently, it occurred to us that it might be feasible to use our Monte Carlo simulation programs for solving the inverse problem of elemental analysis, namely, the problem of obtaining elemental concentrations from the measured spectrum of a sample of unknown composition. The generally recognized difficulty in performing analysis, for example, by neutron capture gamma-ray spectroscopy, is that the gamma-ray response of any of the elements in the sample is a function of the amounts of all the other elements that are present in the sample. This destroys the linearity between the counting rate for an element and its weight fraction in the sample. This is generally true of most analysis situations and is particularly true in the analysis of bulk materials. It is usually very difficult and expensive (or in some cases impossible) to calibrate the analysis system experimentally for all of the elements by taking into account the effects of every other element. An elegant method that is feasible, in principle, for determining the elemental composition is the Library Least Squares (LLS) method as originally proposed by Salmon [6]. In this method, it is assumed that the spectral response resulting from a unit amount of every element that constitutes the sample spectrum (called the library spectrum for that element) is known so that the sample spectrum counting rate in any one of the pulse height channels is a linear combination of the amounts of each of the elements multiplied by the counting rate in the same channel of the library spectra. The amounts of the different elements are then extracted from this set of linear equations by least-squares minimization. This is a very versatile method so long as one can assume linearity between the library spectra and the spectrum of the unknown sample and so long as the library spectra can be obtained for the various elements. It is possible to implement this for practical analysis problems involving thin samples as demonstrated by Gardner and Arinc for the X-ray fluorescence analysis of air filters [7]. The LLS method is powerful because it uses all of the information that is present in the measured spectrum, it yields an estimate of the standard deviation for the elemental amounts, and is capable of detecting elements that may have overlapping peaks in the spectrum. Its application to bulk material analysis such as in borehole logging is complicated by the difficulty of obtaining reliable library spectra of the elements since they are affected by other elements present in the sample. Such spectra are impossible to determine directly by experimental methods and in situations where the LLS method has been utilized in spectral logging [8], it is not clear how the library spectra were determined. On the other hand, if one has an accurate Monte Carlo simulation model, the computation of the library spectra is a very simple bookkeeping task within the code.

This paper presents some preliminary results of the use of Monte Carlo simulation in conjunction with the application of the LLS method to analyzers (hereafter referred to as the MC-LLS method). We start with a discussion of our approach to Monte Carlo simulation of radiation analyzer systems. The MC-LLS method and the results of its application to X-ray fluorescence analysis and (n, γ) analysis are pre-

sented next. The paper concludes with a discussion of the MC-LLS method to other problems including spectral tools for borehole logging .

2. MONTE CARLO SIMULATION OF NUCLEAR ANALYZERS

Monte Carlo simulation at the Center for Engineering Applications of Radioisotopes has been pursued for three different types of nuclear analyzers during recent years: (1) X-ray fluorescence analysis, (2) on-line neutron capture prompt gamma ray analysis in the conveyor belt geometry and in the borehole geometry using steady state neutron sources, and (3) pulsed neutron borehole logging including gamma-ray spectroscopy. In all of these cases, the authors have relied on developing specific purpose Monte Carlo codes rather than adapting existing general purpose codes. The specific purpose codes generally can be made to be more computationally efficient than the general purpose codes because the variance reduction methods can be optimally chosen for the specific types of problems, they run on small mini and microcomputers, and they are easier to use than the general purpose codes.

Unlike the general purpose codes such as MCNP [9], our specific purpose codes do not use importance regions and splitting as the primary variance reduction method. In logging problems and other radiation analyzer problems a large number of importance regions are required when this technique is used and tracking of particles through these regions require an extensive amount of computation. Furthermore, the determination of near-optimum importance values necessitates the use of other transport codes and computations prior to the start of the Monte Carlo simulation [1]. The primary variance reduction method that is incorporated widely in our codes is the statistical estimator at each interaction site. For example, in an (n, γ) problem, at each interaction site, the capture gamma rays from a sampled element are generated and their scores in the detector(s) are estimated and tallied to give the unscattered photon score. Additionally, the scattered photons are followed and their score for scattering toward and interacting in the detector(s) are also estimated and tallied to yield the scattered photon scores. The authors have developed a very efficient algorithm [10] for forcing the scattered particles towards cylindrical detectors which makes this an efficient and powerful variance reduction method. Only the energy distribution of the photons which interact in the detector(s) is computed using Monte Carlo. This distribution is then convolved with the spectral response function of the detector to generate the simulated pulse height spectra. The detector response functions are predetermined as fitted analytical functions of photon energy for the various features of a photon detector pulse-height spectrum. The methodology for the determination of these spectral response functions is described by Yacout, et al [11] for Si(Li) detectors and by Jin, et al [12] and Lee, et al [13] for Ge detectors. The use of the detector response function is another very powerful variance reduction method.

The Monte Carlo code for X-ray fluorescence analysis is described by Yacout, et al [5]. Figure 1 shows a comparison of the X-ray spectrum from a sample of austenitic stainless steel containing six elements excited by a ^{109}Cd source with the Monte Carlo simulated spectrum for the same sample. It is clear that the fluorescence region of the spectrum agrees almost exactly with the Monte Carlo simulation. The

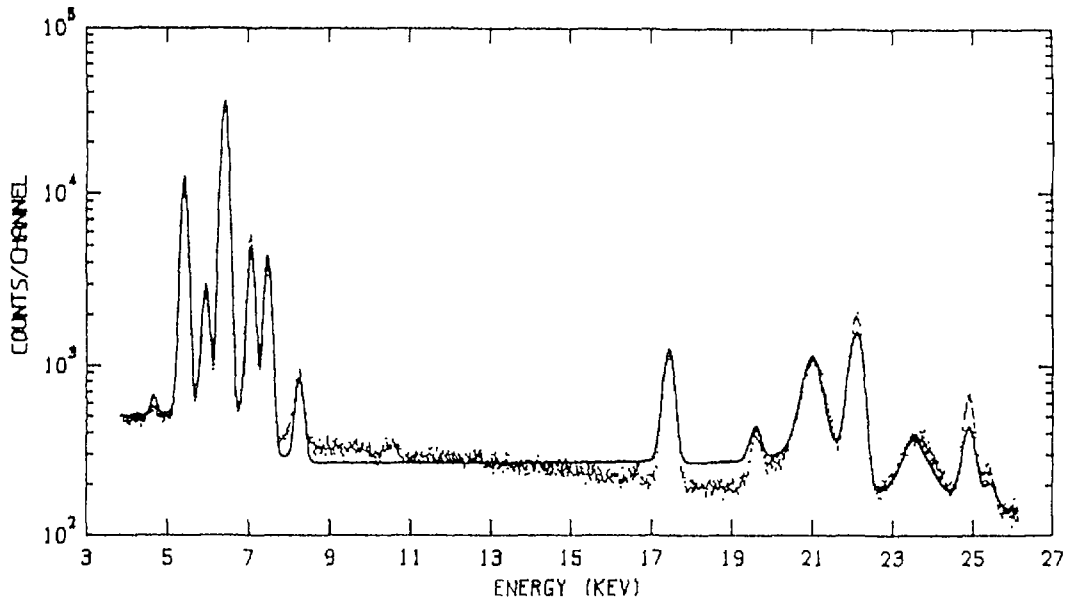


Figure 1. X-ray fluorescence spectrum from austenitic stainless steel (dots are experimental data, line is Monte Carlo simulation).

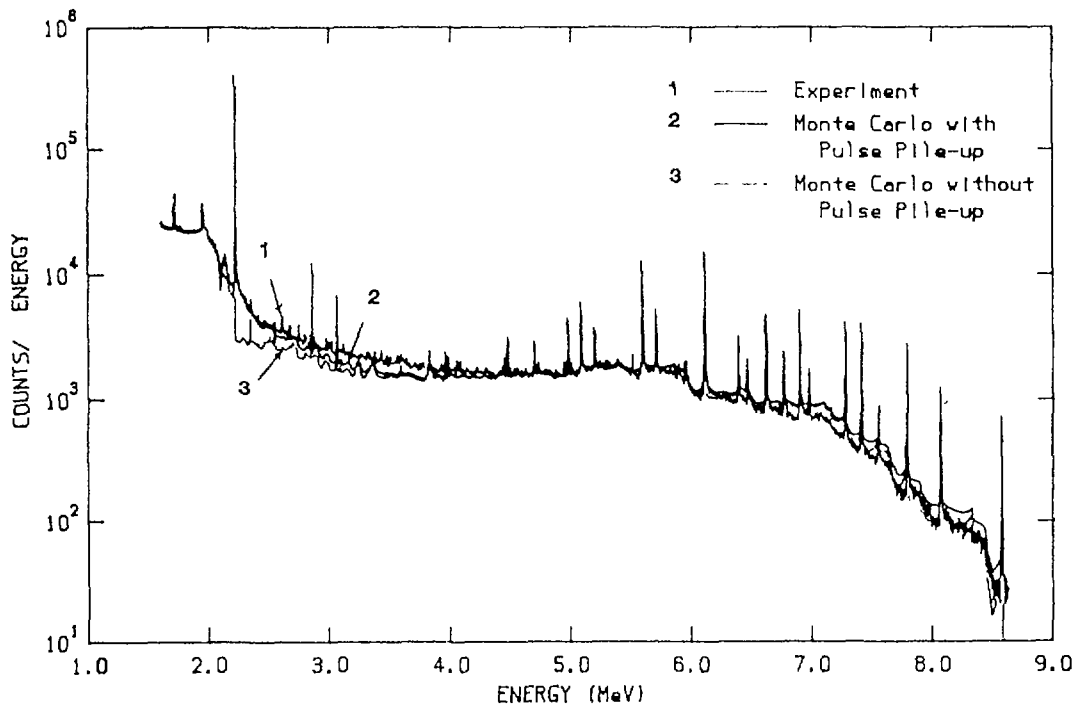


Figure 2. Comparison of the experimental spectrum to the Monte Carlo spectrum (corrected for pulse pile-up) for the (n, γ) analysis of a NaCl solution in borehole geometry.

source backscatter spectrum shows some disagreement, mainly because the detector response function had not been determined adequately for the backscatter source energy range.

The Monte Carlo simulation of (n, γ) analysis in the borehole geometry is discussed by Jin, et al [4] for a laboratory system containing a ^{252}Cf neutron source and a 39% Ge detector in a sonde that was centrally located in a large cylindrical tank of salt water. Figure 2 shows the comparison of the experimental spectrum for this case with the Monte Carlo simulation. The Monte Carlo spectrum corrected for pulse pile up agrees closely with the measured spectrum.

It is clear from these results that the approach of Monte Carlo simulation combined with the detector spectral response convolution is capable of accurate forward simulation of pulse-height spectra from nuclear analyzers. Figure 3 shows the gamma-ray spectrum from a pulsed neutron logging tool with a 14 MeV, 60 microsecond duration pulse and a Ge detector [3]. No data is as yet available to benchmark this spectrum, but it illustrates that the pulsed neutron Monte Carlo model has the capability of simulating photon pulse-height spectra within any specified time interval after the neutron burst .

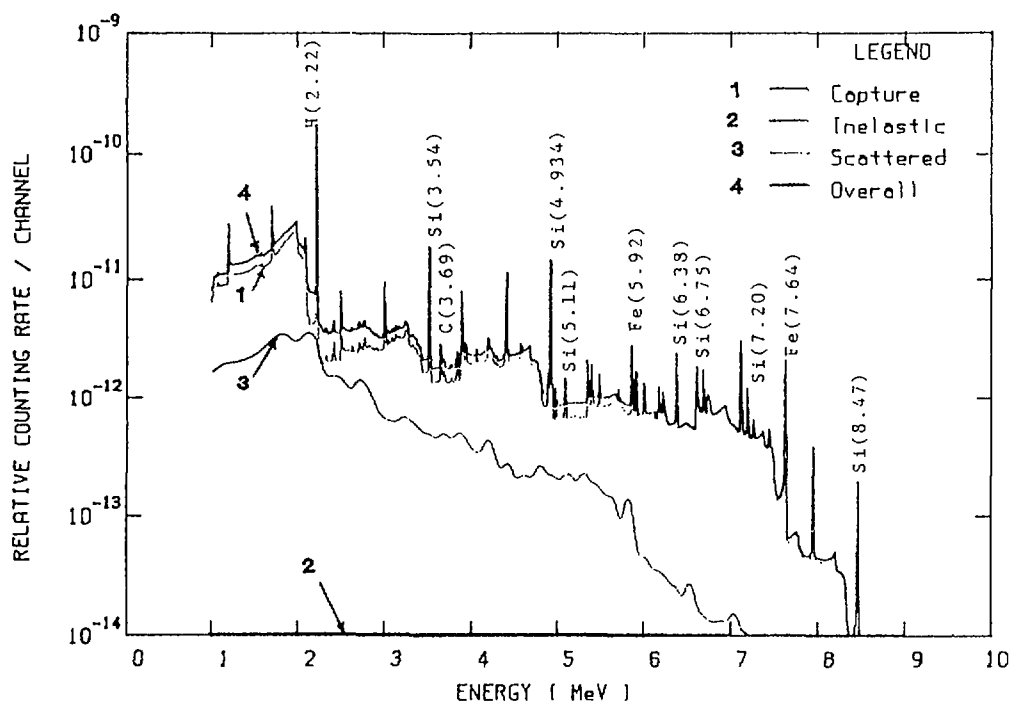


Figure 3. Monte Carlo generated spectrum for a pulsed neutron spectral tool within 600 – 800 μ sec from neutron burst. Fresh water in borehole, oil in quartz formation.

3. THE MONTE CARLO - LIBRARY LEAST-SQUARES METHOD

The basic requirement in applying the MC-LLS principle is an accurate forward simulation model which takes into account all of the interelement effects. The interelement effects naturally become a part of the Monte Carlo results because the

Monte Carlo simulation includes all of the natural interaction mechanisms between the radiation and the medium. In X-ray fluorescence simulation the interelement effects occur primarily by the enhancement of X-ray intensities of a given element due to the secondary and tertiary excitations of that element by the X-rays from elements of higher atomic number and the absorption of X-rays from a given element by the elements with lower atomic number. In (n, γ) analyzers, the interelement effects arise from the competition between the various elements for scattering and absorption of neutrons and photons. In Monte Carlo simulation, all of these effects are accounted for using fundamental physics parameters and known interaction probabilities. Thus a Monte Carlo simulation code is able to generate all of the required library spectra simply by keeping track of the individual scores from all of the photons that are generated by each of the elements provided that the elemental composition of the sample is known. Unfortunately, it is this composition that the analyst is trying to obtain and so the MC-LLS procedure must start with an approximate initial estimate of the composition. In X-ray analysis, such an estimate of the composition might be obtained by estimating the peak areas in the measured sample spectrum and correcting them for the differences in the jump ratio, and the fluorescence yield of the different elements assuming an infinitely thick sample and only primary excitation [14]. In (n, γ) analysis, the initial estimate of the composition might be obtained by correcting the peak areas for differences in their neutron absorption cross sections, their capture gamma-ray yields, and the peak efficiencies of the detector for the different gamma-ray energies. With an approximate initial estimate C_{i1} for the concentration of element i in sample 1, let us assume that we obtain from the Monte Carlo simulation M_{ij1} as the counting rate per unit concentration of element i in channel j for sample 1. Then, if E_{ju} is the measured counting rate in channel j for the sample of unknown composition, we can write

$$E_{ju} \simeq \sum_{i=1}^m C_{i1} M_{ij1} + e_{ju} \quad (1)$$

where e_{ju} is the random error in channel j for the unknown sample. We proceed to solve this equation by minimizing the sum of the squares of the error. Thus we wish to minimize

$$s = \sum_{j=1}^n [E_{ju} - \sum_{i=1}^m C_{i1} M_{ij1}]^2 \quad (2)$$

Minimization of s with respect to C_{i1} gives a set of m linear equations that can be solved for a new estimate of the vector of elemental concentrations C_{i2} ($i = 1, 2, \dots, m$). If C_{i2} is sufficiently close to C_{i1} , we accept C_{i2} as the elemental concentration vector of the sample. If not, we use C_{i2} as the new concentration vector and regenerate the library spectra for a sample of this composition. In most analyzer problems, it is expected that the library spectra computed using an assumed composition will be sufficiently accurate to require no more than one such iteration. Rather than use the C_{i2} vector as the new estimate of the elemental composition, it might be possible to accelerate the convergence of the iteration scheme by adjusting the elemental concentrations based on the residuals of the library least-squares search, but this will have to be investigated.

The MC-LLS procedure offers possibilities other than simply searching on elements which generate significant photon intensities. There may be elements which do not produce significant photon intensities but contribute, nevertheless, by particle scattering to the overall spectrum. A typical example is oxygen in the case of the thermal neutron induced capture gamma ray spectra. If one were to generate library spectra also based on the element of neutron or gamma-ray scattering in an (n, γ) analyzer, it might be possible to use those libraries to obtain the elemental amounts of the scattering element such as oxygen. In any radiation analyzer system the contribution to the measured spectrum from the surrounding media are very significant; for example, in the case of spectral logging, the measured spectra contain contributions from the tool, the borehole, the casing, and the cement region. The library spectra from these regions must be incorporated into the MC-LLS procedure in addition to the elemental spectra from the formation.

4. PRELIMINARY RESULTS FOR ENERGY DISPERSIVE X-RAY FLUORESCENCE ANALYZERS

Table I shows the results of a simulated application of the MC-LLS method for a Cu-Ni alloy. The actual elemental composition of this material is shown in the first column. The pulse-height spectrum of the fluorescent X rays and the source backscatter was simulated by Monte Carlo and this spectrum was used as the spectrum of the unknown sample. The second column of Table I shows the composition that was used with Monte Carlo simulation to give a first estimate to compute the library spectra. Figure 4 shows one of these library spectra. The photons which backscattered from this element and was detected are included as part of the library spectrum. The source was assumed to be the silver X rays from ^{109}Cd . The third column in Table I gives the composition that was generated by a linear LLS calculation as described in Section 3. The agreement of this composition with the actual composition of the sample (column 1) is excellent and no iteration is necessary. The subsequent pairs of columns show other assumed compositions and the corresponding LLS values. Note that the calculated values do not deviate significantly from the actual composition unless the guessed values of the weight fractions of the minor constituents, Fe and Mn, are far from the actual values.

Table I.
Simulated Results for the Application of MC-LLS
to Energy Dispersive X-ray Fluorescence Analysis

Element	Actual (%)	Assumed (%)	LLSQ (%)	Assumed (%)	LLSQ (%)	Assumed (%)	LLSQ (%)
Cu	69.5	60.0	69.3	35.0	68.3	25.0	67.3
Ni	29.2	35.0	29.7	50.0	30.8	25.0	31.9
Fe	0.42	2.50	0.43	6.00	0.43	25.0	0.36
Mn	0.46	2.50	0.48	9.00	0.47	25.0	0.34

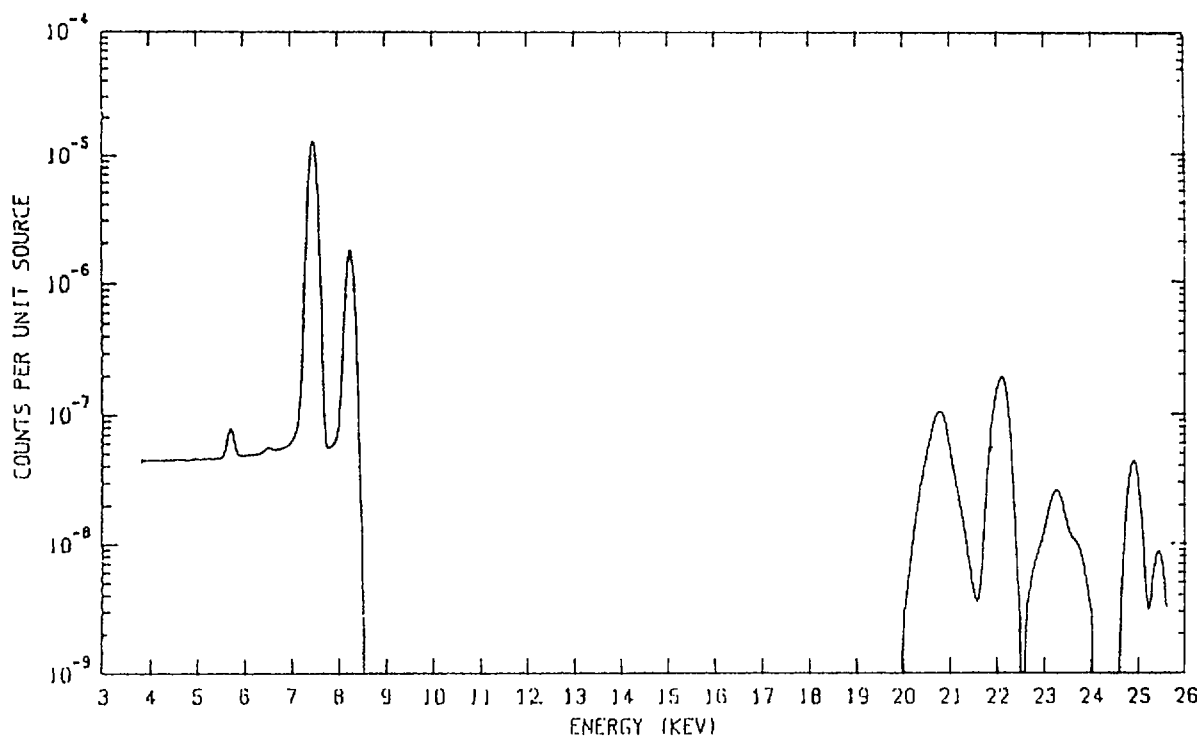


Figure 4. Nickel fluorescent X-ray and source backscatter spectrum generated by Monte Carlo for a Cu-Ni alloy (see Table I for composition)

Similar simulations have been conducted for several other cases of the same alloy and for an austenitic stainless steel containing six elements. The results for all these cases essentially conform to the results of Table I .

5. PRELIMINARY RESULTS FOR NEUTRON CAPTURE PROMPT GAMMA-RAY ANALYZERS

Simulation of the (n, γ) analysis problems are currently underway for a coal analyzer model in the conveyor belt geometry as described by Jin, et al [4]. The system contains a source of ^{252}Cf fission neutrons incident on a rectangular bed of coal and the capture gamma rays are detected using either a Ge or a NaI(Tl) detector in transmission geometry. The coal sample was assumed to contain the concentrations of elements that are shown in Table II. In addition to the elemental spectra from these elements, the Monte Carlo code also generates the pulse height spectra due to the fission gamma rays and the capture gamma rays that are produced by elements in the shielding and other components of the system. Figure 5 shows the total spectrum from the entire system and the library spectrum of chlorine as a typical spectrum simulated by Monte Carlo and the response function for a 39% Ge detector. One of the authors (RPG) is presently developing a spectral response function for large NaI(Tl) detectors. A preliminary version of this response function was also used to study the applicability of the MC-LLS method to coal analysis. Using the total spectrum and the library spectra that exactly constituted the total spectrum, a search was made on the coal composition. Oxygen was not included in the search since its contribution to the total spectrum was insignificantly small (about four orders of magnitude less than the total spectrum). The results as shown in Table II (column 4) verify that the MC-LLS

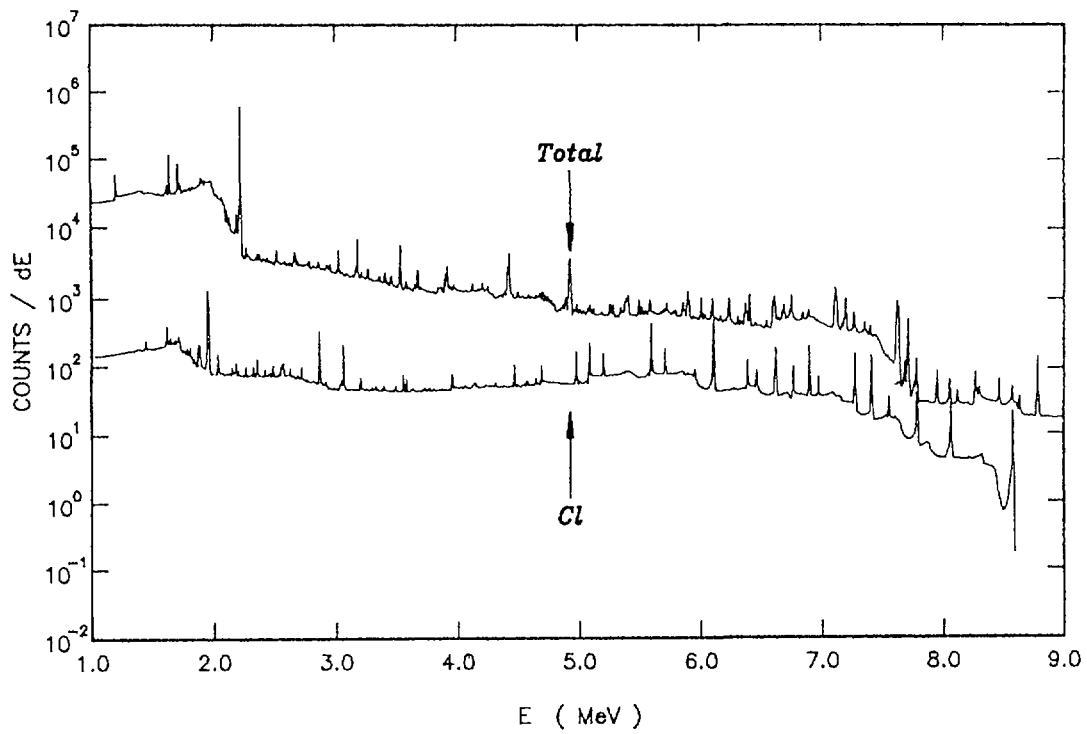


Figure 5 Monte Carlo Simulated Spectra for Coal and One of Its Constituents (Cl)

Table II.
Simulated Results for the Application of MC-LLS
to Neutron Capture Prompt Gamma-ray Analysis of Coal

Element	Actual (%)	Assumed (%)	LLSQ (%)
H	4.853	4.853	4.853
C	48.503	48.503	48.490
N	3.475	3.475	3.475
Al	0.788	0.788	0.789
Si	12.509	12.509	12.510
S	8.000	8.000	8.000
Cl	0.128	0.128	0.128
Ca	0.175	0.175	0.175
Ti	0.042	0.042	0.042
Fe	1.423	1.423	1.423
O	20.000	—	—
Na	0.0444	0.0444	0.0442
Mg	0.0596	0.0596	0.0610

procedure is valid. A search made with oxygen included in the set of libraries gave negative values for the weight fraction of oxygen, presumably due to roundoff error in the matrix inversion for the library least-squares analysis. It is quite likely that the MC-LLS procedure as implemented in this investigation will not have sensitivity for those elements which only make minor contributions to the overall spectrum. Work is currently underway to generate Monte Carlo spectra from a coal sample with a different composition from the one given in Table II. Then these spectra will be used to calculate the composition of the coal given in Table II .

6. DISCUSSION, CONCLUSIONS, AND FUTURE WORK

We have established that specific purpose Monte Carlo simulation codes combined with detector response functions can yield accurate pulse-height spectrum simulations for X-ray fluorescence and (n, γ) analyzers. Preliminary investigations show that these codes may be used to generate library spectra for the library least-squares search method for the elemental analysis of samples. In principle, the Monte Carlo - Library Least Squares analysis principle offers a powerful method that could be exploited in the analysis of formations using spectral logging tools.

The practical limits on the successful application of this method will likely depend on the number of elements to be included in the analysis and their relative contributions to the total pulse height spectrum of the sample. Studies are presently underway to investigate these limits and to determine the optimum implementation of the MC-LLS method .

ACKNOWLEDGEMENTS

The authors would like to acknowledge the support of the National Science Foundation through Grant No. CBT-8311425 and the interest, encouragement, and financial support provided by the Amoco, Mobil, Standard Oil, and ARCO oil companies through an industrial associates program supporting the Center for Engineering Applications of Radioisotopes .

REFERENCES

1. Butler, J., "A forward look at the calibration and correction of nuclear logging tools", SPWLA Twenty-Eighth Annual Logging Symposium, Paper INV-NU, June 29-July 2 (1987).
2. Gardner, R.P., Verghese, K., Use of Monte Carlo methods in the calibration and design optimization of radiation gauges and analyzers, *Isotopenpraxis* 19 10 (1983) 329.
3. Choi, H.K., Verghese, K., Gardner, R.P., Monte Carlo simulation of the temporal and spectral responses of the pulsed neutron logging principle, *Nucl. Geophys.* 1 (1987) 71.

4. Jin, Y., Gardner, R.P., Verghese, K., A Monte Carlo model for the complete pulse-height spectral response of neutron capture prompt γ -ray analyzers for bulk media and borehole configurations, Nucl. Geophys. 1 (1987) 167.
5. Yacout, A.M., Gardner, R.P., Verghese, K., Monte Carlo simulation of the X-ray fluorescence spectra from multielement homogeneous and heterogeneous samples, Advances in X-Ray Analysis (Proc. 35th Annual Denver Conference) -in Press.
6. Salmon, L., Analysis of gamma-ray scintillation spectra by the method of least squares, Nucl. Instr. Methods, 14 (1961) 193.
7. Arinc, F., Gardner, R.P., Wielopolski, L., Stiles, A.R., Application of the least-squares method to the analysis of XRF spectral intensities from atmospheric particulates collected on filters, Adv. X-Ray Anal., 19 (1975) 367.
8. Westway, P., Hertzog, R., Plasek, R.E., Neutron-induced gamma ray spectroscopy for reservoir analysis, Trans. Soc. Pet. Eng., 275 (1983) 553.
9. "MCNP-Monte Carlo neutron and photon transport code", Rep. LA-7396-M, Los Alamos Monte Carlo Group, Los Alamos, NM (1981).
10. Mickael, M., Gardner, R.P., Verghese, K., An improved method for estimating particle scattering probabilities to finite detectors, Nucl. Sci. Engg., (in press).
11. Yacout, A.M., Gardner, R.P., Verghese, K., A semi-empirical model for the X-ray Si(Li) detector response function, Nucl. Instr. Methods, A243 (1986) 121.
12. Jin, Y., Gardner, R.P., Verghese, K., A semi-empirical model for the gamma-ray response function of germanium detectors based on fundamental interaction mechanisms, Nucl. Instr. Methods, A242 (1986) 416.
13. Lee, M.C., Verghese, K., Gardner, R.P., Extension of the Semi-Empirical Germanium Detector Response Function to Low Energy Gamma Rays, Nucl. Instr. Methods, (in press).
14. Gardner, R.P., Ely, R.L., Radioisotope Measurement Applications in Engineering, Reinhold Publishing Corp., (1967) 365.

ADVANCES IN BULK ELEMENTAL ANALYSIS USING NEUTRON INTERACTIONS

T. GOZANI
Science Applications International
Corporation,
Sunnyvale, California,
United States of America

Abstract

Recent advances in on-line bulk elemental analysis using nuclear interactions with thermal and fast neutrons are reviewed. Three aspects of the advances are emphasized: very high count-rate gamma ray spectroscopy that maintained the energy fidelity, presence of discrete and continuum gamma rays in high energy region resulting from 14 MeV neutron interactions, and advanced data analysis incorporating a-priori knowledge.

1. INTRODUCTION

The production of gamma-rays resulting from neutron interactions in matter often provides invaluable information on the elemental composition. If the energy of the neutrons is very low, ("thermal") radiative capture (n,γ) yields a wealth of very specific and sharp gamma-rays which form the basis for the prompt neutron gamma activation analysis (PGNAA). If the energy of the neutrons is high ("fast"), such as those generated by a (D,T) nuclear reaction (14 MeV), different but also specific gamma rays are produced through ($n,x\gamma$) type nuclear reactions, where x can be any charged particle such as a proton, alpha, deuteron or triton, and one or two neutrons. The most common ($n,x\gamma$) reaction is the inelastic neutron scattering ($n,n'\gamma$). Hence the name, prompt inelastic neutron activation analysis (PINAA).

The (n,γ) reactions of thermal neutrons and the ($n,x\gamma$) reaction of fast neutrons are quite complementary to each other. Whereas the (n,γ) cross section is very low, for most light elements, e.g., Li, Be, B, C, N, O, and also Na, Mg, Al, with notable exception of hydrogen, the ($n,x\gamma$) cross-section for these elements is quite respectable. Furthermore, the yield and specificity of the gamma rays from ($n,x\gamma$) is very high.

Advances in the use of PGNAA were reviewed two years ago [1]. The key factors contributing to those advances were mainly hardened high resolution Ge detectors, careful, but elaborate use of accurate analytical and computational tools (n and γ coupled transport codes) to design measurement systems and interpret results, and stable high count rate gamma ray spectroscopy systems. These and other factors are highlighted in Figure 1.

In the current review, further significant advances in very high count rate gamma ray spectroscopy will be discussed as well as two other important issues: nuclear data for fast neutron interactions and advanced data analysis and interpretation which can greatly improve the results and the efficiency of methods under use.

RECENT SUCCESSFUL INDUSTRIAL APPLICATIONS OF CAPTURE NEUTRON GAMMA RAY TECHNOLOGY

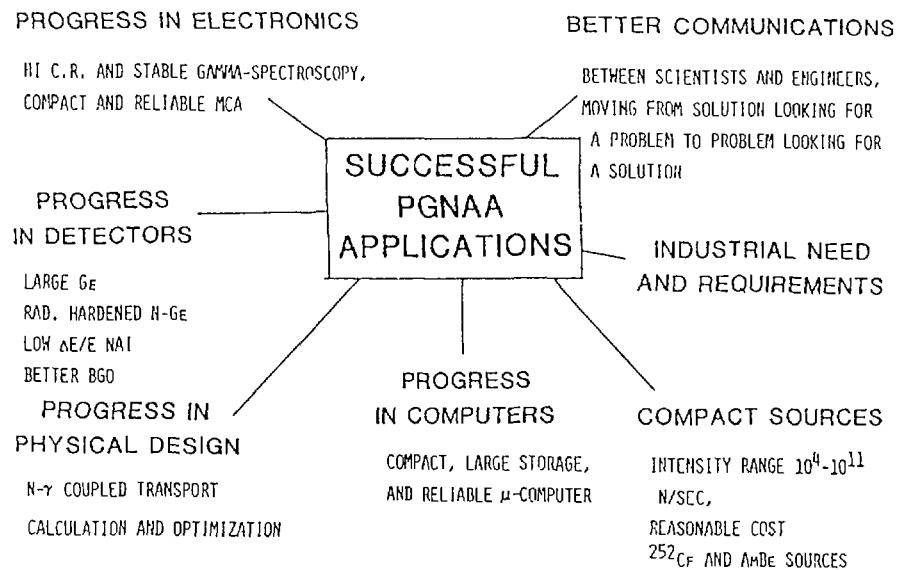


Figure 1. Factors contributing to successful applications of PGNAA.

2. SIGNAL PROCESSOR FOR VERY HIGH COUNT RATE

2.1 Analog Processor

Industrial applications of PGNAA or PINAA most often require very high counting rates in order to keep the measurement time short enough, at a given level of statistical precision to allow real time process control. In these applications, as in many others, the intensity of the radiation of interest could be several orders of magnitude smaller than the background of other gamma-rays.

Because the relative number of counts of interest is so small, it is critical that in any electronic process:

- o very few valid pulses are lost
- o interfering background is minimized.

The most important way that valid counts can be lost is dead time which happens when the processing of one event prevents a following event from being observed, that is, the system is dead. To minimize this problem, a fast gated system can be used to select relevant events on a fast time scale, so that the slower parts of the electronics are not tied up. This reduces the event rate of the fully processed pulses and as a result, system dead time losses are reduced.

Interfering background can come from the high energy tail of a peak at slightly lower energy or from pile-up. The former is minimized by assuring that good energy resolution is maintained through the signal processing.[2] Pile-up is the more important affect, and it can effectively be mitigated by a two-pronged approach, pile-up suppression and pile-up rejection. An example of a pile-up of two anode pulses from a NaI(Tl) detector resulting from a very high pulse count rate (400,000 cps) is shown in Figure 2.

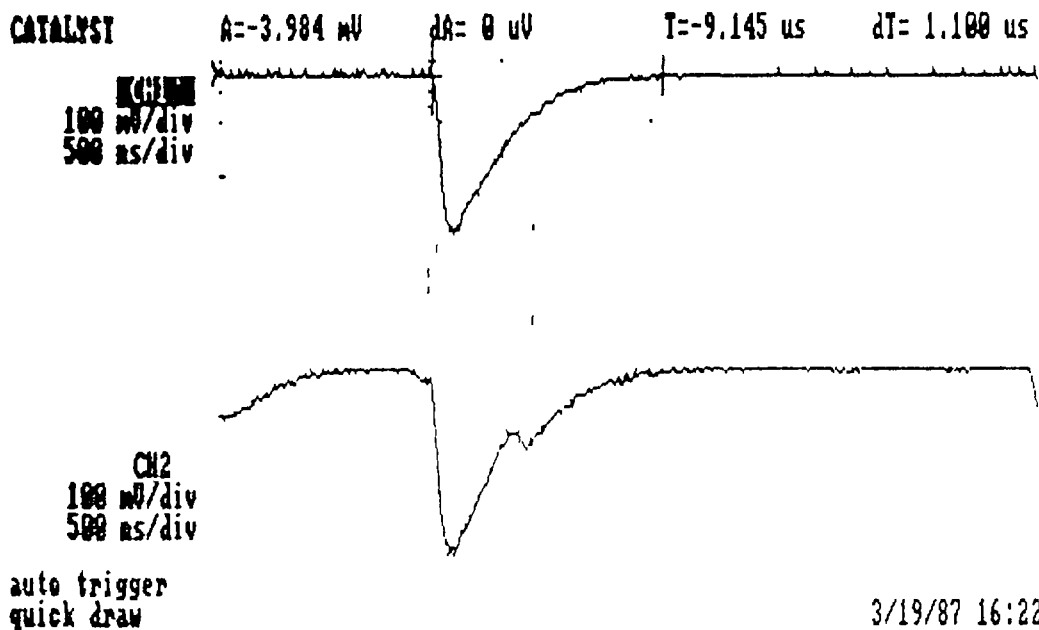


Figure 2. Some examples of NaI anode signal: CH1 represents single event taken at low count rate; CH2 represents signal badly distorted due to the pulse pileup at high count rates.

To overcome these problems, a high counting rate signal processor utilizing time variant filtering was developed.[3] Since the commonly used counting mode pile-up rejector did not improve the characteristics of the system significantly, a more effective pile-up rejector based on pulse length inspection was used

Processing of the photomultiplier anode signal starts with pulse shortening to reduce (suppress) the pile-up rate which is proportional to the pulse width. The roughly exponential light pulses in the NaI(Tl) crystal have a duration of approximately one microsecond. Due to the non-exponential decay components of the NaI(Tl) signal, simple delay line clipping is not satisfactory and a residual tail occurs on the output pulse. This assures fast time recovery of the shaped pulse which is particularly important for pile-up detection.

The signal processor has been experimentally evaluated at high count rates. Since the resolution becomes worse with the reduction of clipping time, because of loss of collected scintillation light, a compromise must be made between resolution requirement and pile-up effects. The resolution of the system as a function of clipping time for different gamma ray energies was measured. Figure 3 shows the relative deterioration of the resolution as a function of gamma ray energies and clipping time. The resolution deterioration due the pulse shortening becomes less important as the energy increases and the intrinsic component of the resolution becomes dominant.

The effect of random pulse pile-up also has been quantified by measuring the number of "background" counts in the high energy region. Since the real background is very low at this energy, most of the observed counts are due to pile-up. Fig. 4 shows the relative effect of random pile-up as a function of the total count rate using a 100 ns delay line for pulse shaping, with and without pile-up rejecter. The pile-up rejecter incorporated in the processor has reduced the number of piled up counts more than a factor of three, while losing less than 10% of valid counts at the same time.

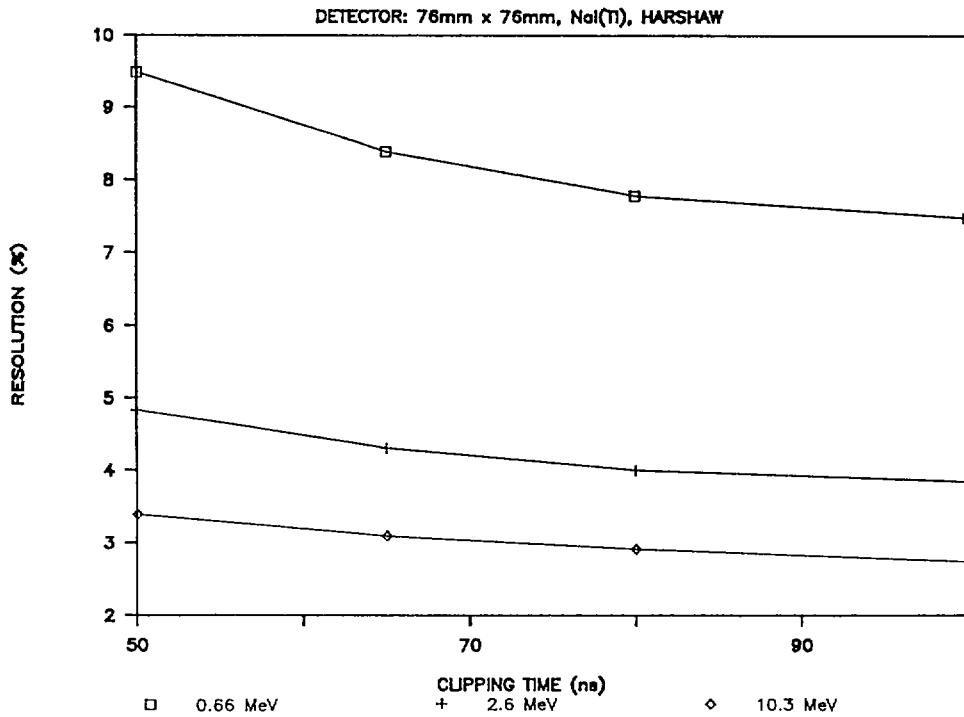


Figure 3. Resolution as a function of shaping delay line length and energy.

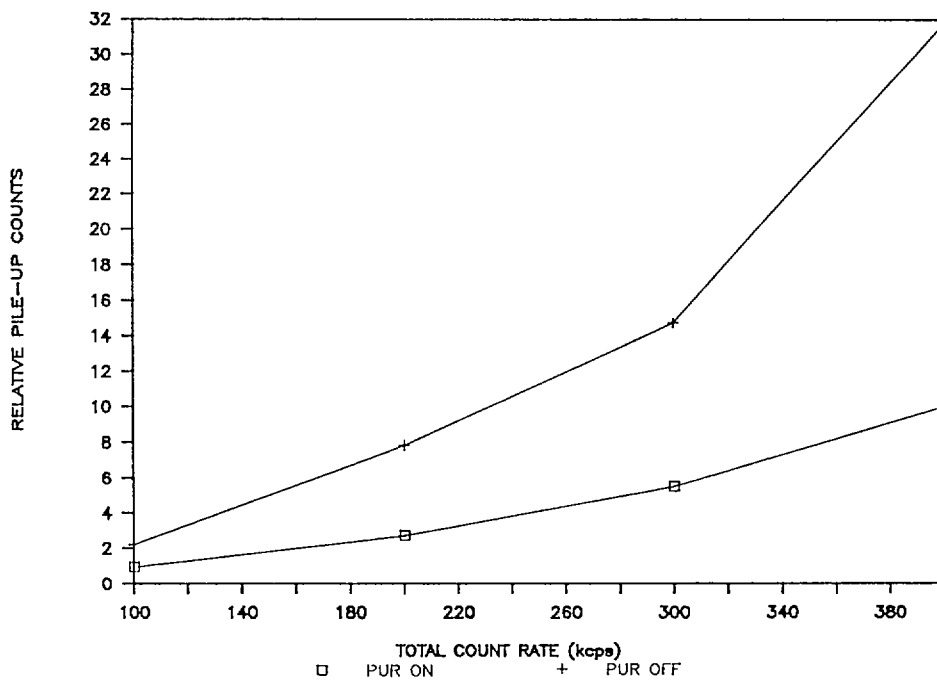


Figure 4. Count rate in high energy pile-up region as a function of total input rate, with and without pile-up rejections.

Fig. 5 shows a spectrum of the 10.8 MeV neutron capture gamma-ray of nitrogen, collected from a melamine sample irradiated by thermal neutrons. The fast neutrons were generated by a Kaman A711 neutron generator. The total average count rate from the detector was 300 kcps. For comparison, a low count rate measurement is shown in the same figure. This figure

clearly demonstrate that much better spectroscopical qualities are maintained at these high count rates as a result of the pile-up suppression and rejection.

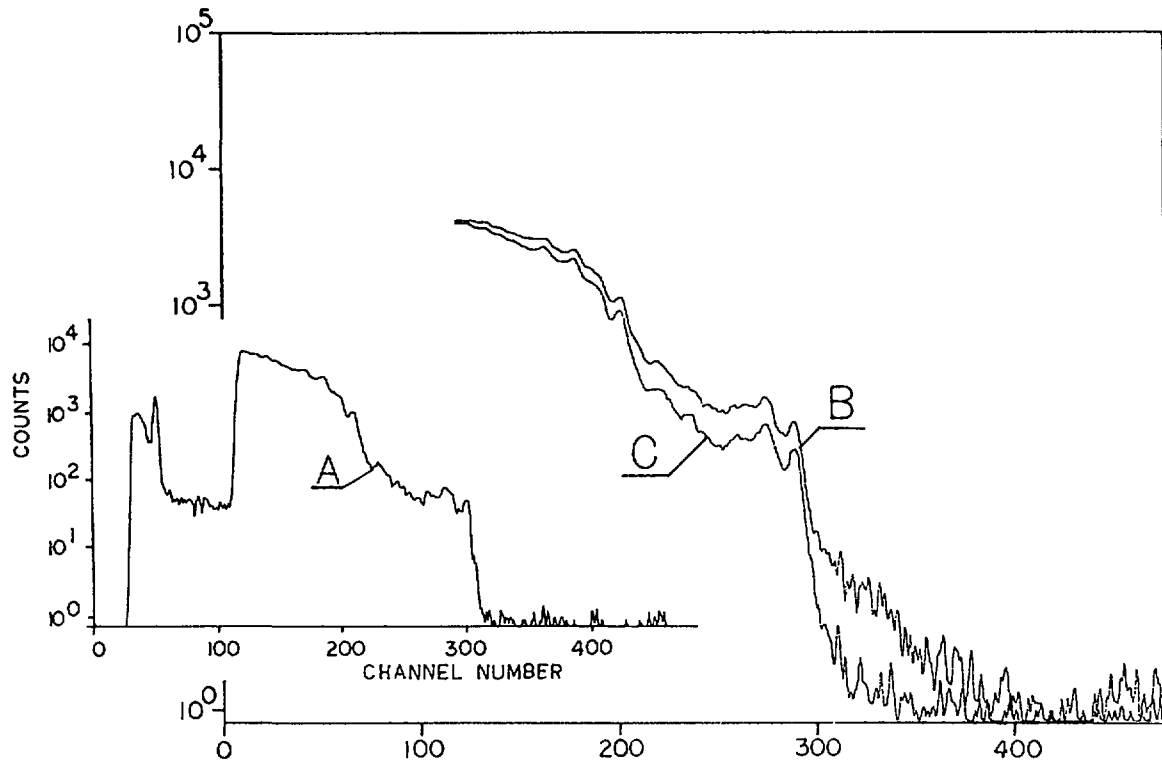


Figure 5. PGNAA spectra of a melamine sample showing the 10.8 MeV nitrogen full energy and escape peaks. A) Whole spectrum insert showing effect of two level thresholds. B) 10.8 MeV region without PUR and C) with PUR.

2.2 Digital Processing

The new analog pulse processor for very high count rate gamma-ray spectroscopy described above may have brought the technology to within its ultimate limits. The essence of the analog pile-up rejection technique is to detect and discard input pulses in which distribution due to pile-up is evident. Circuits of this type can reduce the spectral distortions due to pile-up but they cannot provide information about the events lost from the spectrum due to pile-up. Another recent approach [4] is a digital high rate gamma ray spectroscopy that is becoming realistically feasible. This is a fully digital signal processor. The fast photomultiplier anode pulse shape is treated in a digital form from the very beginning of the readout. The entire pulse shape is digitized by a fast digitizer and a set of processing algorithms is applied to examine and correct the signal for noise, baseline and pile-up distortion. The corrected pulses are integrated to measure the detected energy corresponding to a conventional multichannel spectrum analyzer. All details of the pulse shape are treated in a digital form. No electronics are used between the photomultiplier and digitizer, eliminating the usual amplification, filtering baseline restoration, etc. Since each individual anode pulse is digitized, it can be analyzed and corrected (rather than rejected) for pile-up effect from a preceding or following pulse.

The performance of a basic digital processing system [4] has been studied using a weak $^{241}\text{AmBe}$ source emitting 4.43 MeV gamma-ray in the presence of 1000 stronger ^{137}Cs source emitting .662 MeV rays. The total detector count rate was 400,000. The trigger threshold level was set just below the single escape of 4.43 MeV (3.92 MeV). The pulse height distribution with standard high count rate commercial amplifier MCA system is shown in Figure 6a. The poor energy resolution and substantial pile-up above the full energy peak of 4.43 MeV are obvious. With the full digitized signal corrected for pile-up, the resolution has improved considerably and the pile-up all but eliminated. The current system for digital signal

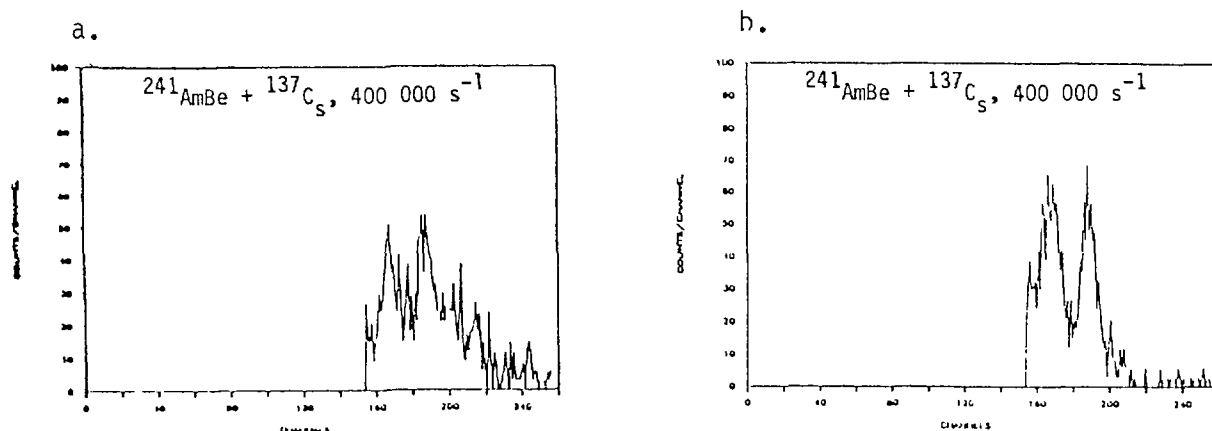


Figure 6. This figure illustrates the effect of the pile-up correction algorithm on 4.43 MeV $^{241}\text{AmBe}$ energy line; (a) uncorrected and (b) corrected, at the same total count rate of $4 \times 10^5 \text{ s}^{-1}$.

processing that demonstrated this remarkable performance is still cumbersome and expensive. However, it is believed that with new and more reliable and less expensive flash ADC and buffer circuits, an economical and flexible system will be ready for implementation with PGNA and PINAA equipment within the next few years.

3. FAST NEUTRON INTERACTIONS

In a neutron reaction with incident energy of 14 MeV, the residual nucleus in general, is left in one of its excited levels and will decay to its ground level directly, or through a cascade, by emission of characteristic gamma rays. Thus a measurement of energies and intensities of these gamma rays will facilitate a quantitative assessment of elemental concentration in the irradiated object. Evidently a similar assessment is also feasible by using thermal neutrons and observing the ensuing characteristic capture gamma-rays. However the total cross-sections for the production of gamma-rays by irradiation of, e.g., C, N or O by 14 MeV neutrons, are significantly greater than the corresponding cross-sections for radiative capture of thermal neutrons. Furthermore, when pulsed 14 MeV neutron source is used, as is common in bore-hole logging, both types of interaction can be employed: the $(n, x\gamma)$ interaction during the pulse of the fast neutrons and thermal capture during the die-away time of the thermal neutron population.

The magnitude of the total cross-section for production of prompt gamma rays (lines and continuum), was reviewed.[5] Experimental data for 26 target nuclei ranging from ^{10}B to ^{239}Pu were reviewed. A comparison between the gamma production cross-section of 14 MeV and thermal neutron is

given in Table I. It is apparent that with the exception of H and possibly ^{10}B , the total cross-sections for gamma ray production with 14 MeV neutron are significantly larger than those obtained from the radiative capture of thermal neutrons. Hence the appeal of employing $(n, x\gamma)$ reactions for elemental composition of light elements, especially C, N and O, in bulk samples.

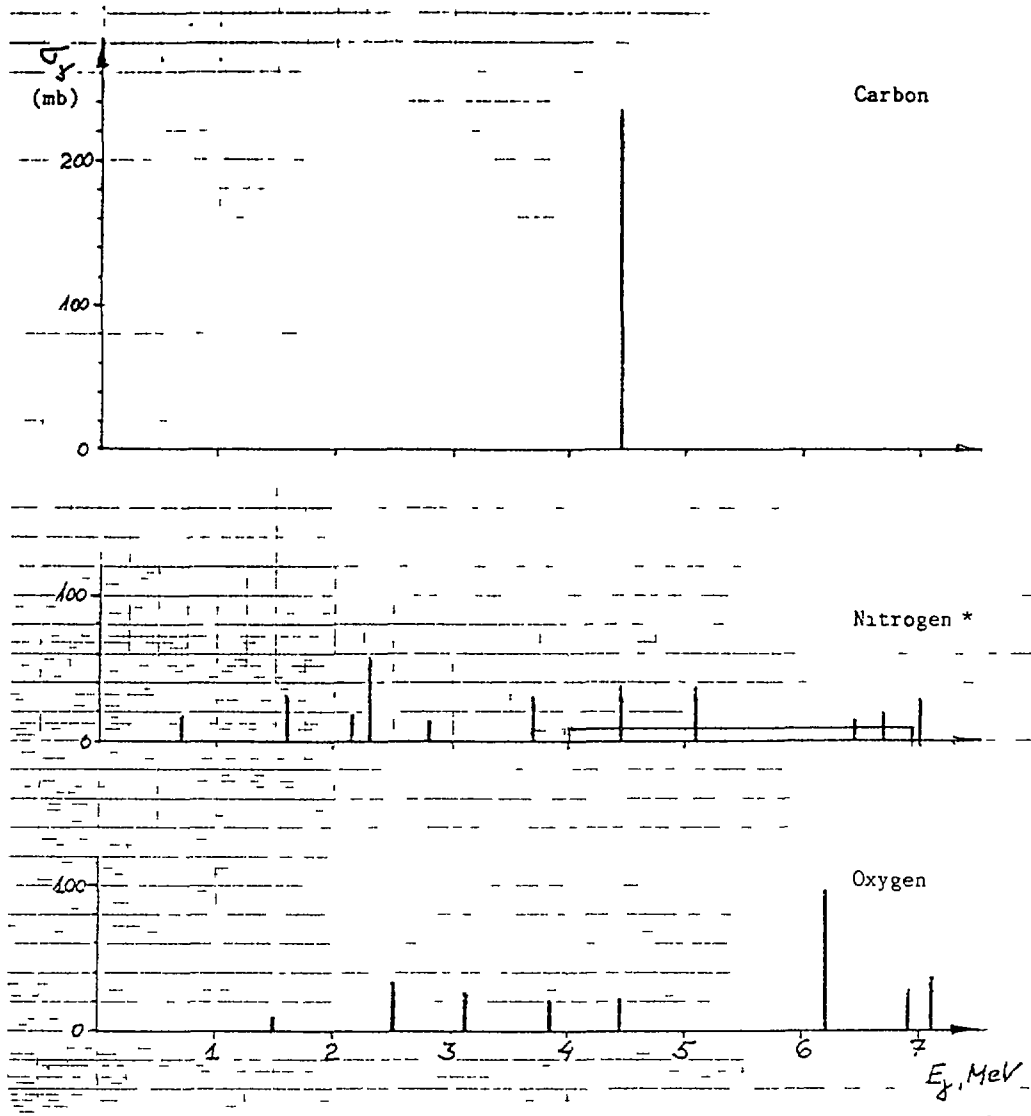
Table I. Total cross sections of production of gamma-rays ($0.5 \leq E \leq 12$ MeV) at $E_n=14$ MeV and at thermal neutron energies for $10 < A < 239$ and $A < 64$, respectively.

Target	($E_n=14$ MeV) (mb)	(E_{th}) (mb)
H	0	330
Li	(0)	3.6
Be	(0)	0.9
B	(160)	100
C	230	3.5
N	314	75
O	474	0.19
Na	1486	530
Mg	1445	51
Al	1832	231
Si	1620	177
P	2515	172
S	2419	530
Ti	4010	7840
Fe	4490	2590
Cu	5985	4500
Zn	5570	760
Zr	5830	185
Mo	6800	2550
Cd	7192	2450
In	6815	194
Sn	6480	626
Ta	9000	20500
W	10400	18400
Hg	9400	372
Pb	6500	171
Bi	11680	34
^{235}U	20632	98300
^{239}U	10546	22000
^{239}Pu	23150	269

The potential and present (and so far limited) use of PINAA require a good knowledge of the various cross-sections and the relative intensities ("Branching Ratio") of the product gamma rays. This is important for the determination of the elemental composition and also to assess presence of possible backgrounds in various regions of interest.

Through the review of the experimental data, and the basic physical principles, a relatively simple model was developed that allowed us to calculate the production of both the discrete and continuum gamma rays. [5]

The partial cross-sections for the production of discrete gamma ray lines in carbon and to a lesser extent in nitrogen and oxygen have relatively simple structures (see Figure 7). This figure shows significant cross-sections over the entire energy spectrum including the 4 to 7 MeV region.



*The flat level from 4 to 7 MeV represents a very rough estimate of the production cross-section per 100 KeV for continuum gamma rays in that energy region.

Figure 7 Yield of gamma-ray lines in neutron bombardment at $E_n=14$ MeV of Carbon, Nitrogen, and Oxygen.

However, somewhat heavier elements such as Na, Mg, Al, Si, Cl, Fe, etc., show also significant partial cross-sections for production of discrete lines with values above 5 mb up to 6 to 7 MeV. For example, aluminum and chlorine, which may be present in the measurement surrounding (e.g., NaCl) or in structural material (e.g., Al members), show discrete lines above 5 MeV (see Figures 8 and 9). The emphasis here on the high energy region of the spectrum is motivated by the fact that the S/N ratio there would be higher. Heavier elements tend to have fewer or no gamma ray lines resulting from $(n,x\gamma)$ reaction about 3 to 4 MeV.

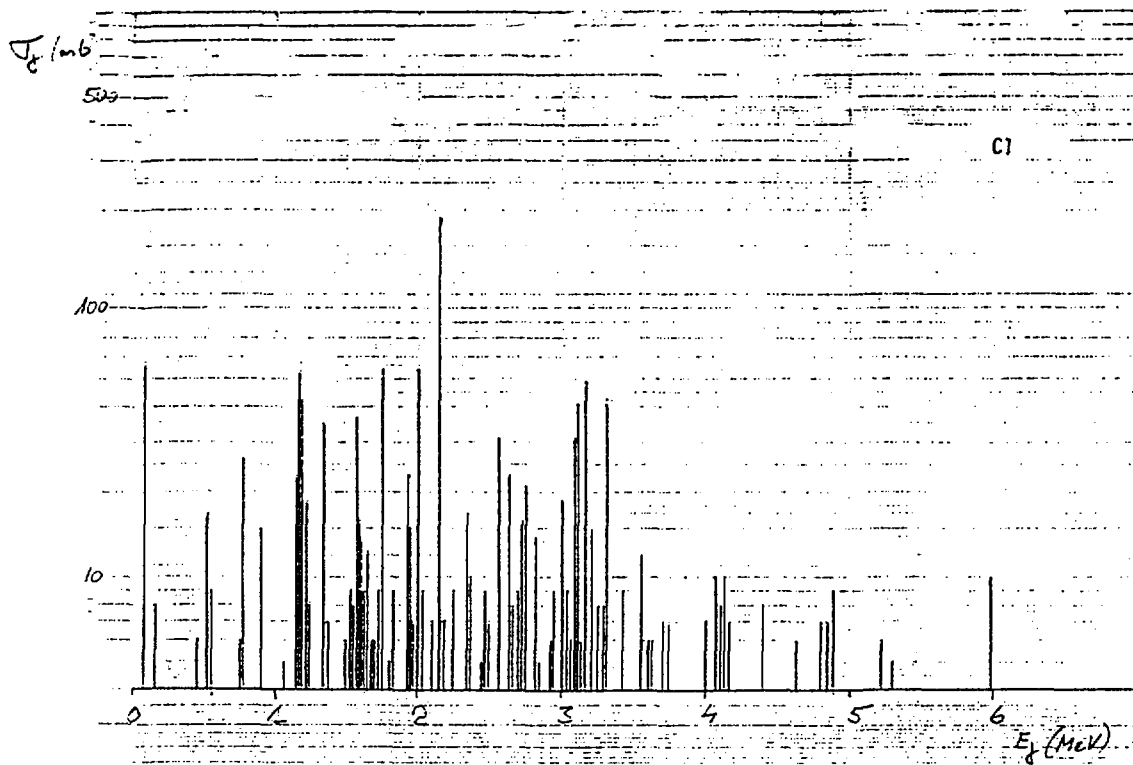


Figure 8. Partial gamma-ray production cross-sections in (n,XY) reaction on Cl, using 14 MeV neutrons.

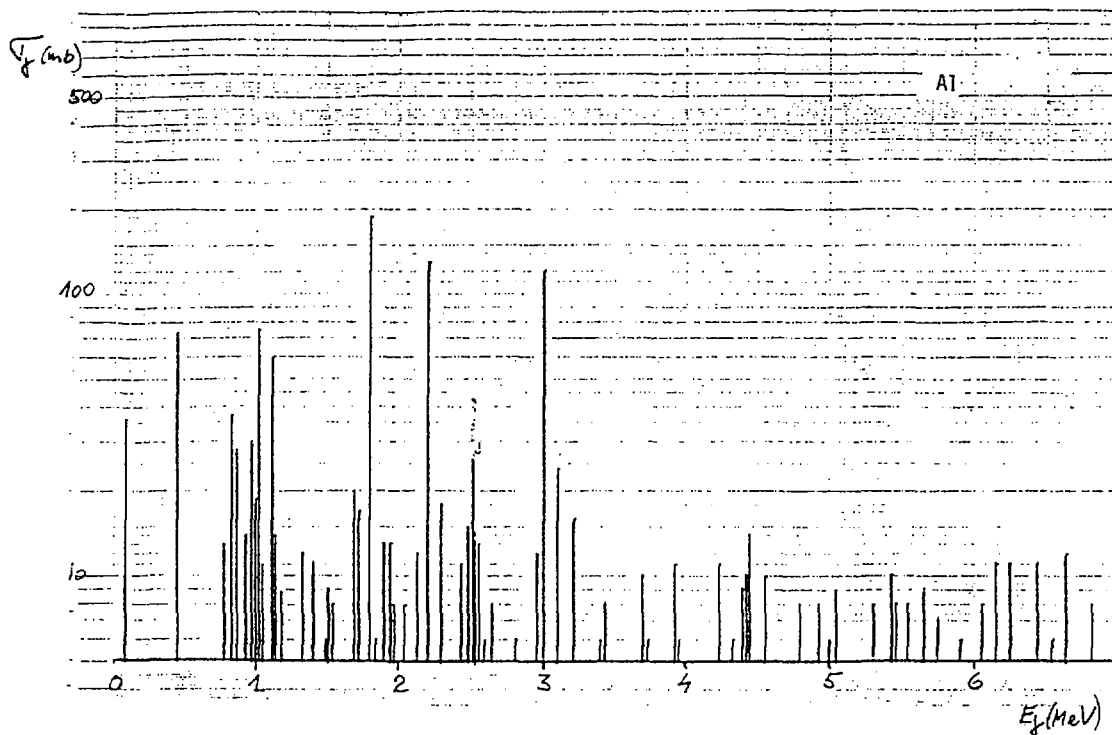


Figure 9. Partial gamma-ray production cross-section in (n,XY) reaction on Al, using 14 MeV neutrons.

In addition to the possible presence of weak but significant discrete gamma lines in the high energy region in light and medium-light elements, also unresolved (continuum) gamma rays must be considered. Integrated, over energy, such cross-section of the order of 50 mb per MeV could be typical. The intensity of the resulting gamma rays, as measured by a medium resolution detector such as NaI(Tl) or BGO is then equivalent to a discrete line intensities at 6 MeV with values of the order of 10 mb. This is, in effect, higher than many of the discrete line intensities in that energy region. The relative magnitude of the continuum cross-section in nitrogen is shown, as an example, in Figure 7. The presence of discrete and continuum gamma rays as the results of (n,x γ) reactions with 14 MeV neutrons in light and medium elements has not been hitherto recognized in PINAA applications. The existence of these phenomena should not, by any means invalidate the usefulness of the PINAA methods, but rather its recognition could improve PINAA accuracy and range of applicability.

4. ADVANCED DATA ANALYSIS

Most on-line instruments use a fixed calibration between the instrument response and the desired quantity of interest, for example, between the number of transmitted gamma rays and the total density of material in a pipe. In general, these calibrations are linear (or perhaps contain a simple function like a logarithm), even though the underlying physics of the situation is nonlinear and complicated by many different effects. In even a simple example like a pipe gauge, the response of the system will change not just with density but with type of material, void fraction, etc. In the more complex systems like elemental analyzers a lot of error-causing interactions are "swept under the rug" of the linear calibration. In these complex systems, several linear equations are solved simultaneously; often, there is some degree of interdependence between the equations. Especially in the case where the equations are not fully independent, it is possible for errors to propagate through the calibration and produce nonsensical results. Anyone who has worked with these instruments for a while has probably seen a case where a correlation in the minerals present caused a wierd reading, or the presence of some new element (like chlorine) made the instrument go wild.

Common to all of these kinds of problems is the fact that, highly embarrassing to the instrument developer, any one of the field guys standing around could tell you that that certain reading is nonsensical. This is important - it is obvious to any human being that the result is in error. All one needs to do is find a way to incorporate this kind of a check into the machine. There are a variety of techniques for doing this, including regularization, a priori information, expert systems or any of a number of other artificial intelligence techniques.

Regularization is the most developed and most mathematically straightforward of the techniques. It is often used in NaI spectra deconvolution or imaging.

Using a priori information is also often done with these kinds of systems. Indeed, in some sense the original linear calibration used the a priori information about the relation between the instrument reading and the quantity of interest. Here, that is taken to mean using knowledge about things the instrument cannot measure; for example, a known correlation between moisture content and chlorine content, which might effect an instrument trying to measure sulfur.

Expert systems and other artificial intelligence techniques are still at the edge of technology and have not been widely applied in this field. These systems can use both a priori information about the material being measured and knowledge of the instrument's response to cope with widely varying conditions and to not make nonsensical errors.

5. REFERENCES

- [1] GOZANI, T., "Physics of Recent Applications of PGNAAs for On-Line Analysis of Bulk Materials," Neutron Capture Gamma-Ray Spectroscopy, Raman, S., Ed., AIP Publication (1985).
- [2] GOZANI, T., "High Counting Rate Gamma Spectroscopy," American Nuclear Society Transaction, Vol. 15, No. 2 (1972).
- [3] DRNDAREVIC, V., RYGE, P., GOZANI, T., "A Signal Processor for High Counting Rate Gamma Ray Spectroscopy with NaI(Tl) Detectors," to be published in IEEE Transactions on Nuclear Science.
- [4] DRNDAREVIC, V., GOZANI, T., RYGE, P., "Gamma Ray Spectroscopy at High Counting Rates By Digital Signal Processing," to be published.
- [5] Sawa, P and Gozani, T , Evaluation of gamma ray production by 14 MeV neutrons in light and medium elements, To be published.

THE ASSAY OF GOLD AND PLATINUM IN ROCKS AND ORES — AN OPTION

C.G. CLAYTON
Tregaron, Dyfed,
United Kingdom

Abstract

Since the low concentrations of gold and platinum in prospective ore bodies inhibit the effective use of neutron techniques in borehole logging equipment, consideration has been given to the routine use of activation analysis for multiple sample assay at ground level for the purpose of establishing the viability of a prospective ore body. The potential of small electron and proton Linacs are discussed and it is shown that electron Linacs can be regarded as the origin of a relatively intense source of thermal neutrons and the proton Linac as a source of fast neutrons of identified maximum energy. The possibility of analysing 2 to 3 kg samples of gold and platinum at the ppm level is discussed and particular consideration is given to self-shielding effects in gold when using thermal neutrons. This problem is resolved by using the proton Linac and fast neutron activation analysis.

1. INTRODUCTION

Gold and platinum are the most valuable metals currently being mined and interest in both these elements, and in the discovery and development of new deposits, is very high. Unfortunately, the problem of establishing the economic viability of a potential ore deposit can be difficult and costly since acceptable ore grades may be deep underground and spatial heterogeneity of the metal within the ore body can be substantial.

In such a situation borehole logging as an alternative to core analysis ought to be attractive, but the low grades of gold and platinum which are encountered (ppm and sub-ppm) coupled with their particular neutron interaction properties (cross-section and half-life) and the magnitude and nature of potential interferences, in particular, prohibit the method being used. In this latter context, Boyle, (1) for example, lists 43 elements along with the rare earths which may be found in association with gold - although they do not all occur in the same deposit.

Although effective borehole logging for gold and platinum appears to be discounted at the present time, it is pertinent to question whether fast or thermal neutron activation could be an acceptable method of analysis for the very large number of samples (collected from ground surveys and from borehole cores) which are required to assess the grade of a potential ore body. Significantly greater flexibility in technique is possible for measurements at ground level than can be accommodated in borehole logging systems. However, because of the low concentrations of gold and platinum involved a relatively intense neutron source is required.

In this context recent developments in small electron and proton accelerators are changing the outlook. They offer the possibility of

providing an intense thermal or fast neutron flux at a controlled energy and over a mass of 2-3 kg of crushed rock. This latter characteristic is very attractive since, by pre-mixing small samples, a more representative result can be achieved by a single measurement.

From considerations of cost, size and mobility the discussion can be limited to electron linear accelerators with a terminal energy of 15 Mev at 100 μ A beam current and to proton linear accelerators operating at 5 Mev with a mean current of 1 mA.

The electron Linac is regarded as a source of thermal neutrons. With a suitable target surrounded by an efficient moderator a thermal neutron flux of about 10^{10} n/cm²/s can be generated over a mass of 2 to 3 kg of crushed rock. If required, after use the facility can be dismantled, transported and re-assembled at other sites.

The development of radio-frequency quadropole focussing(2) for low energy particle acceleration now permits relatively high beam currents to be generated at several Mev energy in a compact structure(3,4) and, with a thick lithium target for example, allows a high neutron yield ($>10^{12}$ n/s) to be obtained. The neutron energies are controlled by the proton energy and the fast neutrons generated are used to induce radioactivity in the material to be analysed. By suitable choice of proton energy the γ -ray yield from a selected analyte can be maximised and potential interferences from reactions with higher threshold energies can be eliminated.

2. THE ELECTRON LINEAR ACCELERATOR

Small electron linear accelerators with an energy in the range 5 to 15 Mev and an average beam current of 100 to 1,000 μ A are now available commercially and recent developments have resulted in substantial reductions in size, increase in mobility and simplification of the controls. With a suitable combination target for the (e^- , γ), (γ ,n) reactions and, surrounded by an efficient moderator, they provide a means of generating an intense thermal neutron flux over a substantial volume which is several orders of magnitude greater than is possible from available radioisotope sources and comparable with the flux in a small reactor. Uranium and beryllium can be regarded as alternative neutron sources: uranium provides the higher yield (Fig.1), but beryllium is more attractive operationally.

2.1. The electron linear accelerator with a uranium target.

Figure 2 is a schematic diagram of a tungsten-uranium target assembly for a 15 Mev, 100 μ A linear accelerator. It is preferred to generate bremsstrahlung by using a primary tungsten target which is coupled to a uranium secondary target which acts as the principal neutron source, the neutrons being generated through the reaction $U(\gamma, nf)$. The merit of this arrangement lies in the higher thermal conductivity and melting point of tungsten compared with uranium, and the more acceptable mechanical properties.

By using tungsten as the electron target the possibility of uranium, overheating and swelling due to the phase change at $\approx 650^\circ\text{C}$ is avoided and servicing the electron target is also facilitated since the uranium,

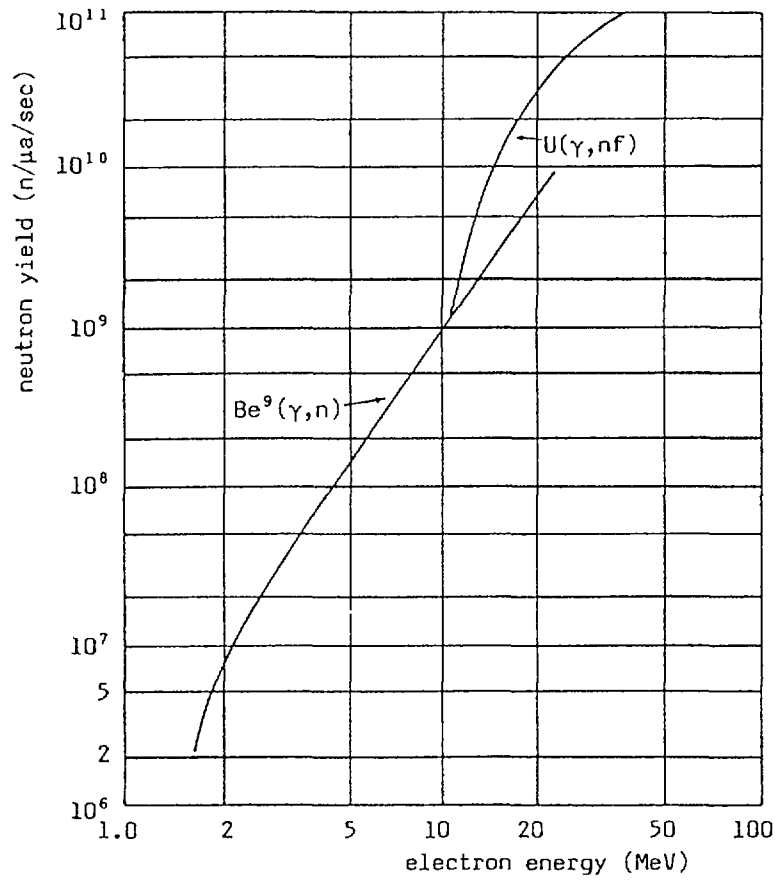


FIG. 1. Comparison of neutron yields from ${}^9\text{Be}(\gamma, n)$ and $\text{U}(\gamma, nf)$ thick targets.

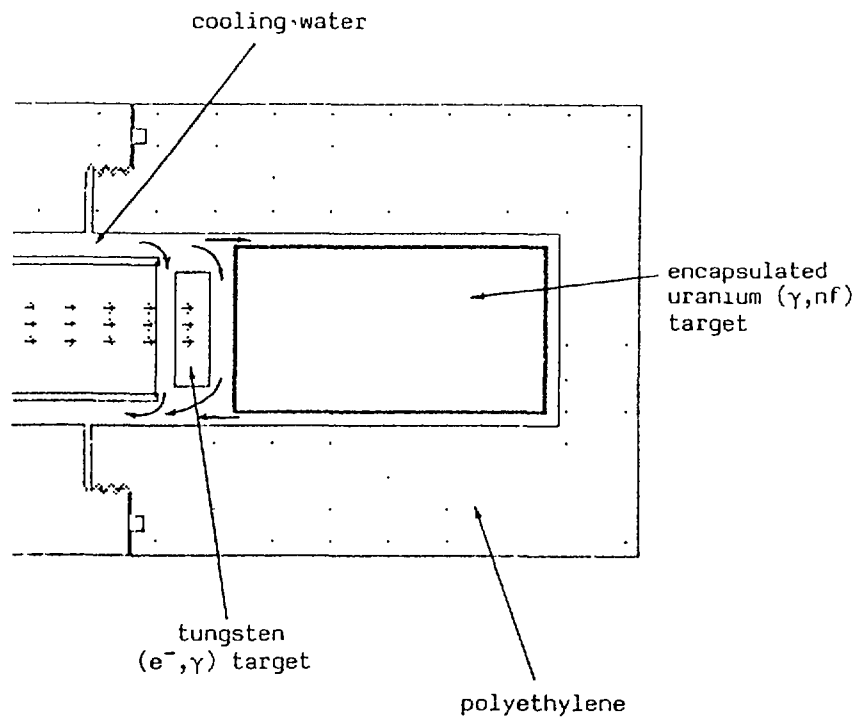


FIG. 2. Coupled tungsten-uranium target for electron linear accelerator.

which becomes radioactive through the (n,γ) and (n,f) reactions can be removed and isolated.

Figure 3 gives the neutron yield from various elemental targets for electrons in the energy range 10 to 40 MeV (5), the estimated yield from a uranium target at 15 MeV and 100 μA being 2.25×10^{12} n/s. The reduction in yield by using a composite tungsten-uranium target instead of a single uranium target is within 10 per cent of the value given above. The neutron energy distribution is given in Fig.4. It is interesting to note that the peak occurs at about 300 keV and that about 90 per cent of the neutron yield has an energy below 2.8 MeV.

This yield can be compared with a neutron output of 2.3×10^9 n/s from a 1 mg ^{252}Cf source which is a reasonable standard of comparison taking into account the requirement for continuous shielding of the isotope source.

2.2 Some characteristics of a beryllium target.

A beryllium target has some attractive characteristics when compared with uranium. The macro-absorption cross-section is very low [$\Sigma_a = 1.23 \times 10^{-4} \text{cm}^{-1}$] and the macro-scattering cross-section is relatively high [$\Sigma_s = 0.865 \text{cm}^{-1}$]. Consequently, the source itself makes a significant contribution to the total moderating power of the system.

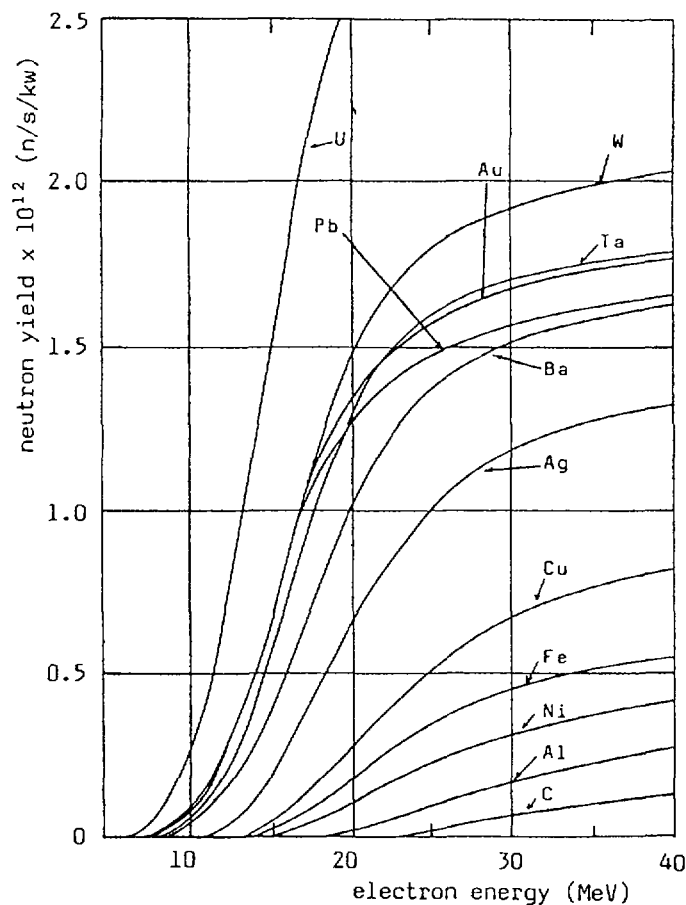


FIG. 3. Neutron yield from various elemental targets for electrons in the energy range 10 to 40 MeV.

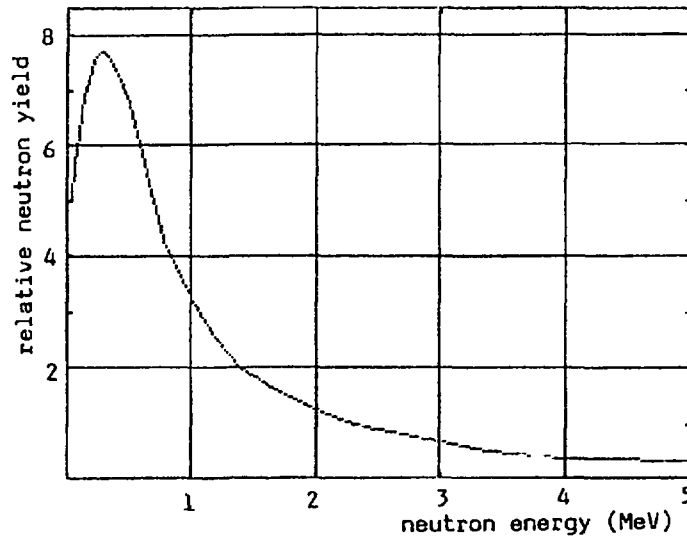


FIG. 4. Neutron energy distribution for 15 MeV electrons on a thick target of natural uranium.

The activation cross-section is approximately equal to Σa and the activation products have either a very long half-life (2.7×10^6 y) or a very short half-life (0.80s) so that induced radioactivity is negligible. Beryllium also has a high melting point and a high thermal conductivity.

To maximise the neutron yield it is preferable to use tungsten as the (e^-, γ) converter and to couple this mechanically to the beryllium which then operates solely as the (γ, n) source. As the angular distribution of the γ -rays from the tungsten is highly focussed in the forward direction, as can be seen in Fig. 5, a simple cylindrical shape for the beryllium target in an arrangement such as that shown in Fig. 2 is adequate.

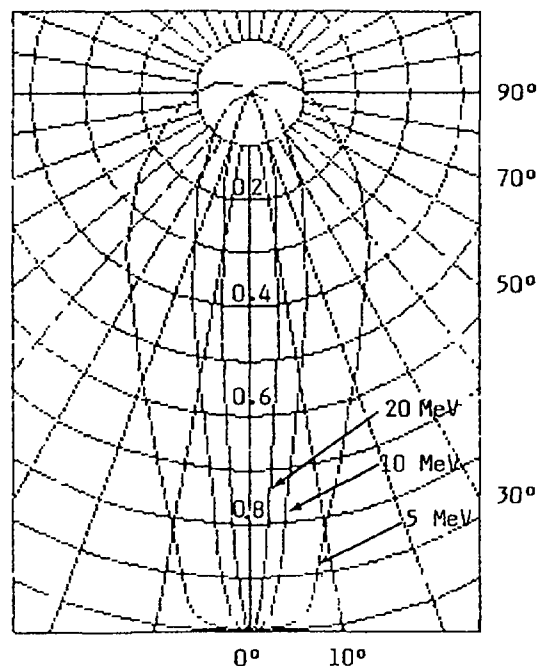


FIG. 5. Angular distribution of bremsstrahlung at a distance of 0.1 cm from a tungsten target of 0.325 cm thickness for electrons of 5, 10 and 20 MeV. Relative intensities to the intensity at 0° are given.

Since data on the neutron yield from a tungsten-beryllium combination was not available, this was calculated for a tungsten thickness of 5 g/cm^2 and a path length of 5 cm for the γ -rays in beryllium. This length was a compromise between increasing the neutron yield and decreasing the thermal flux over a surrounding mass (2-3 kg) of rock to be analysed.

The result of this calculation gave a yield of $2.65 \times 10^{10} \text{ n/s}$.

2.3 A thermal neutron source for analysing about 2 kg of crushed rock.

The possibility of generating a uniform thermal neutron flux over about 2 kg of crushed rock has been examined recently by Clayton and Coleman(6) for a range of primary neutron energies and Fig.6 is reproduced from this work. It shows that for a polythene sphere of 100 cm radius within which the sample is contained in a zone between 4 and 8 cm radius, an acceptably uniform flux distribution over essentially siliceous or calcareous rocks can be obtained.

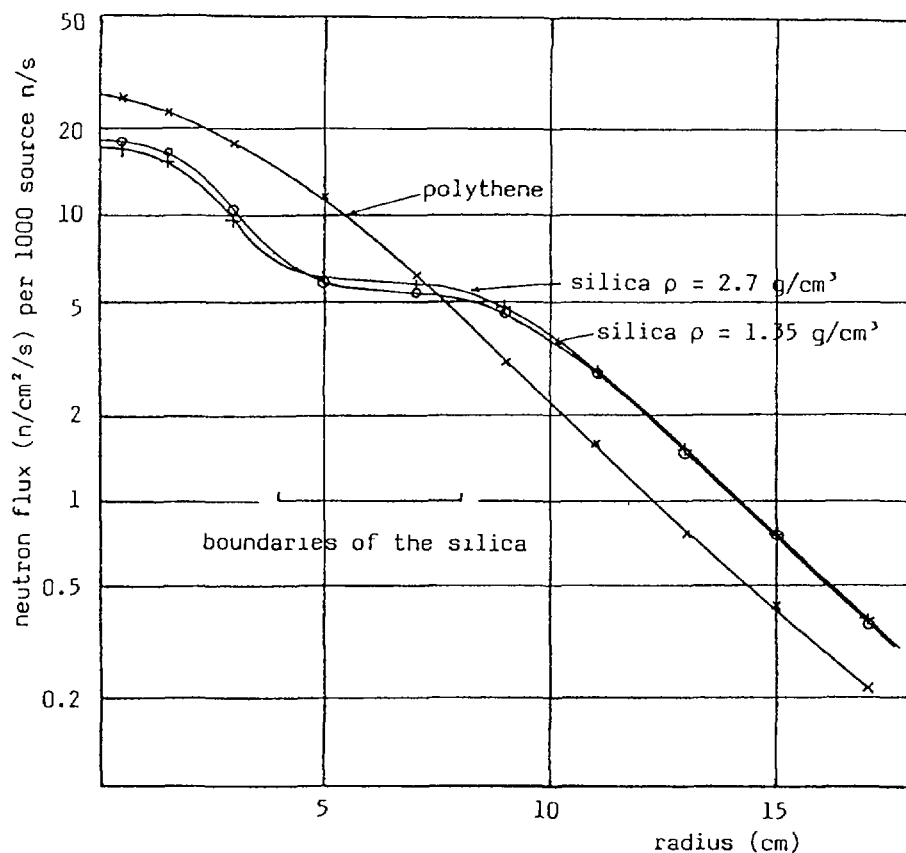


FIG. 6. Variation of thermal neutron flux with radius in a polythene sphere containing about 2 kg silica in a zone between radii at 4 and 8 cm.

For a uranium target terminating a 15 MeV, 100 μ A beam accelerator the thermal neutron flux over a 2 kg rock is calculated as $2 \times 10^{10} \text{ n/cm}^2/\text{s}$. This is about 10 times higher than available from a 1 mg ^{252}Cf source and large enough to allow many important on-site analyses to be carried out on relatively large masses of rocks and minerals which would otherwise not be possible. An outline diagram of an operational assembly is shown in Fig.7.

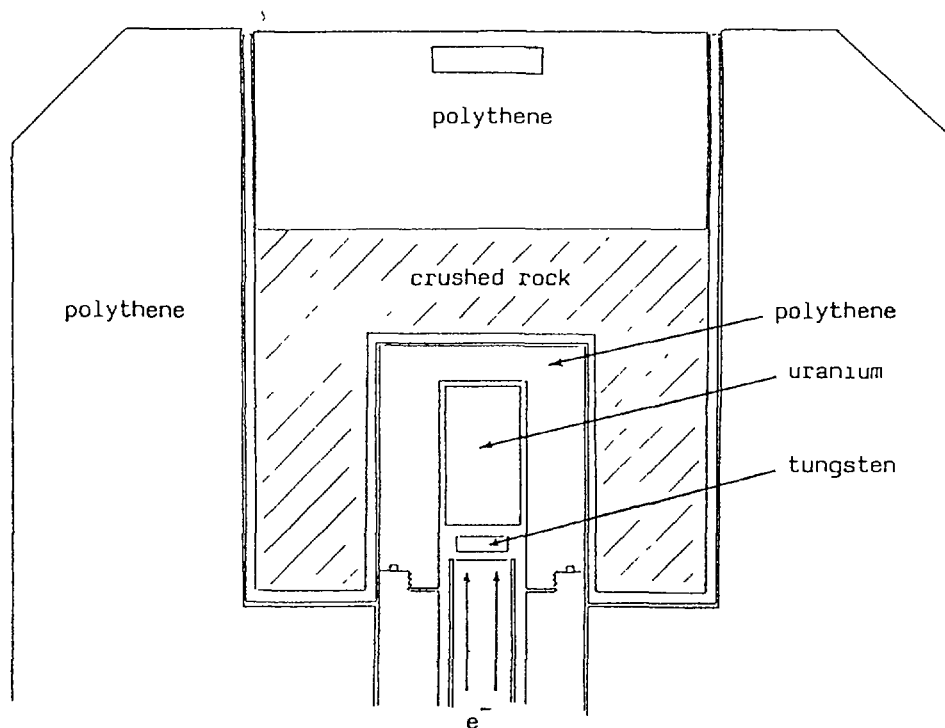


FIG. 7. Schematic diagram of an irradiation assembly for about 2 kg rock sample around the target of an electron linear accelerator.

2.4 Application of an accelerator-based facility for analysing platinum and gold.

2.4.1 Measurement of platinum concentrations in chromitite ores by thermal neutron activation analysis.

The measurement of platinum concentrations in the Merensky Reef in the Bushveld igneous complex in South Africa has been considered. In this occurrence, the platinum, which varies in concentration between about 15 and 18 ppm occurs in chromitite segregations in the lower part of the reef. The country rock is dunite. The range of mineral concentrations in chromitite are given in Table 1 and the average concentrations in dunite in Table 2. The virgin formation normally consists of bands of chromitite within the dunite.

After mining some mixing of the two ores is likely. In the example considered intimate mixing is assumed. Although this is not strictly true it represents a worst case since the main constraint to a rapid measurement of platinum comes from manganese which occurs in the dunite. It is also assumed that the concentration of Cr_2O_3 in chromitite is 35 per cent and the concentration of chromitite in dunite is 20 per cent.

The activation route is shown in Fig. 8. It is considered to be the only practical option in spite of the relatively low abundance of ^{198}Pt (7.21%). The activation product (^{199}Pt) decays at a relatively high rate ($\lambda = 3.75 \times 10^{-4} \text{ s}^{-1}$) into a long-lived daughter (^{199}Au) which allows the effect of short-lived interferences (e.g. ^{56}Mn) to be overcome.

TABLE 1. RANGE OF CONCENTRATIONS OF MINERALS
IN CHROMITITE

Mineral	Concentration range wt.%
Cr ₂ O ₃	30 - 48
Al ₂ O ₃	11.0 - 31.4
FeO	11.4 - 22.4
MgO	7.6 - 16.4
Fe ₂ O ₃	0.5 - 7.1

TABLE 2. AVERAGE CONCENTRATIONS OF MINERALS
IN DUNITE

Mineral	Average concentration wt.%
MgO	37.9
SiO ₂	38.3
FeO	9.4
Fe ₂ O ₃	3.6
Al ₂ O ₃	1.8
CaO	1.0
P ₂ O ₅ , Na ₂ O	0.2
TiO ₂ , K ₂ O, MnO	0.1
H ₂ O	4.8
CO ₂	0.4

Using the data given in Tables 1 and 2 for a 2 kg sample of mixed dunite and chromitite and a thermal neutron flux of 1.3×10^{20} n/cm²/s following irradiation for one hour, the induced activity is first dominated by γ -rays from ⁵⁶Mn.

Assuming a counting efficiency of 1 per cent for the 158 keV and 208 keV γ -rays from ¹⁹⁹Au and 0.1 per cent for the γ -rays from ⁵⁶Mn, the calculated countrates immediately after irradiation are

$$1.86 \times 10^6 \text{ c/s for } ^{56}\text{Mn}$$

and, $1.83 \text{ c/s for } ^{199}\text{Au}.$

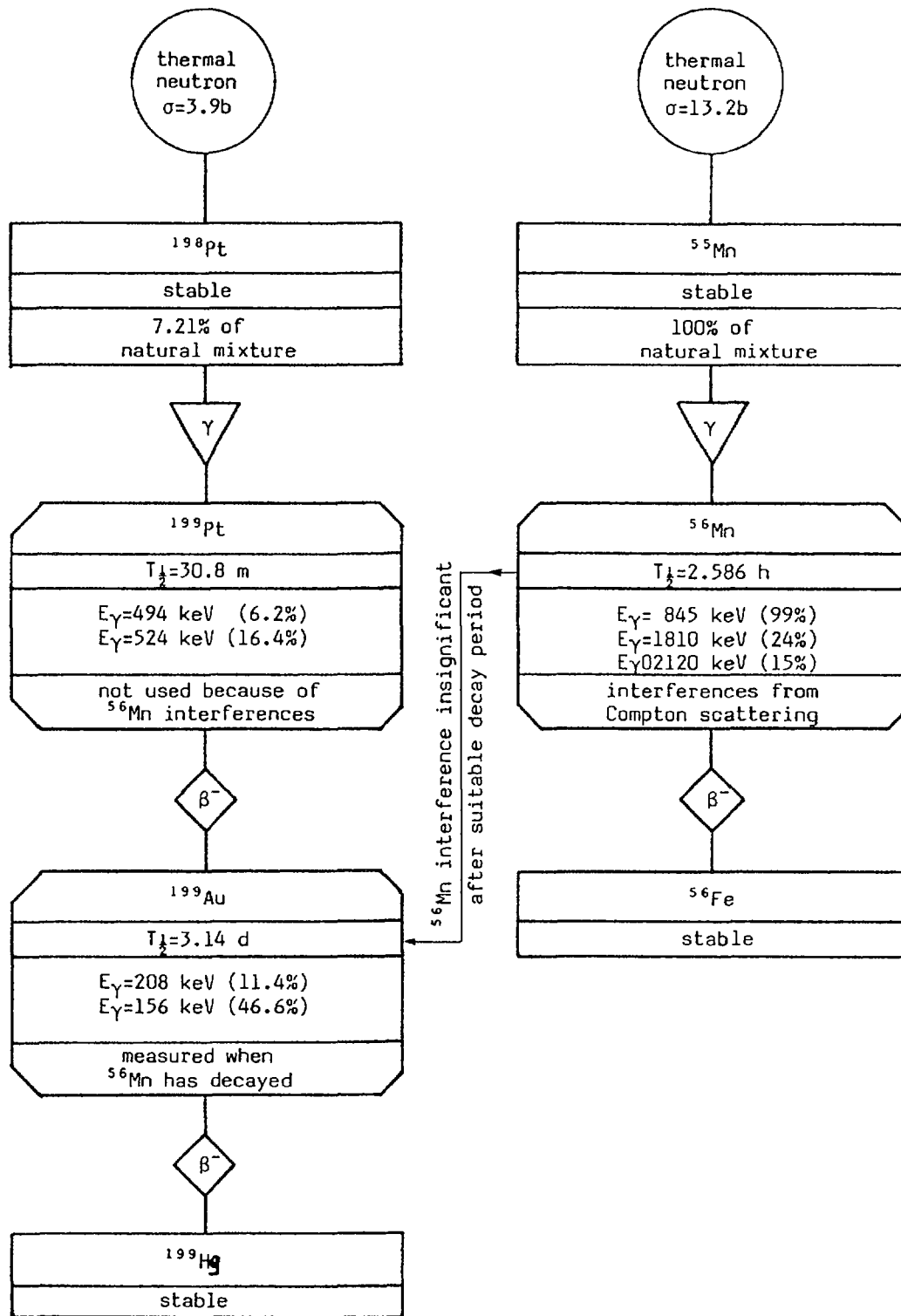


FIG. 8. Diagrammatic irradiation and decay scheme to avoid strong interference from ^{56}Mn in the measurement of platinum concentration.

For 1,000 counts registered, the optimum delay before counting is about 2.5 days when the accuracy of determining the platinum concentration (at 3.3 ppm) is 4.27% (2σ). At 1 ppm platinum concentration the optimum delay before counting is somewhat longer (≈ 3 days) and the accuracy is reduced to 18.2% (2σ): i.e. + 0.2 ppm.

It is worth noting that manganese concentrations differing by a factor 50 times from that considered can be accommodated simply by increasing, or decreasing the time before counting by about 1 day.

Thus, with an on-site accelerator facility, very low concentrations of platinum can be assayed in relatively large masses of rock provided a delay before assay of about 3 days can be tolerated.

2.4.2 Measurement of gold concentrations in rocks and ores by thermal neutron activation analysis.

The conventional method for analysing gold in gold-bearing ores is by fire assay based on samples which vary in mass between about 10 and 100g. An alternative method which is rapid, accurate and instrumental, and which can accommodate large samples (so as to improve representation) is of strong interest at the present time.

Reactor activation analysis is an established method for measuring gold concentrations. The high thermal neutron cross-section of gold and high reactor thermal flux enable low gold concentrations (<1 ppm) to be measured with short irradiation times. The relatively long half-life of ^{198}Au ($T_{1/2} = 2.7$ days) has the advantage that interferences from other elements (e.g. Fe, Mn, Na, As, Cu) typically found in many gold-bearing ores (and in gold concentrates) can readily be allowed for after a few days delay before measurement of the intensity of the 412 keV γ -ray on which the gold concentration is based. However, reactor activation analysis is usually inconvenient for routine use: reactors are rarely close to operational sites and acceptable samples are generally small and only a few grammes in weight.

For the analysis of gold from fine-grained deposits, activation analysis is a straightforward technique. However, care must be exercised when analysing gold from placer deposits and from other types of deposit in which gold may be in a particulate form. Errors may then occur in the analysis due to self-absorption of thermal neutrons and, when the Cd ratio is less than 50 (approx.), due to the strong epithermal resonance at 5eV (Fig. 9).

It is worth noting that in the thermal columns of high flux reactors, where small sample activation analysis is often carried out, Cd ratios >1,000 are typical. In some low flux reactors, which are also used for routine activation analysis, Cd ratios may be <10. Since Cd ratios <50 can be expected from accelerator neutron sources, consideration of errors due to epithermal neutron absorption is required.

Apart from self-shielding it is necessary to consider the possibility of flux depression around individual gold particles. However, this is not a problem if the dimensions of the gold particles are small compared to the transport mean free path in the host rock: flux depression is then insignificant. For a siliceous rock the transport mean free path is approximately 10 cm and compares with a few 100 μm for the largest gold particles generally found. Flux depression can therefore be ignored.

The self-shielding factor in gold has been treated in two parts: for thermal neutrons and for neutrons above the Cd cut-off (taken as 0.55 eV). For thermal neutrons self-shielding factors for plates and spheres were regarded as giving an adequate representation of the shapes

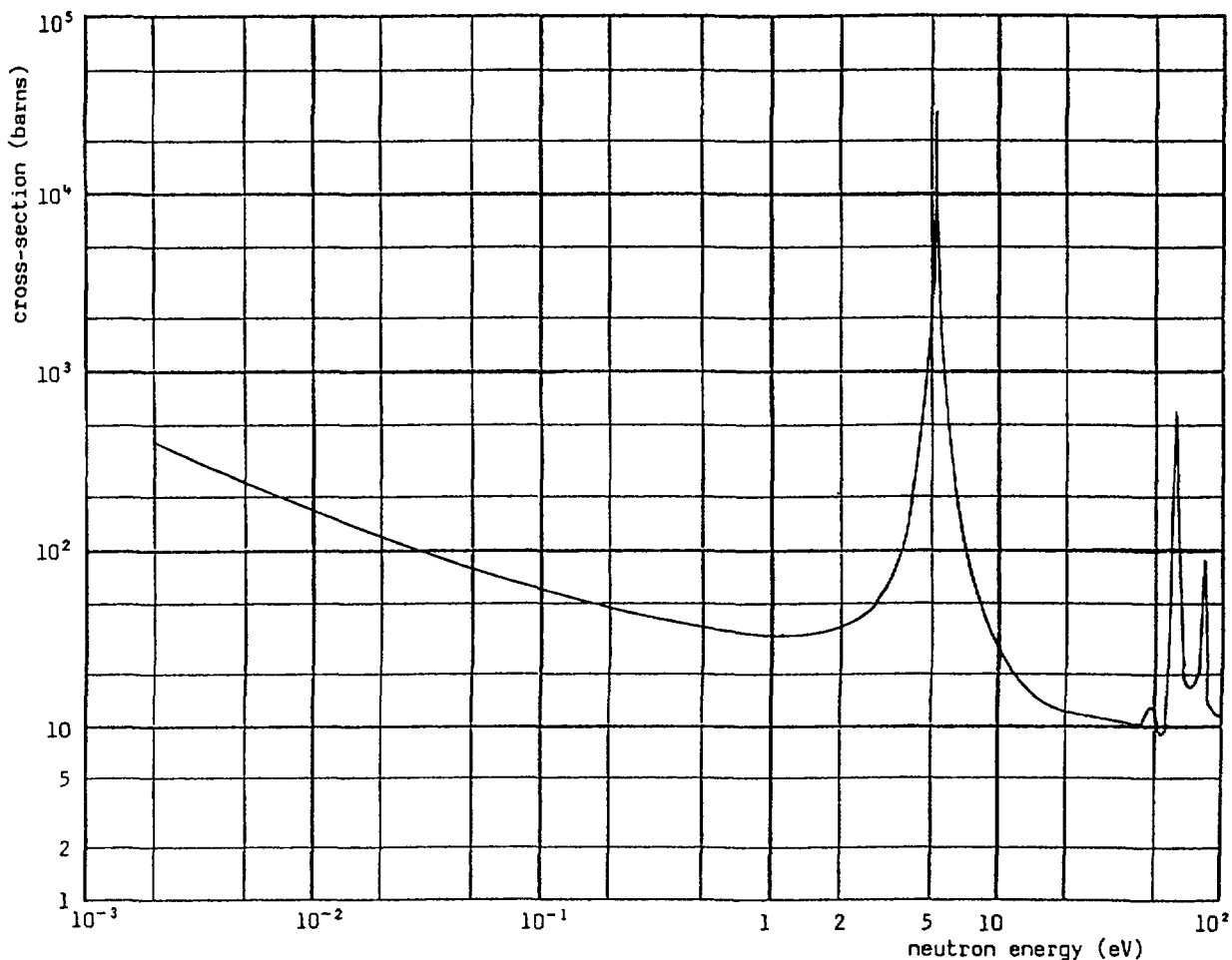


FIG. 9. The total cross-section for gold between 10^{-3} eV and 10^2 eV.

of gold particles. For epithermal neutrons, since the self-shielding factors become very large, only plates were considered.

The self-shielding factors calculated for gold spheres are given in Fig.10 from which it is apparent that the self-absorption factor exceeds 5 per cent at $r = 0.012$ cm and exceeds 20 per cent only at $r = 0.054$ cm.

The epithermal self-shielding factor is shown in Fig.11 as a function of gold plate thickness. It is clear that for a plate of thickness only $1 \mu\text{m}$ self-absorption exceeds 10 per cent and at $10 \mu\text{m}$ it is about 50 per cent.

These results indicate that, without regard to the sample containment, activation analysis using an electron Linac as a primary source of thermal neutrons can only be used for those types of geodeposit for which the probability of occurrence of particles with dimensions $>10^{-4}$ cm (approx.) is low.

Avoidance of epithermal neutron absorption can be achieved by enclosing the sample to be analysed and the calibration sample within thin envelopes of an element with the same epithermal resonance characteristics as gold, i.e. gold or silver. In theory gold is ideal, but in practice it would become highly radioactive. A more

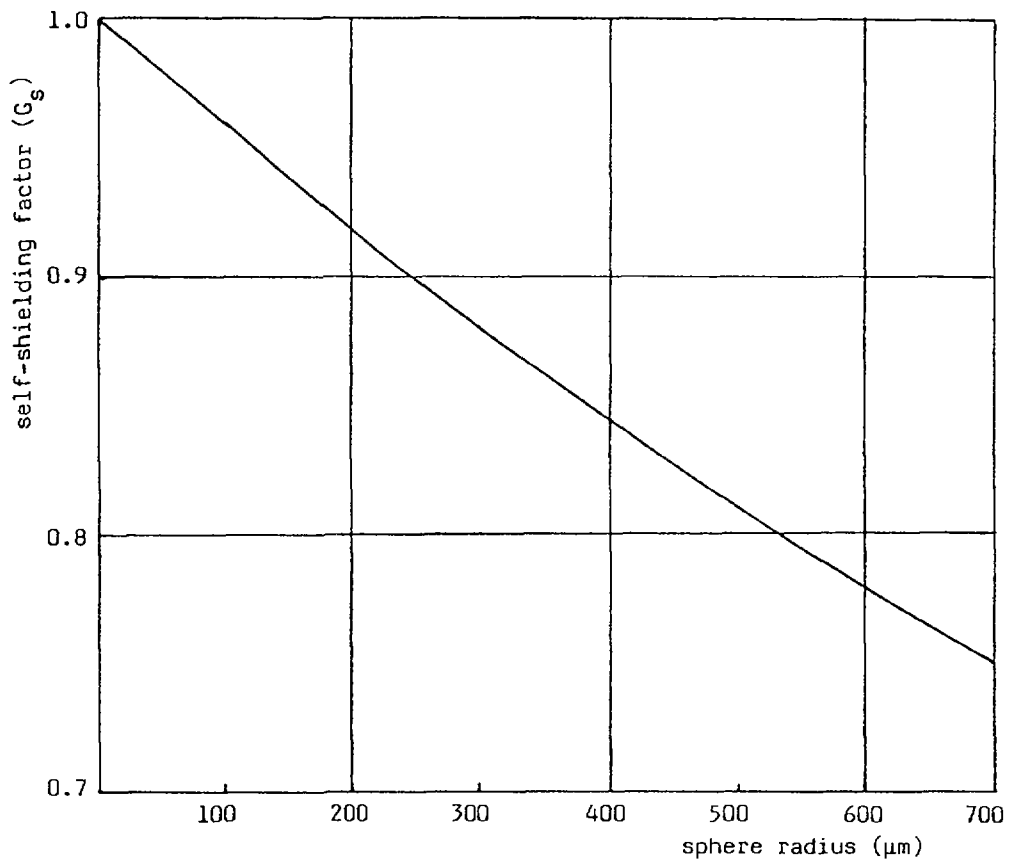


FIG. 10. Variation in the self-shielding factors for thermal neutrons with the radius of gold spheres.

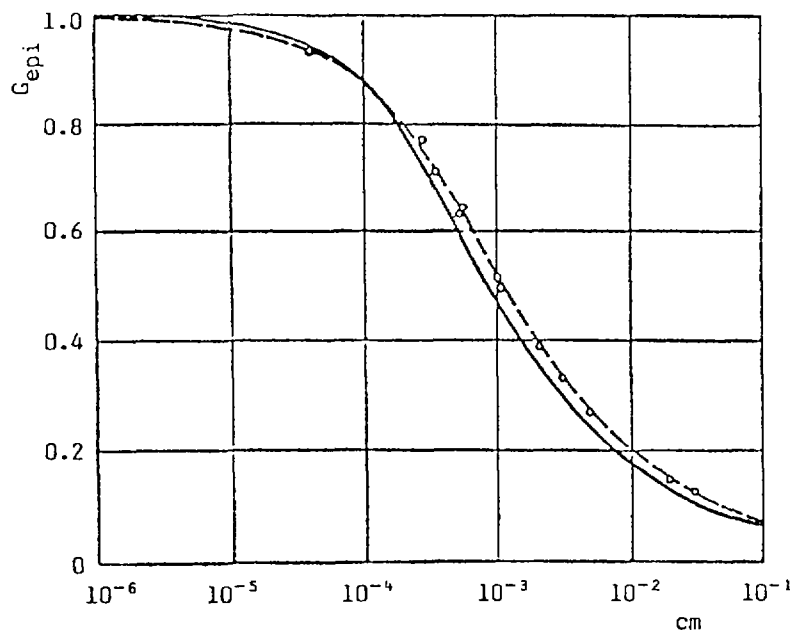


FIG. 11. The epithermal shielding factor for gold plates as a function of thickness.

—o—o— measured values
 ————— calculated values

satisfactory solution is to use silver. The (n, γ) cross-section of silver has significant resonances between 1 eV and 500 eV as can be seen in Fig. 12. The principal peak virtually overlaps the gold peak at 5 eV and activation of silver is less than gold, and silver is less expensive. When epithermal neutron self-absorption effects are overcome, thermal neutron activation analysis can be used for grain sizes up to about 0.05 cm (approx.) It appears that analysis of gold in placer deposits by this method is generally unacceptable - a result which is in conflict with the conclusion of Plant and Coleman (7).

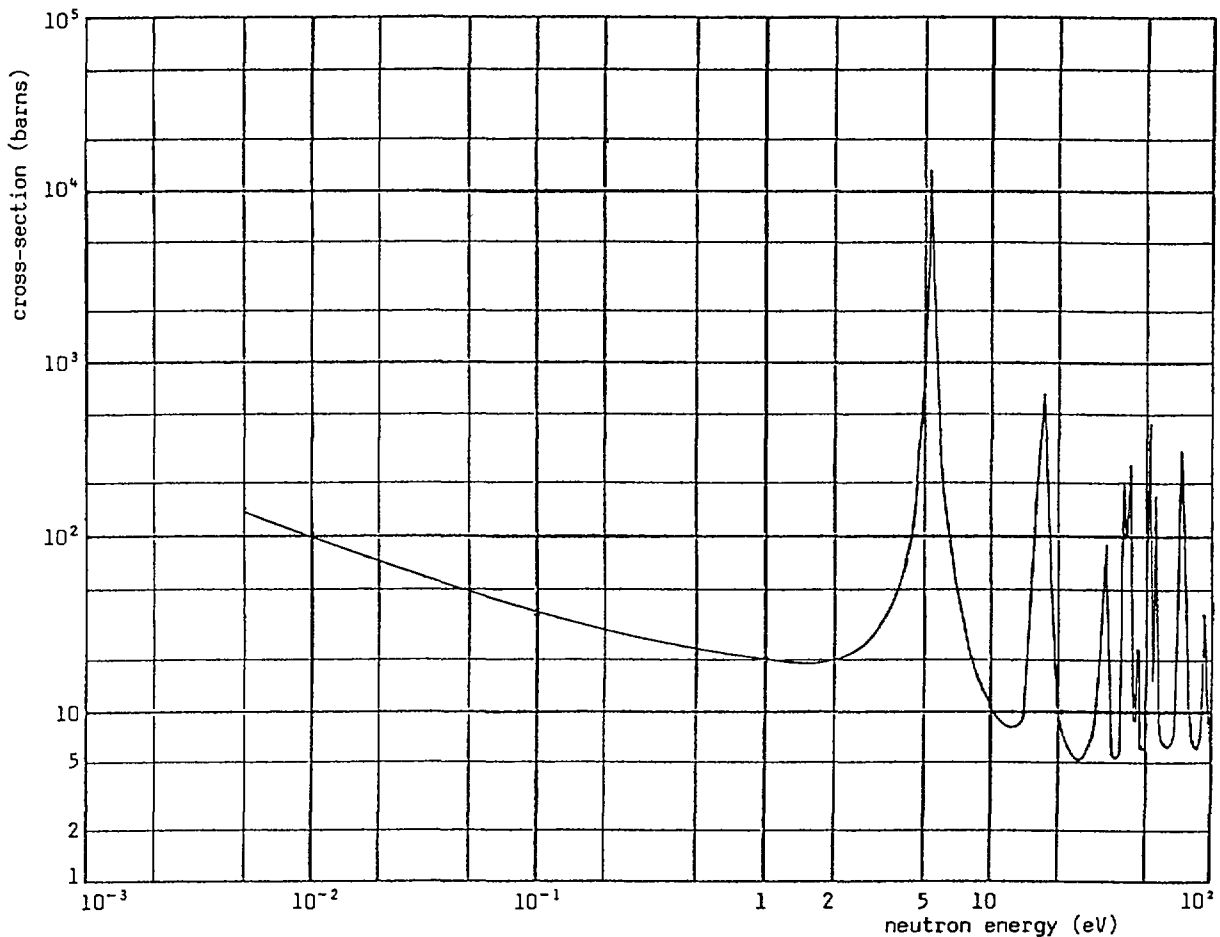


FIG. 12. The total cross-section for silver between 10^{-3} eV and 10^2 eV.

3. THE PROTON LINEAR ACCELERATOR.

The development of the radio frequency quadrupole structure [RFQ] for proton acceleration at low energies has opened up the possibility of energy selective activation analysis being carried out at exploration sites (and at mines and mineral processing plants).

The neutron yield from several possible targets has been considered but, for most applications, the favoured reaction is ${}^7\text{Li}(p, n){}^7\text{Be}$. The neutron yield from this reaction has been extensively tabulated by Liskean and Paulsen (8) and the cross-section for high yield fits very well to the proton energies available from small accelerators. A possible target design is shown schematically in Fig. 13.

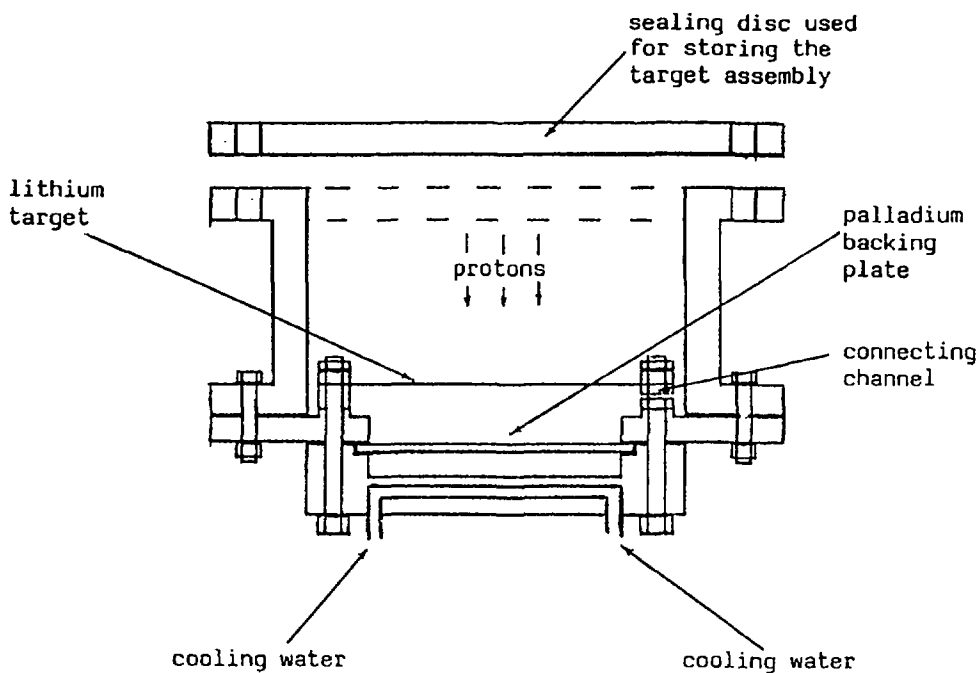


FIG. 13. Schematic diagram of a lithium target assembly.

The lithium is never exposed to high differential pressures and is only exposed to atmosphere for the short time (seconds) during which the target holder is being attached to the flight tube. The palladium acts as a sink for protons which penetrate the lithium target - when the lowest neutron energy needs to be controlled.

3.1 Analysis of gold in rocks and ores.

The potential problems associated with particle self-absorption are avoided by using the fast reaction $^{197}\text{Au}(n, n'\gamma)^{197m}\text{Au}$ as the route for gold analysis. The cross-section for this reaction is given in Fig. 14 along with the cross-sections for the $^{28}\text{Si}(n, p)^{28}\text{Al}$, $^{27}\text{Al}(n, p)^{27}\text{Mg}$ and $^{27}\text{Al}(n, \alpha)^{24}\text{Na}$ reactions which are the major potentially interfering reactions from the rock forming elements - especially in the Witwatersrand Reef.

It is seen that for a proton energy of 4.5 MeV, which equates with the highest neutron energy of 2.85 MeV at 0, overlap of a significant proportion of the $^{197}\text{Au}(n, n'\gamma)$ reaction is obtained whilst avoiding the $^{28}\text{Si}(n, p)$ and $^{27}\text{Al}(n, \alpha)$ reactions and accepting only a small fraction of the possible yield from the $^{27}\text{Al}(n, p)$ reaction. If very high aluminium concentrations are encountered a small reduction in the proton energy can be made.

The variation in neutron intensity from a lithium target of thickness $16.4 \text{ mg/cm}^2 (= 0.0308 \text{ cm})$ for a proton energy of 4.5 MeV is exhibited graphically in Figs. 15 and 16 (9).

Using the above data, a count of $400 \pm 20 (1\sigma)$ is calculated for a HpGe detector (efficiency 4%) for 1 ppm gold in a 3 kg sample of crushed rock after an irradiation of 30s, transfer time of 3s and counting time of 30s. In practice, uncertainty in the count might be increased by

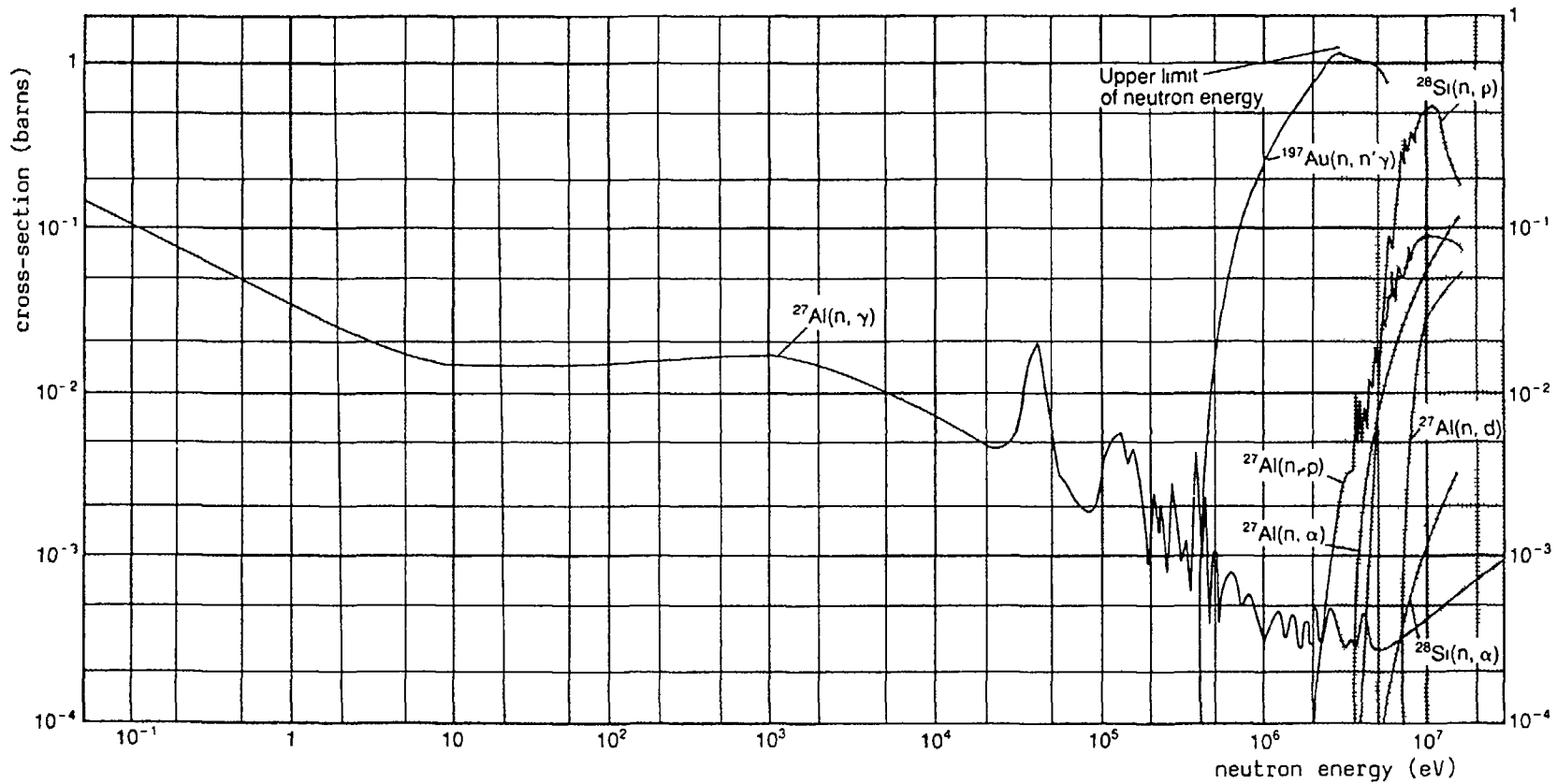


FIG. 14. Cross-sections (barns) of the $^{27}\text{Al}(n,\gamma)$, $^{27}\text{Al}(n,p)$, $^{27}\text{Al}(n,\alpha)$, $^{27}\text{Al}(n,d)$, $^{28}\text{Si}(n,p)$, $^{28}\text{Si}(n,\alpha)$ and $^{197}\text{Au}(n,n'\gamma)$ reactions.

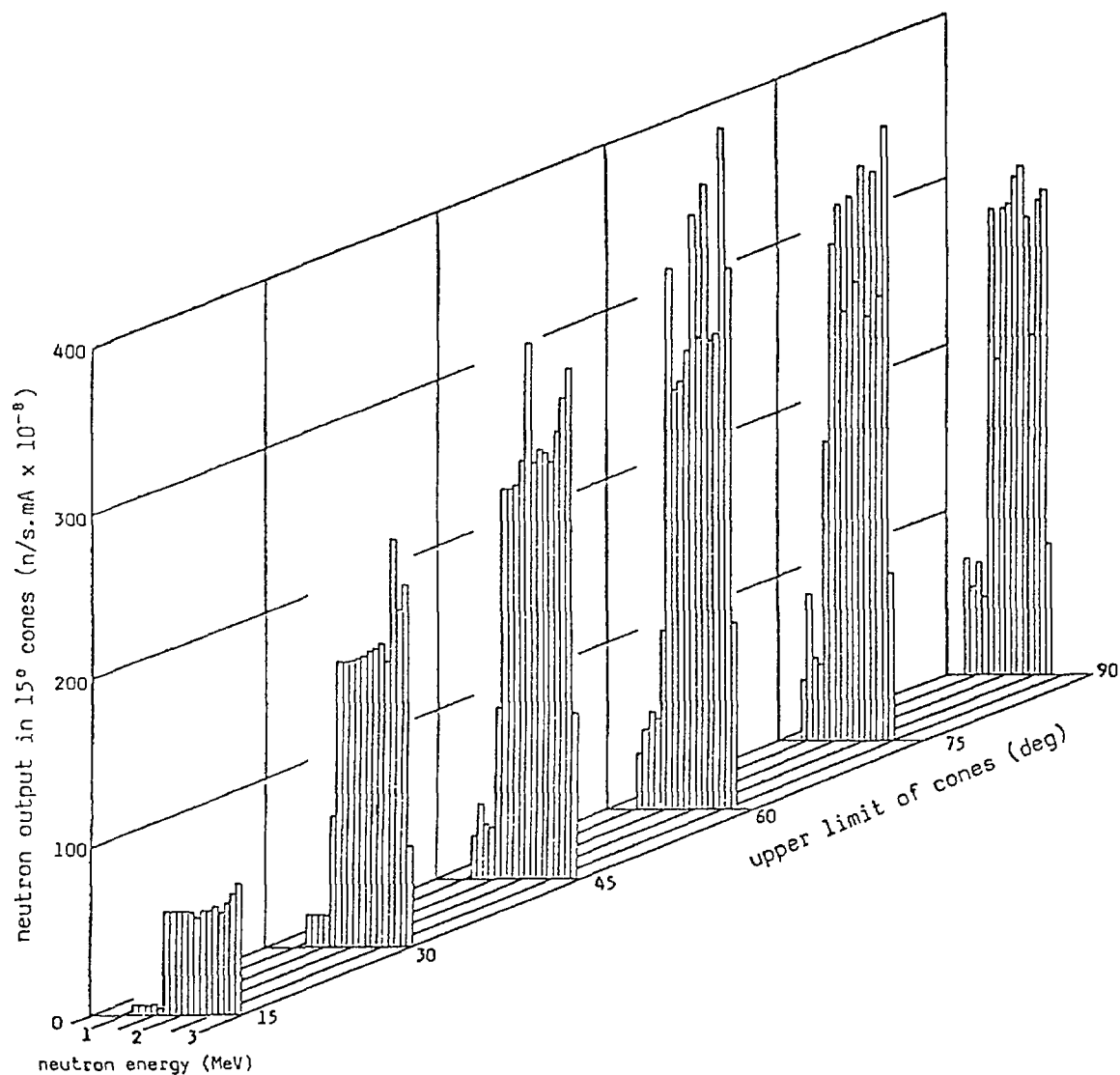


FIG. 15. Neutron output from the lithium target (0-90°).

interference from the $\text{Al}(n,p)$ reaction, depending on the concentration of aluminium present. For a lithium target of about 5 cm diam. which would require some form of beam scanning, the heat dissipation in the lithium is only about 1 watt/cm which is well within the acceptable limit.

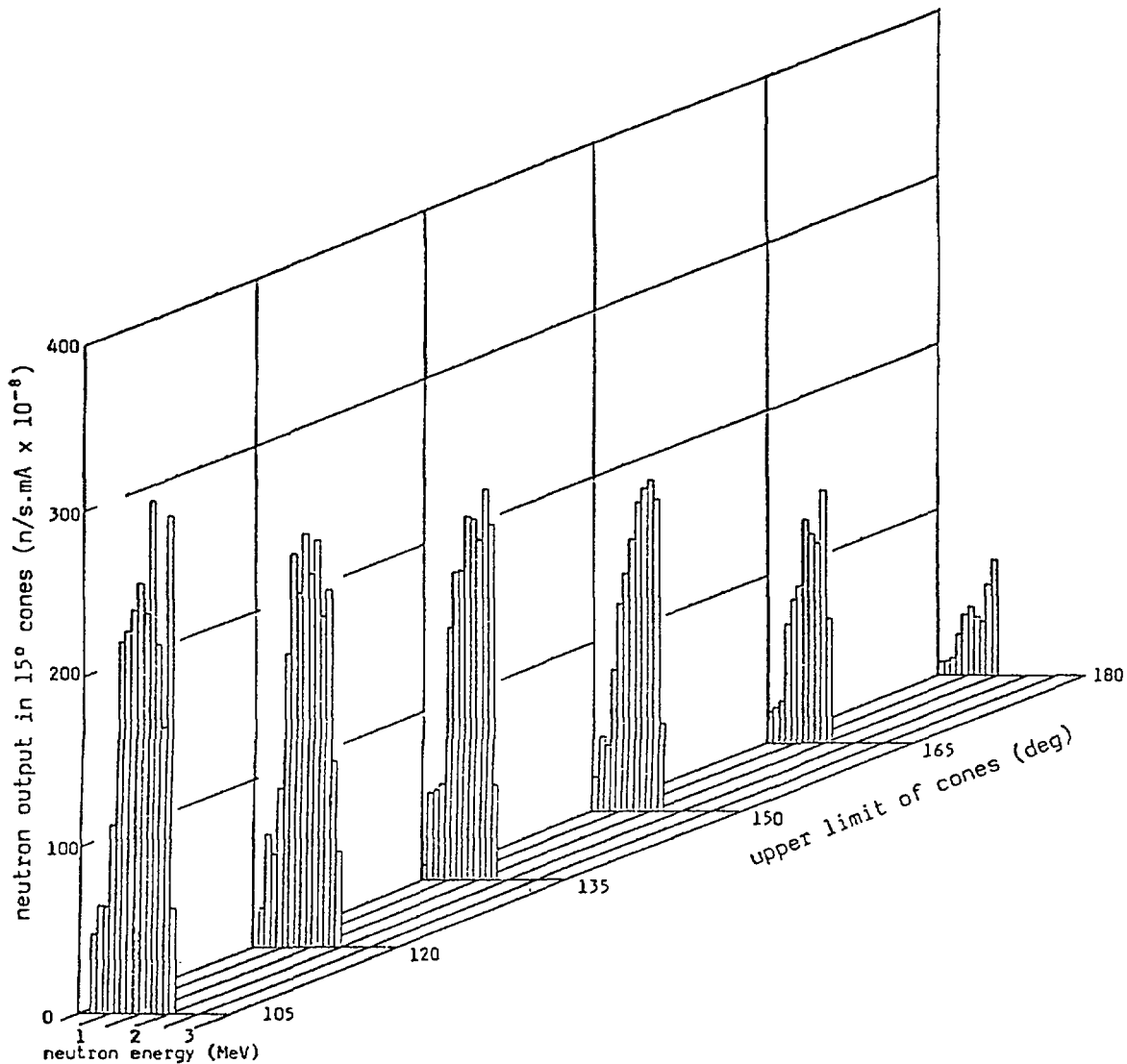


FIG. 16. Neutron output from the lithium target (90-180°).

CONCLUSIONS

Compact electron linear accelerators operating to 15 MeV, 100 μ A beam current and with W-U [(e⁻, γ) (γ ,nf)] or W-Be [(e⁻, γ) (γ ,n)] targets and an efficient neutron moderator can be used to generate a thermal flux of about 10⁹n/cm²/s over 2-3 kg of rock. This is adequate to allow selected elements at concentrations from <1 ppm upwards in rocks and ores to be measured.

The accurate analysis of gold by thermal neutron activation is restricted to deposits with particulate gold in the size range less than a few μ m or, if a suitable epithermal neutron absorber is used as a container for sample and standard, to a size range less than a few hundred μ m.

With the same system platinum concentrations of about 1 ppm in chromitite can be measured to an accuracy of a few per cent. If manganese is present a delay before assay of 2-3 days may be required.

Small proton Linacs with low energy ion injection into a RFQ section can be used to generate fast neutrons with some energy selection to overlap the cross-section of the analyte and to be below the threshold of potential competing reactions.

Using a proton Linac the thermal and epithermal self-absorption in gold particles can be avoided and gold analysed to sub-ppm concentrations via the reaction $^{197}\text{Au}(n, n'\gamma)^{197\text{m}}\text{Au}$.

REFERENCES

1. BOYLE, R.W. The geochemistry of gold and its deposits. Geological Survey Bulletin 280. Geological Survey of Canada, Ottawa, Canada (1979)
2. KAPCHINSKII, M. and TEPLYAKOV, V.A. Linear ion accelerator with spatially homogeneous strong focussing. Prib. Tech. Eksp. No. 2, 19 (1970).
3. CHIDLEY, B.G., McMICHEAL, G.E. and SCHRIBER, S.O. Canutron-A clean accelerator neutron generator. Nucl. Instrs. and Methods. B10/11, 888 (1985).
4. SCHRIBER, S.O., LONE, M.A., CHIDLEY, B.G., de JONG, M.S., KUSHNERIUK, S.A. and SELANDER, W.N. A compact neutron source for research and industrial applications. IEE Trans. Nucl. Sci., NS-30, 1668 (1983).
5. SWANSON, W.P. Calculation of neutron yields released by electrons incident on selected materials. Stanford Linear Accelerator Centre, Report SLAC-PUB-2042 (1977).
6. CLAYTON, C.G. and COLEMAN, C.F. Thermal and epithermal n-flux distributions for particular isotopic and mono-energetic neutron sources in spheres of selected materials relevant to bulk minerals analysis. To be published in Nuclear Geophysics.
7. PLANT, J. and COLEMAN, R.F. Application of neutron activation analysis to the evaluation of placer gold concentrations. Geochemical Exploration 1972, 373 (Inst. Mining and Metall., London, 1973).
8. LISKEAN, H. and PAULSEN, A. At. Data Nucl. Data Tables, 15, 58 (1975)

LIST OF PARTICIPANTS

Dr. J. Charbucinski
CSIRO,
Division of Mineral Engineering
P.O.Box 124
Port Melbourne, Victoria 3207
Australia

Dr. Q. Bristow (Chairman)
Head, Instrumentation R&D Section
Mineral Resources Division
Geological Survey of Canada
601 Booth Street
Ottawa, Ontario K1A 0E8
Canada

Dr. P.G. Killeen
Borehole Geophysics Section
Mineral Resources Division
Geological Survey of Canada
601 Booth Street
Ottawa, Ontario K1A 0E8
Canada

Dr. Sun Hancheng
Institute of Atomic Energy
Division of Physics
P.O.Box 275 (15)
Beijing
People's Republic of China

Dr. J.L. Pinault
Bureau de Recherches Géologiques
et Minières
B.P. 6009
F-45060 Orléans cedex 2
France

Dr. M. Dede
Institute of Experimental Physics
Kossuth University
Bem tér 18/a - P.O.Box 105
H-4001 Debrecen
Hungary

Dr. M. Yagi
Central Technical Laboratory
Japan Petroleum Exploration Co., Ltd.
3-5-5 Midorigaoka, Hamura-machi
Nishitama-gun, Tokyo
190-11 Japan

Dr. A. Kreft
Institute of Physics and Nuclear
Techniques
Academy of Mining & Metallurgy
Mickiewicza 30
30-059 Kraków
Poland

Dr. U. Woznicka
Institute of Nuclear Physics
Applications
ul. Radzikowskiego 152
31-342 Kraków
Poland

Dr. C.G. Clayton
Argoed Hall
Tregaron, Dyfed, SY25 6JR
United Kingdom

Prof. R.P. Gardner
Centre for Engineering Applications
of Radioisotopes
North Carolina State University
Department of Nuclear Engineering
Box 7909
Raleigh, NC 27695-7909
U.S.A.

Dr. T. Gozani
Science Applications International Corp.
1257 Tasman Drive
Sunnyvale, CA 94089
U.S.A.

Dr. W.R. Mills
Manager, Petrophysics Research
Mobil Research and Development Corporation
P.O.Box 819047
Dallas, TX 75381-9047
U.S.A.

Dr. F.E. Senftle
U.S. Geological Survey
Physics Building
Mail Stop 990
Reston, Virginia 22092
U.S.A.

Dr. J.S. Schweitzer
Schlumberger-Doll Research Centre
Old Quarry Road
Ridgefield, Connecticut 06877-4108
U.S.A.

Dr. C.W. Tittle
Professor of Physics
Consultant to
Gearhart Industries, Inc.
P.O. Box 1936
Fort Worth, TX 76101
U.S.A.

Prof. D.A. Kozhevnikov
Kathedra of Geophysical Research
in Boreholes
Ghubkin's Moscow Institute of Oil
Chemistry and Gas Industry
Moscow 117917
USSR

Dr. R. Rosenberg
IAEA
P.O. Box 100
A-1400 Vienna
Austria

(Scientific Secretary)